INSTABILIDADE DO DESENVOLVIMENTO E EVOLUÇÃO MORFOLÓGICA EM *Carollia perspicillata* (LINNAEUS, 1758) (CHIROPTERA: PHYLLOSTOMIDAE)

LUCAS DE OLIVEIRA CARNEIRO

UNIVERSIDADE ESTADUAL DO NORTE FLUMINENSE DARCY RIBEIRO - UENF

CAMPOS DOS GOYTACAZES - RJ

AGOSTO DE 2024

I

INSTABILIDADE DO DESENVOLVIMENTO E EVOLUÇÃO
MORFOLÓGICA EM *Carollia perspicillata* (LINNAEUS, 1758)
(CHIROPTERA: PHYLLOSTOMIDAE)

LUCAS DE OLIVEIRA CARNEIRO

Tese apresentada ao Centro de Biociências da Universidade Estadual do Norte Fluminense Darcy Ribeiro, como parte das exigências para a obtenção do título de doutor em Ecologia e Recursos Naturais

Orientador: Dr. Leandro Rabello Monteiro

CAMPOS DOS GOYTACAZES - RJ

AGOSTO DE 2024

INSTABILIDADE DO DESENVOLVIMENTO E EVOLUÇÃO MORFOLÓGICA EM *Carollia perspicillata* (LINNAEUS, 1758) (CHIROPTERA: PHYLLOSTOMIDAE)

LUCAS DE OLIVEIRA CARNEIRO

> Tese apresentada ao Centro de Biociências da Universidade Estadual do Norte Fluminense Darcy Ribeiro, como parte das exigências para a obtenção do título de doutor em Ecologia e Recursos Naturais

Aprovada em: 28 de Agosto de 2024

Comissão examinadora:

Documento assinado digitalmente
DANIELA MUNHOZ ROSSONI
Data: 25/11/2024 15:37:27-0300
Verifique em https://validar.iti.gov.br

_____

Dra. Daniela Munhoz Rossoni (Florida State University)

Documento assinado digitalmente
GUSTAVO LAZZARO REZENDE
Data: 21/11/2024 16:09:54-0300
Verifique em https://validar.iti.gov.br

_____

Prof. Gustavo Lazzaro Rezende (Universitat de València)

Documento assinado digitalmente
RENAN MAESTRI
Data: 26/11/2024 09:26:00-0300
Verifique em https://validar.iti.gov.br

_____

Prof. Renan Maestri (Universidade Federal do Rio Grande do Sul)

Documento assinado digitalmente
LEANDRO RABELLO MONTEIRO
Data: 26/11/2024 09:37:48-0300
Verifique em https://validar.iti.gov.br

_____

Prof. Leandro Rabello Monteiro (UENF)

(Orientador)

Agradescimentos

Sumário

Lista de figuras

Introdução:

Capítulo 1:

Capítulo 3:

Lista de tabelas

Introdução:

Capítulo 2

Capítulo 3

Resumo

A incapacidade de tamponar desvios no desenvolvimento, e gerar o fenótipo ótimo para um determinado ambiente é chamada de instabilidade do desenvolvimento (ID). Existem evidências de que a ID está inversamente associada à aptidão. A ID gera imprecisão no desenvolvimento, que pode ser medida, em organismos bilaterais, por diferenças entre os lados (assimetria). Poucos estudos avaliaram um grande número de caracteres para mostrar a existência de um efeito sistêmico da ID. A correlação de assimetrias em diferentes caracteres, além de ser evidência de um efeito sistêmico da ID, pode ser utilizada como ferramenta para o estudo da integração morfológica no desenvolvimento, além da ocorrência de módulos. O objetivo principal deste estudo foi avaliar a existência de instabilidade no desenvolvimento sistêmica (como atributo do indivíduo) e sua relação com os padrões de integração e modularidade regulando a variabilidade fenotípica intra e interpopulacional no morcego *Carollia perspicillata*. Para alcançar este objetivo, foram examinadas as assimetrias flutuantes (AF) e correlações entre componentes de diferentes complexos morfológicos (membros anteriores, posteriores e crânio) em amostras distribuídas ao longo de sua distribuição geográfica. As correlações entre as assimetrias foram baixas, mas um modelo misto hierárquico aponta que a variação de assimetria está mais concentrada no nível dos indivíduos que dos caracteres. O efeito da ID foi associado negativamente com a importância funcional dos caracteres (FA da asa < FA do crânio < FA dos membros posteriores). O que sugere um tamponamento diferencial reduzindo os efeitos sistêmicos da ID de características funcionalmente importantes. Os padrões de integração de desenvolvimento e estática no crânio foram marcados pela estruturação de caracteres adjacentes. No nível evolutivo, esse complexo morfológico apresentou um padrão mais complexo e mais forte de integração. Os padrões integrativos de desenvolvimento e estático (particularmente na mandíbula) se assemelham ao observado para nectarívoros da família Phyllostomidae enquanto o estático e o evolutivo ao padrão conhecido para frugívoros especializados (subfamília Stenodermatinae). No nível de desenvolvimento dos membros, pela primeira vez se observou módulos distintos integrando falanges e metacarpos em asas de morcegos. Padrão que se alinha ao conhecimento da biologia do desenvolvimento dessas estruturas. No nível estático, membros anterior e posterior apresentam relativa independência, como observado

em outros grupos em que membros estão sujeitos a gradientes de seleção diferentes. Assim como no crânio, a integração evolutiva foi maior e mais complexa nos membros. Esses resultados indicam que gradientes de seleção reorganizam os padrões de associação entre os componentes desses complexos morfológicos.

Palavras-Chave: Assimetria flutuante, Aptidão, Imprecisão do desenvolvimento, Estresse ambiental, Integração morfológica.

Abstract:

The inability to buffer disturbances in development and generate the optimal phenotype for an environment is called developmental instability (DI). There is evidence that DI is inversely associated with fitness. DI generates imprecision in development, which can be measured, in bilateral organisms, by differences between sides (fluctuating asymmetry – FA). Few studies have evaluated a large number of characters to show the existence of a systemic effect of DI. In addition to being evidence of a systemic effect of DI, the correlation of asymmetries in different characters can be used as a tool to study developmental morphological integration and modularity. The main objective of this study was to evaluate the existence of systemic developmental instability (as an individual property) and its relationship with the patterns of integration and modularity regulating intra- and interpopulational phenotypic variability in the bat *Carollia perspicillata*. To achieve this objective, the asymmetries and correlations among components of different morphological complexes (forelimbs, hindlimbs and skull) were measured in samples distributed throughout its geographic range. The correlations between the asymmetries were low, but a hierarchical mixed model for asymmetries in trait sets indicated that the variation is concentrated at the individual level nested within trait level. The effect of DI was negatively associated with the functional importance of the characters (Wing FA < Skull FA < Hindlimb FA), indicating that differential buffering reduces the systemic effects of DI on functionally important traits. The patterns of developmental and static integration in the skull were characterized by a strong association between adjacent traits. At the evolutionary level, this morphological complex presented a more intricate pattern with higher correlations. Both developmental and static patterns (particularly in the mandible) resemble those observed for nectarivores of the Phyllostomidae family, while the static and evolutionary patterns resemble those known for specialized frugivores (subfamily Stenodermatinae). In the wings, distinct modules integrating phalanges and metacarpals at the developmental level were observed for the first time in bats. This pattern is in line with the knowledge of the developmental biology of these structures. At the static level, forelimbs and hindlimbs are relatively independent, as observed in other groups in which limbs are subject to different selection gradients. Evolutionary integration was also stronger and more complex than developmental and static patterns in the limbs. These results indicate

that selection gradients reorganize the association patterns among the components of these morphological complexes.

Introdução

Os processos evolutivos responsáveis pela diversidade de fenótipos complexos têm intrigado gerações de pesquisadores, sendo abordada de modo transversal em diferentes linhas de pesquisa (Bonner, 1988; Soyer e Bonhoeffer, 2006; Deline *et al.*, 2018; Verd *et al.*, 2019). A investigação dos padrões de associação entre as estruturas que compõem os organismos auxilia a compreensão da diversidade morfológica e, em maior escala, da diversidade biológica (Marroig *et al.*, 2009; Zelditch, 2022). O conhecimento sobre os padrões de diversidade morfológica em linhagens que passaram por radiações adaptativas, por exemplo, permite a compreensão do papel da divergência morfológica durante a diversificação desses clados (Monteiro e Nogueira, 2010; Rossoni *et al.*, 2019; Reaney *et al.*, 2020; Vinciguerra e Burns, 2021; Rossoni *et al.*, 2024).

O surgimento dos organismos complexos, formados pela associação de estruturas pluricelulares distribuídas em diferentes níveis de organização, foi em parte possível por conta da organização modular desses organismos (Hansen e Houle, 2008; Payne e Wagner, 2018; Verd *et al.*, 2019). Um sistema modular é formado por componentes quase-independentes, ou seja, que podem operar de modo integrado, mas ao mesmo tempo são relativamente independentes ou "dissociáveis" (Callebaut, 2005).

Integração morfológica e modularidade

Os padrões de associação entre os diferentes componentes de uma estrutura morfológica, medidos pela correlação de caracteres fenotípicos, decorrem da integração entre esses componentes e podem ser usados para descrever essa hierarquia de desenvolvimento (Esteve-Altava, 2017; Zelditch e Goswami, 2021). Esses padrões são dependentes do compartilhamento de vias de sinalização reguladoras da embriogênese, trajetórias de desenvolvimento, ou limitações impostas por seleção natural, associadas à performance (Klingenberg, 2014; Melo *et al.*, 2016; Hall e Moody, 2018). A modularidade é inferida pela forte associação entre componentes pertencentes a um grupo (módulo), que apresentam reduzida ou nenhuma associação com elementos de outros grupos

(Klingenberg, 2009). Mesmo as respostas evolutivas decorrentes de seleção não são independentes dos processos de desenvolvimento, já que a seleção age sobre a variação produzida na embriogênese (Hendrikse *et al.*, 2007; Olson, 2019). Dessa forma a associação entre genótipo e fenótipo por meio do desenvolvimento pode ser compreendida pela predisposição nas direções de variação fenotípica (Klingenberg e Monteiro, 2005; Hendrikse *et al.*, 2007). Essa tradução do genótipo em fenótipo sob efeito de demandas funcionais pode ser observada no esquema conceitual proposto por Wagner e Altenberg (1996) (Figura 1) para a tradução do mapa genotípico em fenótipo através do desenvolvimento (Porto *et al.*, 2016).
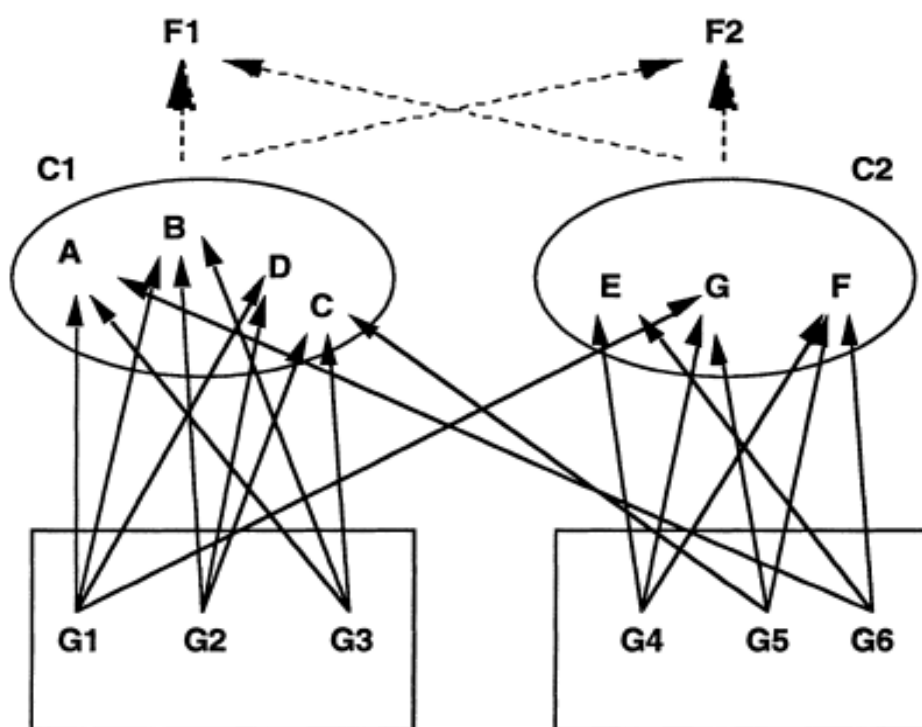
Figure 1: Representação de dois módulos de caracteres fenotípicos (C1 e C2). C1 apresenta os caracteres A, B, C e D enquanto C2 os caracteres E, F, G. Ambos os módulos servem às funções F1 e F2, embora cada um deles apresente uma função primária (C1 tem F1 como função primária enquanto C2 tem F2). F2 apresenta efeito fraco em C1 (em comparação a F1) e vice-versa. O fenótipo modular reflete uma estrutura genética modular, porque os efeitos pleiotrópicos dos genes G1, G2, G3 incidem basicamente sobre em C1, enquanto os genes G4, G5, G6 tem seu efeito concentrado em caracteres do complexo C2. Há mais efeitos pleiotrópicos nos caracteres dentro de cada complexo do que entre eles. Figura retirada de Wagner e Altenberg (1996).

Os conceitos de integração e modularidade estão envolvidos em certa ambiguidade, tanto em relação às definições quanto em relação às metodologias

empregadas na investigação dos fenômenos descritos pelos termos (Esteve-Altava, 2017; Zelditch e Goswami, 2021). De maneira geral, integração e modularidade são entendidos como conceitos complementares que representam duas faces de uma mesma moeda (Wagner e Altenberg, 1996; Esteve-Altava, 2017; Zelditch e Goswami, 2021) e que portanto, devem ser discutidos em conjunto (Klingenberg, 2013). Além disso, a descrição quantitativa de integração e modularidade não se restringe a conjuntos de caracteres sem sobreposição, mas deve levar em consideração a intensidade de integração, hierarquia e sobreposição entre módulos (Wagner e Altenberg, 1996).

Diferentes níveis de integração e modularidade podem ser reconhecidos de acordo com os mecanismos por trás desses padrões (Klingenberg, 2014), embora a maioria das pesquisas sobre integração e modularidade se concentre no nível estático—análises realizadas amostras homogêneas da mesma espécie (Klingenberg, 2014). Efeitos pleiotrópicos de genes podem produzir respostas correlacionadas de diferentes estruturas ou parte de uma estrutura—integração genética (Wagner e Altenberg, 1996; Klingenberg, 2014). Processos ou fatores de desenvolvimento compartilhados podem aumentar a associação entre diferentes características—integração no desenvolvimento (Klingenberg, 2008). Funções compartilhadas entre caracteres podem gerar padrões de integração funcional, os quais podem surgir por efeitos seletivos ou mesmo diretos como a remodelagem óssea resultante de forças aplicadas em uma estrutura (Zelditch *et al.*, 2008). Restrições no desenvolvimento e gradientes de seleção associados a demandas funcionais também podem atuar na associação entre caracteres que são selecionados em conjunto em um nível interpopulacional ou interespecífico—integração evolutiva (Cheverud, 1996; Monteiro e Nogueira, 2010). Estudos que analisam diferentes níveis de integração e modularidade ainda são raros, apesar de seu potencial para esclarecer o papel da associação de diferentes causas entre caracteres (Klingenberg, 2014; Sherratt e Kraatz, 2023).

O potencial evolutivo (*evolvability*), definido pela capacidade apresentada por um sistema biológico de gerar variabilidade fenotípica herdável—adaptativa ou neutra (Brown, 2014; Payne e Wagner, 2018), apresenta papel central na Biologia Evolutiva do Desenvolvimento (Hendrikse *et al.*, 2007), e tem ganhado espaço na Biologia Evolutiva como um todo (Brown, 2014; Payne e Wagner, 2018). A investigação do potencial evolutivo de uma população, para uma dada

característica fenotípica, requer a consideração de informações sobre o desenvolvimento ontogenético dessa característica (Hendrikse *et al.*, 2007). A importância da biologia do desenvolvimento para a compreensão dos processos evolutivos (em especial os adaptativos), se dá por ser a variabilidade fenotípica (sobre a qual age a seleção natural) a tradução da variabilidade genética—que apresenta herdabilidade (Hendrikse *et al.*, 2007) pelos processos de desenvolvimento. A compreensão da evolução de estruturas morfológicas complexas depende do entendimento dos processos de desenvolvimento da morfologia e das fontes de variabilidade que sobre eles incidem (Marroig *et al.*, 2009; Hall e Moody, 2018). A hierarquia da organização do desenvolvimento tem, portanto, papel fundamental na predição de modificações evolutivas conjuntas ou independentes entre diferentes partes do corpo (Hendrikse *et al.*, 2007; Marroig *et al.*, 2009; Hall e Moody, 2018).

A investigação de associações entre a assimetria de estruturas bilaterais apresenta uma alternativa para a dissociação da influência de fatores de desenvolvimento de ambos os gradientes de pleiotropia e seleção na modelagem de padrões de integração e modularidade (Klingenberg, 2008; Klingenberg, 2022). Como os dois lados do corpo compartilham o mesmo genótipo e (em animais dotados de mobilidade) compartilham o mesmo ambiente, espera-se que as pequenas diferenças aleatórias entre eles tenham se acumulado como impressão nos dois eventos de desenvolvimento replicados (Van Dongen, 2006). Assim, a correlação de assimetrias (com sinal) entre dois caracteres indica origem de desenvolvimento compartilhada (Klingenberg, 2008; Klingenberg, 2014).

Assimetria flutuante e instabilidade no desenvolvimento

A assimetria de estruturas bilaterais é amplamente usada como marcador de instabilidade no desenvolvimento (Palmer e Strobeck, 2003; Graham, 2021). Esta se origina com o acúmulo de pequenas diferenças aleatórias entre estruturas que apresentem simetria bilateral. Sob a perspectiva de um desenvolvimento ideal, não haveria diferença entre os membros direito e esquerdo de um animal bilateral, uma vez que essas estruturas compartilham o mesmo genótipo e ambiente (Konuma *et al.*, 2014). A assimetria mede a imprecisão do desenvolvimento do indivíduo (Leamy e Klingenberg, 2005; Graham, 2020;

Graham, 2021). Quando a ID é a principal responsável pelas assimetrias individuais, é observado um padrão populacional de variação das assimetrias, chamado assimetria flutuante (AF) (Figura 2). Neste contexto é esperado que valores medidos para assimetrias individuais assumam uma distribuição leptocúrtica com média zero, na qual a maior parte da variação se concentra próxima do centro embora a distribuição apresente caudas longas (Van Dongen *et al.*, 1999), ou seja, a maioria dos indivíduos apresenta pouca assimetria e alguns indivíduos muito assimétricos ocorrem em maior frequência que o esperado em uma distribuição Normal.
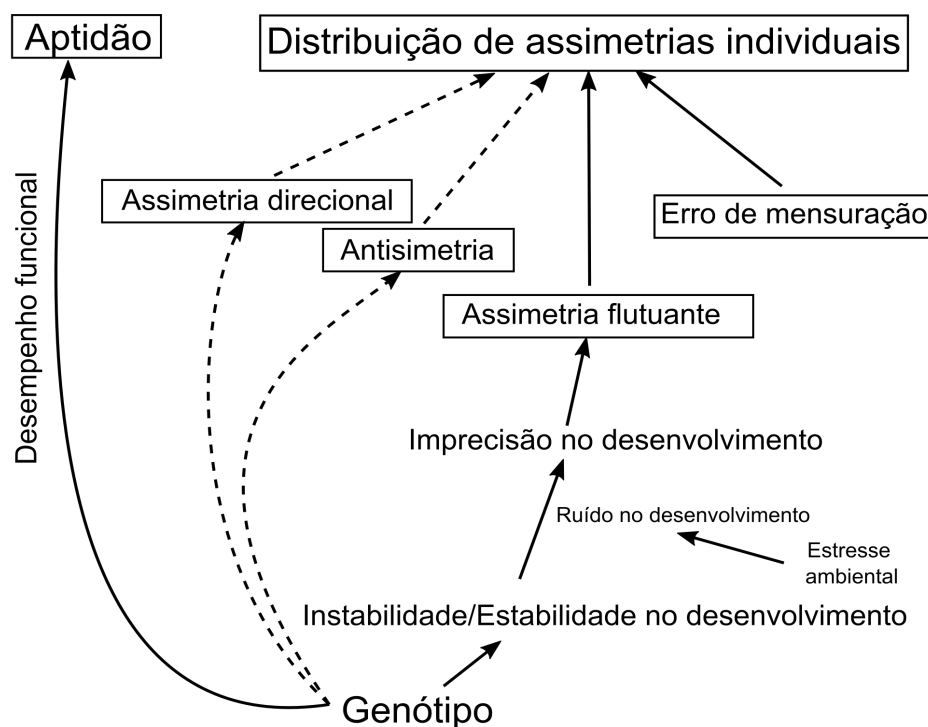
Figure 2: Diagrama causal mostrando o modelo conceitual da relação entre os diferentes tipos de assimetria, desenvolvimento e aptidão, baseado em Gangestad e Thornhill (1999) e Klingenberg (2003). Diferenças genotípicas e processos biológicos devem levar a um ajuste entre aptidão e assimetria individual, mas este pode ser obscurecido por uma mistura de processos biológicos e problemas metodológicos. Os termos em caixas correspondem a padrões de distribuição. As linhas tracejadas mostram caminhos que, quando presentes, são parte do desenvolvimento normal e possivelmente adaptativo. Figura modificada de Monteiro et al. (2019).

Outras formas de assimetria precisam ser consideradas por constituírem parte do desenvolvimento ideal dos indivíduos e serem geneticamente determinadas em algumas espécies (Van Dongen, 2006; Klingenberg, 2015) (Figura 2). A assimetria direcional leva ao desenvolvimento maior de um lado

específico em relação ao outro, o que gera uma distribuição assimétrica com média diferente de zero. Já a antissimetria é caracterizada pelo desenvolvimento maior de um dos lados, sem que haja um padrão em relação a qual lado será mais desenvolvido, dessa forma a distribuição das assimetrias será bimodal com média dos valores zero (Palmer e Strobeck, 2003). Estes padrões de assimetria podem inclusive ser adaptativos e não estão associados à ID, devendo ser excluídos em estudos de AF. O estudo da instabilidade no desenvolvimento, seus padrões de variação e covariação entre caracteres fenotípicos, assim como sua associação com aptidão, abre uma janela de oportunidade para incorporar processos de desenvolvimento aos níveis de variação entre organismos e populações.

Sistema modelo e objetivos do estudo

Morcegos são organismos modelo para diferentes temas em ecologia e evolução (Fenton *et al.*, 1992; Monteiro e Nogueira, 2010; Dumont *et al.*, 2012). Questões relativas à função e integração em diferentes membros são melhor compreendidas quando diferentes membros (ou elementos dentro dos membros) apresentam funções diferentes, fazendo com que a sobreposição entre modelos de desenvolvimento e funcionais não seja absoluta (Young e Hallgrímsson, 2005). *Carollia perspicillata* (Linnaeus, 1758) (Figura 3), em particular, é uma das espécies de morcego mais estudadas (Fleming, 1988) e considerada um modelo emergente na investigação de diferentes questões biológicas (Cretekos *et al.*, 2005; Rasweiler *et al.*, 2010; Martinez-Cerdeño *et al.*, 2017). Esta espécie é amplamente distribuída por toda a região Neotropical e é encontrada em alta abundância em toda a sua distribuição, possivelmente por apresentar tolerância à perturbações ambientais (Bernard e Fenton, 2003; Mellado *et al.*, 2018). Sua dieta é composta principalmente de frutos do gênero *Piper* (Parolin *et al.*, 2016) entre outros encontrados no sub-bosque de florestas, bem como artrópodes e pólen (Cloutier e Thomas, 1992). Apresenta um sistema de acasalamento poligínico com defesa de recursos, no qual os machos defendem ativamente territórios dentro de abrigos reprodutivos, os quais serão escolhidos pelas fêmeas durante a estação reprodutiva (Fleming, 1988).

Figure 3: *Carollia perspicillata* fotografado na Reserva Biológica União. Foto de Marcelo R. Nogueira.

Monteiro *et al.* (2019) observaram que a assimetria do comprimento do antebraço em *C. perspicillata* está negativamente relacionada à sobrevivência e reprodução na espécie, sendo considerada um potencial marcador de aptidão (*fitness*). Esses autores mostraram também que a sobrevivência aparente varia temporalmente, seguindo uma tendência de associação positiva com a pluviosidade sazonal, possivelmente relacionada à maior disponibilidade de alimentos na estação chuvosa. Estudos posteriores mostraram, nessa mesma população, que indivíduos (em particular machos) com antebraços mais assimétricos apresentaram menor resposta imunológica (Mellado *et al.*, 2024a). Outras medidas de desempenho, como força de mordida e gasto energético do voo não apresentaram clara relação com a assimetria do antebraço (Monteiro, L. R. dados não publicados). Este resultado corroborou parcialmente a hipótese de Monteiro *et al.* (2019) de que a assimetria do antebraço não apresentava relação com o desempenho funcional dinâmico (que depende do movimento de partes do corpo) (Husak *et al.*, 2009), mas sim com um componente de desempenho regulatório, baseado na homeostase e processos fisiológicos. A associação com o desempenho regulatório seria mais compatível com a hipótese de um efeito sistêmico da ID.

Apesar de existirem evidências de efeitos indiretos de um efeito sistêmico da ID na relação da assimetria do antebraço com componentes da aptidão, ainda existem questões em aberto sobre como a ID seria expressa em outros caracteres morfológicos, que podem pertencer a outros módulos de desenvolvimento ou funcionais. Carneiro *et al.* (2023) demonstraram, na população do Sudeste do Brasil estudada por Monteiro *et al.* (2019) e Mellado *et al.* (2024a), que diferenças nos padrões de movimento observados entre machos e fêmeas da espécie (Charles-Dominique, 1991; Rocha *et al.*, 2017) podem estar relacionadas a um padrão previamente desconhecido de dimorfismo sexual na asa da espécie. Diferenças nas asas resultantes de pequenas mudanças no comprimento de metacarpos e falanges específicos influenciam o consumo de energia durante o voo, de modo que machos e fêmeas têm morfologias otimizadas para o voo em diferentes áreas de seu habitat (Carneiro *et al.*, 2023). Mesmo com a existência de um efeito sistêmico da ID, é possível que existam mecanismos de tamponamento localizados em conjuntos de caracteres cuja função não comporta um acúmulo de diferenças assimétricas (Polak *et al.*, 2003).

O objetivo principal deste estudo foi avaliar a existência de instabilidade no desenvolvimento sistêmica (como atributo do indivíduo) e sua relação com os padrões de integração e modularidade regulando a variabilidade fenotípica intra e interpopulacional no morcego *Carollia perspicillata*. Para alcançar este objetivo, foram examinadas as correlações observadas nos componentes de diferentes complexos morfológicos, em populações do morcego *C. perspicillata* (membros anteriores, posteriores e crânio) distribuídas ao longo de sua distribuição geográfica.

A tese foi organizada em quatro capítulos, sendo o primeiro sendo o primeiro uma revisão sobre metodologias aplicadas ao estudo da integração morfológica e modularidade, o segundo um teste da hipótese da ID sistêmica, que prevê a existência de correlações entre as assimetrias sem sinal (absolutas) dos diferentes complexos morfológicos (Van Dongen, 2006). Caso a assimetria esteja associada a um prejuízo funcional direto, espera-se que caracteres com maior importância relativa para a performance funcional dos indivíduos (partes da asa como comprimento do antebraço e falanges) apresentem menor nível de AF em relação aos complexos menos relevantes funcionalmente, como os membros posteriores. Espera-se que ocorra variação da AF em diferentes populações, com

maiores valores observados em populações sujeitas a condições mais estressantes. Considerando a diminuição da sobrevivência e massa corporal em *C. perspicillata* documentada em períodos de seca prolongada (Monteiro *et al.*, 2019; Mellado *et al.*, 2024b), comparamos a AF entre populações oriundas de ecoregiões florestais com populações oriundas de áreas abertas e mais secas, como Cerrado e Caatinga.

Os capítulos seguintes examinaram a integração de elementos ósseos (crânio e pós-crânio separadamente) em diferentes níveis de variação (Klingenberg, 2014) em populações de *C. perspicillata*. A integração no desenvolvimento foi avaliada pelas correlações de assimetrias com sinal (variação intra-individual). A integração estática (intra-populacional) foi avaliada a partir das correlações entre médias dos lados esquerdo e direito (dados simetrizados) dentro das populações (resíduos intra-populacionais). A integração evolutiva foi avaliada pelas correlações dos dados simetrizados entre as médias calculadas por população. Os padrões de integração foram descritos e comparados com modelos teóricos baseados em processos de desenvolvimento (Young e Hallgrímsson, 2005; Monteiro e Nogueira, 2010), e com padrões estimados para níveis de variação entre linhagens e guildas de morcegos filostomídeos disponíveis na literatura (Monteiro e Nogueira, 2010). A combinação de resultados da variação de ID com a integração de diferentes elementos ósseos em um contexto multinível, permitiu uma discussão mais aprofundada sobre a organização do fenótipo, assim como dos mecanismos responsáveis pela variação a partir da divergência na função dos membros.

Descrição da amostragem

Para a realização dos capítulos 2–4 foram examinados 310 espécimes de *C. perspicillata* provenientes de 36 localidades ao longo da distribuição da espécie (Tabela 1; Figura 4). Os espécimes tiveram o crânio fotografado em vista ventral e mandíbula em vista lateral (tanto do lado direito quanto do esquerdo). Foram tomadas 12 medidas lineares nos membros anterior e posterior desses espécimes. Detalhes da amostragem são apresentados no decorrer dos capítulos.
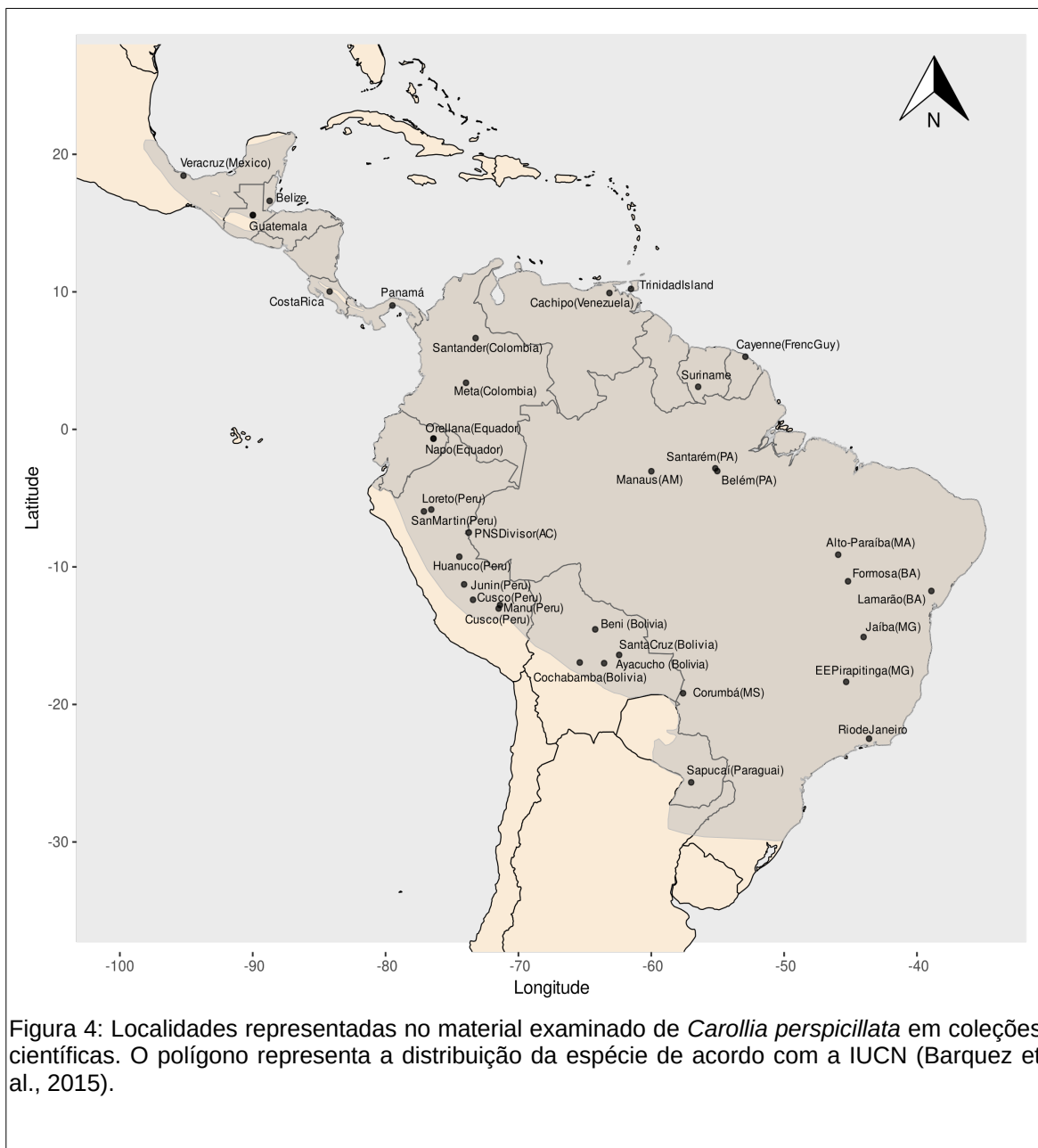
Figura 4: Localidades representadas no material examinado de *Carollia perspicillata* em coleções científicas. O polígono representa a distribuição da espécie de acordo com a IUCN (Barquez et al., 2015).

Table 1: Localidades representadas no material examinado de *Carollia perspicillata* em coleções científicas e tamanho amostral por localidade.

Localidade	Tamanho amostral
Alto-Paraíba (MA)	3
Ayacucho(Peru)	2
Belém(PA)	6
Belize	16
Beni(Bolivia)	11
Cachipo(Venezuela)	1
Cayenne(FrencGuy)	6
Cochabamba(Bolivia)	21
Corumbá(MS)	1
Costa Rica	8
Cusco(Peru)	7
Cusco(Peru)	1
EE Pirapitinga(MG)	9
Formosa(BA)	3
Guatemala	16
Huanuco(Peru)	6
Jaíba(MG)	9
Junin(Peru)	2
Lamarão(BA)	1
Loreto(Peru)	1
Manaus(AM)	14
Manu(Peru)	25
Meta(Colombia)	5
Orellana(Equador)	6
Panamá	2
PNSDivisor(AC)	33
RiodeJaneiro	29
San Martin(Peru)	17
Santa Cruz(Bolivia)	29
Santander(Colombia)	3

Localidade	Tamanho amostral
Santarém(PA)	2
Sapucaí(Paraguai)	3
Suriname	6
Trinidad Island	3
Veracruz(Mexico)	3
Napo(Equador)	1

Referências bibliográficas

Barquez, R., Perez, S., Miller, B., Diaz, M. 2015. *Carollia perspicillata*. The IUCN Red List of Threatened Species 2015: e.T3905A22133716. https://dx.doi.org/10.2305/IUCN.UK.2015-4.RLTS.T3905A22133716.en. Acessado em 07 August 2024.

Bernard, E., Fenton, B. (2003). Bat mobility and roosts in a fragmented landscape in central Amazonia, Brazil. *Biotropica* 35:262-277.

Bonner, J.T. (1988). *The evolution of complexity by means of natural selection*. Princeton, New Jersey: Princeton University Press. 272 p.

Brown, R.L. (2014). What evolvability really is. *The British Journal for the Philosophy of Science* 65:1–24.

Callebaut, W. (2005). The ubiquity of modularity. *In*: Rasskin-Gutman, W.C. (eds.) *Modularity understanding the development and evolutionof natural complex systems*. Cambridge, MA: MIT Press Cambridge, MA. p. 3–28.

Carneiro, L.O., Mellado, B., Nogueira, M.R., Cruz-Neto, A.P.d., Monteiro, L.R. (2023). Flight performance and wing morphology in the bat *Carollia perspicillata*: biophysical models and energetics. *Integrative Zoology* 18:876–890.

Charles-Dominique, P. (1991). Feeding strategy and activity budget of the frugivorous bat *Carollia perspicillata* (Chiroptera: Phyllostomidae) in French Guiana. *Journal of Tropical Ecology* 7:243–256.

Cheverud, J.M. (1996). Developmental integration and the evolution of pleiotropy. *The American Zoologist* 36:44–50.

Cloutier, D., Thomas, D.W. (1992). *Carollia perspicillata*. *Mammalian species* :1–9.

Cretekos, C.J. et al. (2005). Embryonic staging system for the short-tailed fruit bat, *Carollia perspicillata*, a model organism for the mammalian order Chiroptera, based upon timed pregnancies in captive-bred animals. *Developmental dynamics: an official publication of the American Association of Anatomists* 233:721–738.

Deline, B., Greenwood, J.M., Clark, J.W., Puttick, M.N., Peterson, K.J., Donoghue, P.C.J. (2018). Evolution of metazoan morphological disparity. *Proceedings of the National Academy of Sciences* 115:E8909-E8918.

Dumont, E.R., Davalos, L.M., Goldberg, A., Santana, S.E., Rex, K., Voigt, C.C. (2012). Morphological innovation, diversification and invasion of a new adaptive zone. *Proceedings of the Royal Society B: Biological Sciences* 279:1797–1805.

Esteve-Altava, B. (2017). In search of morphological modules: a systematic review. *Biological Reviews* 92:1332–1347.

Fenton, M.B. et al. (1992). Phyllostomidae Bats (Chiroptera: Phyllostomidae) as indicators of habitat disruption. *Biotropica* 24:440-446.

Fleming, T. (1988). *The short-tailed fruit bat: a study in plant-animal interactions*. Chicago, USA: Chicago University Press. 365 p.

Gangestad, S.W., Thornhill, R. (1999). Individual differences in developmental precision and fluctuating asymmetry: a model and its implications. *Journal of evolutionary Biology* 12:402–416.

Graham, J.H. (2020). Fluctuating asymmetry and developmental instability, a guide to best practice. *Symmetry* 13:9.

Graham, J.H. (2021). Nature, nurture, and noise: developmental instability, fluctuating asymmetry, and the causes of phenotypic variation. *Symmetry* 13:1204.

Hall, B.K., Moody, S.A. (2018). *Cells in evolutionary biology: translating genotypes into phenotypes-past, present, future*. Boca Raton, Florida: CRC Press. 280 p.

Hansen, T.F., Houle, D. (2008). Measuring and comparing evolvability and constraint in multivariate characters. *Journal of Evolutionary Biology* 21:1201–1219.

Hendrikse, J.L., Parsons, T.E., Hallgrímsson, B. (2007). Evolvability as the proper focus of evolutionary developmental biology. *Evolution and Development* 9:393–401.

Husak, J.F., Irschick, D.J., McCormick, S.D., Moore, I.T. (2009). Hormonal regulation of whole-animal performance: Implications for selection. *Integrative and Comparative Biology* 49:349–353.

Klingenberg, C.P. (2003). A developmental perspective on developmental instability: theory, models and mechanisms. *In*: Polak, M. (eds.) *Developmental instability: causes and consequences*. New York: Oxford University Press. p. 14–34.

Klingenberg, C.P. (2008). Morphological integration and developmental modularity. *Annual Review of Ecology, Evolution, and Systematics* 39:115–132.

Klingenberg, C.P. (2009). Morphometric integration and modularity in configurations of landmarks: tools for evaluating a priori hypotheses. *Evolution & Development* 11:405–421.

Klingenberg, C.P. (2013). Cranial integration and modularity: insights into evolution and development from morphometric data. *Hystrix, the Italian Journal of Mammalogy* 24:43-58.

Klingenberg, C.P. (2014). Studying morphological integration and modularity at multiple levels: concepts and analysis. *Philosophical Transactions of the Royal Society B: Biological Sciences* 369:20130249.

Klingenberg, C.P. (2015). Analyzing fluctuating asymmetry with geometric morphometrics: concepts, methods, and applications. *Symmetry* 7:843–934.

Klingenberg, C.P. (2022). Shape asymmetry — what's new?. *Emerging Topics in Life Sciences* 6:285–294.

Klingenberg, C.P., Monteiro, L.R. (2005). Distances and directions in multidimensional shape spaces: implications for morphometric applications. *Systematic Biology* 54:678–688.

Konuma, J., Yamamoto, S., Sota, T. (2014). Morphological integration and pleiotropy in the adaptive body shape of the snail-feeding carabid beetle Damaster blaptoides. *Molecular Ecology* 23:5843–5854.

Leamy, L.J., Klingenberg, C.P. (2005). The genetics and evolution of fluctuating asymmetry. *Annual Review of Ecology, Evolution and Systematics* 36:1-21.

Marroig, G., Shirai, L.T., Porto, A., de Oliveira, F.B., De Conto, V. (2009). The Evolution of Modularity in the Mammalian Skull II: Evolutionary Consequences. *Evolutionary Biology* 36:136–148.

Martinez-Cerdeño, V. et al. (2017). The bat as a new model of cortical development. *Cerebral Cortex* 28:3880–3893.

Mellado, B., Carneiro, L.d.O., Nogueira, M.R., Herrera M, L.G., Cruz-Neto, A.P., Monteiro, L.R. (2024a). Developmental instability, body mass, and reproduction predict immunological response in short-tailed bats. *Current Zoology* In Press:zoae034.

Mellado, B., de Oliveira Carneiro, L., Nogueira, M.R., Monteiro, L.R. (2024b). Not all size measures are created equal: different body size proxies are not equivalent fitness predictors in the bat *Carollia perspicillata*. *Journal of Mammalian Evolution* 31:9.

Mellado, B.R., Carneiro, L.O., Nogueira, M.R., Monteiro, L.R. (2018). Diversity and seasonality of a Phyllostomid assemblage from the Atlantic Forest of southeastern Brazil. *Mastozoologia Neotropical* 25:363–377.

Melo, D., Porto, A., Cheverud, J.M., Marroig, G. (2016). Modularity: genes, development, and evolution. *Annual Review of Ecology, Evolution, and Systematics* 47:463–486.

Monteiro, L.R., Mellado, B., Nogueira, M.R., Morais-Jr, M.M. (2019). Individual asymmetry as a predictor of fitness in the bat *Carollia perspicillata*. *Journal of Evolutionary Biology* 32:1207–1229.

Monteiro, L.R., Nogueira, M.R. (2010). Adaptive radiations, ecological specialization, and the evolutionary integration of complex morphological structures. *Evolution* 64:724–744.

Olson, M.E. (2019). Spandrels and trait delimitation: No such thing as "architectural constraint". *Evolution and Development* 21:59–71.

Palmer, A.R., Strobeck, C. (2003). Fluctuating asymmetry analyses revisited. *In*: Polak, M. (eds.) *Developmental instability: causes and consequences*. Oxford University Press New York. p. 279–319.

Parolin, L.C., Bianconi, G.V., Mikich, S.B. (2016). Consistency in fruit preferences across the geographical range of the frugivorous bats Artibeus, Carollia and Sturnira (Chiroptera). *Iheringia. Série Zoologia* 106:e2016010.

Payne, J.L., Wagner, A. (2018). The causes of evolvability and their evolution. *Nature Reviews Genetics* 20:24–38.

Polak, M., Møller, A., Gangestad, S., Kroeger, D., Manning, J., Thornhill, R. (2003). Does an individual asymmetry parameter exist? A meta-analysis. *In*: Polak, M. (eds.) *Developmental instability: causes and consequences*. Oxford: Oxford University Press. p. 81–96.

Porto, A., Schmelter, R., VandeBerg, J.L., Marroig, G., Cheverud, J.M. (2016). Evolution of the genotype-to-phenotype map and the cost of pleiotropy in mammals. *Genetics* 204:1601–1612.

Rasweiler, J.J., Badwaik, N.K., Mechineni, K.V. (2010). Selectivity in the transport of spermatozoa to oviductal reservoirs in the menstruating fruit bat, *Carollia perspicillata*. *Reproduction* 140:743–757.

Reaney, A.M., Bouchenak-Khelladi, Y., Tobias, J.A., Abzhanov, A. (2020). Ecological and morphological determinants of evolutionary diversification in Darwin's finches and their relatives. *Ecology and evolution* 10:14020–14032.

Rocha, R. et al. (2017). Does sex matter? Gender-specific responses to forest fragmentation in Neotropical bats. *Biotropica* 49:881–890.

Rossoni, D.M., Costa, B.M.A., Giannini, N.P., Marroig, G. (2019). A multiple peak adaptive landscape based on feeding strategies and roosting ecology shaped the evolution of cranial covariance structure and morphological differentiation in phyllostomid bats. *Evolution* 73:961–981.

Rossoni, D.M., Patterson, B.D., Marroig, G., Cheverud, J.M., Houle, D. (2024). The Role of (Co)variation in Shaping the Response to Selection in New World Leaf-Nosed Bats. *The American Naturalist* 203:E107–E127.

Sherratt, E., Kraatz, B. (2023). Multilevel analysis of integration and disparity in the mammalian skull. *Evolution* 77:1006–1018.

Soyer, O.S., Bonhoeffer, S. (2006). Evolution of complexity in signaling pathways. *Proceedings of the National Academy of Sciences* 103:16337–16342.

Van Dongen, S. (2006). Fluctuating asymmetry and developmental instability in evolutionary biology: past, present and future. *Journal of Evolutionary Biology* 19:1727–1743.

Van Dongen, S., Lens, L., Molenberghs, G. (1999). Mixture analysis of asymmetry: modelling directional asymmetry, antisymmetry and heterogeneity in fluctuating asymmetry. *Ecology Letters* 2:387–396.

Verd, B., Monk, N.A., Jaeger, J. (2019). Modularity, criticality, and evolvability of a developmental gene regulatory network. *eLife* 8:e42832.

Vinciguerra, N.T., Burns, K.J. (2021). Species diversification and ecomorphological evolution in the radiation of tanagers (Passeriformes: Thraupidae). *Biological Journal of the Linnean Society* 133:920–930.

Wagner, G.P., Altenberg, L. (1996). Perspective: complex adaptations and the evolution of evolvability. *Evolution* 50:967–976.

Young, N.M., Hallgrímsson, B. (2005). Serial homology and the evolution of mammalian limb covariation structure. *Evolution* 59:2691.

Zelditch, M.L. (2022). Extending microevolutionary theory to a macroevolutionary theory of complex adaptations. *Evolution* :No prelo.

Zelditch, M.L., Goswami, A. (2021). What does modularity mean?. *Evolution and Development* 23:377–403.

Zelditch, M.L., Wood, A.R., Swiderski, D.L. (2008). Building Developmental Integration into Functional Systems: Function-Induced Integration of Mandibular Shape. *Evolutionary Biology* 36:71–87.

Capítulo 1: Breve histórico e principais metodologias usadas para o estudo da Integração e modularidade em estruturas morfológicas complexas

Resumo

A compreensão dos fenômenos de integração morfológica e modularidade é fundamental para o entendimento da evolução de estruturas morfológicas complexas, assim como para a compreensão da diversidade biológica. A relevância desses fenômenos, associada ao desenvolvimento de tecnologias computacionais, se reflete no crescente número de publicações sobre esses temas. Entretanto, há uma desconexão entre as metodologias usadas e o contexto teórico das análises realizadas nessa área. Historicamente a morfometria tradicional é usada na investigação desses fenômenos, mas nas últimas décadas o uso da morfometria geométrica tem se popularizado. Se por um lado a interpretação da variação morfológica é facilitada nos diagramas da morfometria geométrica, algumas limitações metodológicas podem comprometer o significado biológico das análises de integração e modularidade, as distanciando do contexto teórico em questão. Esta revisão busca revisar as metodologias utilizadas para no estudo de integração e modularidade, a luz da teoria de medição. A análise de associações entre unidades morfogenéticas, definidas como condensações celulares emergentes na formação de estruturas complexas, permite que o conhecimento sobre a ontogenia da estrutura sob análise oriente o estabelecimento de caracteres, assim como a formulação de hipóteses *a priori* sobre os fenômenos de integração e modularidade. Isto permite a conciliação da metodologia morfométrica com o contexto teórico da investigação. Os pesquisadores devem estar atentos ao que está sendo medido e como estas medições se relacionam com o contexto da questão, de modo a manter o significado biológico dos resultados.

Palavras-chave: Evolução morfológica; Biologia Evolutiva do Desenvolvimento; Teoria da Medição, Morfometria geométrica.

Introdução

Os padrões de associação entre os componentes de uma estrutura morfológica complexa (aquela que enquanto estrutura coesa é composta por diferentes unidades; Atchley e Hall 1991), medidos pela correlação entre esses componentes, decorrem da integração entre esses componentes e podem ser usados para descrever a hierarquia de desenvolvimento (Esteve-Altava, 2017; Zelditch e Goswami, 2021). Esses padrões emergem do compartilhamento de vias de desenvolvimento, ou limitações impostas por seleção natural, associadas à performance (Klingenberg, 2014; Melo *et al.*, 2016; Hall e Moody, 2018). A modularidade é inferida pela forte associação entre componentes pertencentes a um grupo (módulo), que apresentam reduzida ou nenhuma associação com elementos fora desses grupos (Klingenberg, 2009). Mesmo as respostas evolutivas decorrentes de seleção não são independentes dos processos de desenvolvimento, já que a seleção age sobre a variação produzida durante o desenvolvimento (Hendrikse *et al.*, 2007; Olson, 2019). De forma que a associação entre genótipo e fenótipo mediado pelo desenvolvimento pode ser compreendida pela predisposição nas direções de variação fenotípica (Klingenberg e Monteiro, 2005; Hendrikse *et al.*, 2007). A tradução do genótipo em fenótipo sob efeito de demandas funcionais pode ser observada no esquema conceitual proposto por Wagner e Altenberg (1996) para a tradução do mapa genotípico em fenótipo através do desenvolvimento (Porto *et al.*, 2016).

A variedade de interpretações sobre integração e modularidade é refletida na variedade de metodologias disponíveis para o estudo desses fenômenos biológicos (Klingenberg, 2013; Zelditch e Goswami, 2021). Essas divergências conceituais/metodológicas, podem gerar problemas de comunicação, uma vez que as diferenças de interpretação sobre os conceitos se refletem na interpretação dos resultados das análises e, por consequência, dos fenômenos biológicos em questão (Melo *et al.*, 2016; Machado *et al.*, 2019; Zelditch e Goswami, 2021). Isso se torna especialmente problemático porque os fenômenos de integração e modularidade são objeto de estudo em diferentes campos das Ciências Biológicas (Esteve-Altava, 2017).

Dados de uma revisão sistemática que avaliou trabalhos publicados entre 1958 e 2015, que investigavam os fenômenos de integração e modularidade com foco em morfologia, indicam um outro problema. 23% desses trabalhos não

apresentaram hipóteses acerca da modularidade e/ou integração a ser testada apenas analisando os padrões de variação morfológica de forma exploratória (Esteve-Altava, 2017). Esse problema não é uma tendência recente na área, visto que já era apontada por Cheverud *et al.*(1989).

O objetivo deste trabalho é revisar as principais metodologias utilizadas para o estudo da integração e modularidade, discutindo a relevância de conceituar e definir caráter sob o prisma da teoria da medição, no contexto das análises de integração e modularidade em estruturas morfológicas complexas, respeitando a natureza multivariada da forma. Essa teoria preconiza que as relações entre medições feitas na investigação de uma questão representem a relação entre os atributos reais do sistema de estudo, de forma que uma medição deve sempre considerar a hipótese sob teste (Krebs, 1987; Houle *et al.,* 2011).

Metodologias aplicadas ao estudo de integração e modularidade

Diferentes metodologias são aplicadas ao estudo dos fenômenos de integração e modularidade em estruturas morfológicas complexas. Análises descritivas qualitativas—*e.g.*, (Gutiérrez-Ibáñez *et al.*, 2014; López-Guerrero *et al.*, 2014), Análises de loci de caracteres quantitativos—*e.g.*, (Konuma *et al.*, 2014; Atkinson *et al.*, 2015), análises de rede—*e.g.*, Schwarz *et al.*, 2008; Ferrarini *et al.*, 2009), entre outras têm sido usadas com esse objetivo, porém constituem uma porção relativamente pequena da produção de conhecimento nesta área (Esteve-Altava, 2017). As metodologias mais comumente aplicadas são baseadas em correlações ou covariâncias obtidas a partir de distâncias lineares (também conhecida como morfometria tradicional) ou coordenadas de marcos anatômicos (morfometria geométrica). Juntas, essas metodologias são usadas em mais de dois terços dos trabalhos publicados (Esteve-Altava, 2017).

Correlação entre variáveis tradicionais

A morfometria tradicional é o meio historicamente usada para o estudo quantitativo da variação de tamanho e forma dos organismos. Essa escola de morfometria se baseia no uso de distâncias lineares (comprimentos, larguras);

ângulos, áreas ou razões entre essas variáveis (Marcus, 1990; Rohlf e Marcus, 1993). A necessidade prática de compreensão sobre a variabilidade de tamanho em humanos, por exemplo, há séculos motiva a busca por formas de medição (Bookstein, 1994). Já durante a segunda metade do século XIX, a chamada escola biométrica tentava entender a variação de forma dos organismos por meio das correlações entre medidas lineares nas estruturas que formavam esses organismos (Bookstein, 1991; Bookstein, 1994; Bookstein, 1996). Uma importante contribuição para o avanço da morfometria tradicional foi dada por Pearson e Davin(1924). Estes autores sugeriram que a tomada de medidas cranianas deveria ser feita ao longo de um mesmo osso, em contraste a medidas tradicionalmente utilizadas em antropologia, com distâncias e ângulos entre pontos de referência (alguns exclusivos) do crânio humano. Dessa forma, as medidas poderiam ser tomadas homologamente em diferentes grupos de mamíferos, para testar a existência de fatores comuns a grupos de caracteres, potencializando o uso das medições para análises no nível evolutivo (Cheverud, 1982). Essa incorporação conceitual permitiu que hipóteses sobre desenvolvimento e/ou funcionais fossem propostas *a priori* (Cheverud, 1995).

O uso de correlações entre distâncias para o estudo dos padrões de integração e modularidade formalmente remonta aos trabalhos de Olson e Miller(1958), que cunharam o termo integração morfológica, analisando matrizes de correlação com métodos descritivos e exploratórios. Berg(1960) adicionou hipóteses funcionais à ideia de plêiades correlacionadas (conjuntos de caracteres morfológicos altamente correlacionados entre si e com baixa correlação em relação a outros conjuntos de caracteres — *Korrelationsplejaden*, no original) de Terentjev(1931). Posteriormente, a metodologia foi conceitualmente muito influenciada pelos trabalhos de James Cheverud—*e.g.* (Cheverud, 1982; Cheverud *et al.*, 1983; Cheverud *et al.*, 1989; Cheverud, 1995). Nesse contexto, matrizes teóricas são construídas de modo que, aos pares, caracteres pertencentes a um módulo hipotético ou a uma estrutura integrada (seja devido ao desenvolvimento e/ou demandas funcionais) recebem valor um (1). Pares de caracteres pertencentes a módulos diferentes recebem valor zero (0). Vale destacar que esse exemplo representa o modelo mais simples possível – que admite correlação total entre os caracteres de um módulo e ausência completa de correlação entre as partes que compõem diferentes módulos, outros valores

poderiam ser atribuídos de modo a permitir que os modelos estivessem mais próximos de condições reais (nas quais a estrutura de correlação seria mais complexa) (Cheverud *et al.*, 1989). Padrões de integração e modularidade podem ser, por exemplo, inferidos pelos coeficientes de correlação de Pearson entre as matrizes de correlação das medições e as matrizes teóricas. Os valores de probabilidade associados podem ser testados por testes de Mantel (Cheverud *et al.*, 1989). Outras metodologias foram propostas, visando contornar questões específicas relacionadas ao contexto de determinadas hipóteses, podendo ainda incluir matrizes de covariância e/ou índices derivados dessas matrizes, além de índices de repetibilidade — *e.g*., (Cheverud, 1982; Cheverud, 1995; Marroig *et al.*, 2009; Porto *et al.*, 2009).

Uma crítica feita a estudos conduzidos com morfometria tradicional é que a forma e o tamanho são medidos em conjunto, não sendo possível uma separação estatística clara entre estas propriedades. A informação sobre a geometria do objeto sob análise seria perdida assim que o instrumento de medição é removido da estrutura (Bookstein, 1991). Adicionalmente, parte das distâncias medidas podem apresentar redundância, e a representação dos dados numericamente em forma de tabelas ou graficamente—como nos *scatter plots* de uma Análise de Componente Principais ou outras análises multivariadas torna sua interpretação complexa (Bookstein, 1991; Rohlf e Marcus, 1993; Mitteroecker e Bookstein, 2007; Zelditch *et al.*, 2012).

A busca pela separação entre forma e tamanho em estudos morfológicos foi muito influenciada pela taxonomia (Jensen, 2003). Nessa escola sistemática, predominava a ideia de que o tamanho seria sensível a plasticidade e variação dependente da idade, o que faria da forma um indicador mais confiável da variação morfológica para a identificação de diferentes táxons (Jolicoeur e Mosimann, 1960; Sundberg, 1989). Independentemente da sua utilidade para a inferência taxonômica, há um robusto corpo de evidências de que o tamanho é importante do ponto de vista funcional e evolutivo—*e.g.*, (Peres-Neto e Jackson, 2001; Marroig e Cheverud, 2005; Nogueira *et al.*, 2009; Marroig e Cheverud, 2010). No contexto das investigações de padrões de integração e modularidade não há justificativa biológica para a necessidade de separação entre forma e tamanho. Durante o desenvolvimento ontogenético, os processos de demografia celular que originam a forma e o tamanho das estruturas morfológicas são em

grande parte compartilhados (Atchley e Hall, 1991; Atchley, 1993; Hall e Miyake, 2000; Hall, 2003). Além disso, efeitos funcionais que incidem sobre a estrutura de covariação dos componentes morfogenéticos podem ser dependentes de demandas biomecânicas relacionadas ao tamanho(Zelditch *et al.*, 2008).

O uso de variáveis tradicionais em estudos sobre integração e/ou modularidade apresenta a vantagem de não impor ao conjunto de dados transformações que desrespeitem o contexto teórico da investigação e preserva a variação local da estrutura morfológica (Houle *et al.*, 2011; Melo *et al.*, 2016). A perda da geometria total do objeto não representa um problema neste caso, uma vez que o objetivo das análises é entender o padrão de covariação entre os caracteres, não à variação de forma da estrutura como um todo (Cheverud, 1995; Marroig *et al.*, 2009; Baab, 2013; Melo *et al.*, 2016).

A noção de homologia entre medidas tomadas em um determinado osso é útil em contextos como o da sistemática (Jensen, 2003), mas captura apenas parcialmente a relação entre as trajetórias de desenvolvimento das unidades morfogenéticas que compõem as estruturas complexas (Atchley e Hall, 1991; Atchley, 1993; Hall, 2003). Isto pode dissociar as medições realizadas do contexto teórico do estudo de integração e modularidade, comprometendo o significado biológico dos resultados (Houle, 2001; Houle *et al.*, 2011; Melo *et al.*, 2016).

Morfometria geométrica e a covariância de marcos anatômicos

A morfometria geométrica (MG) se baseia em coordenadas cartesianas extraídas a partir da posição de marcos anatômicos (Bookstein, 1991). A MG foi apresentada como uma revolução no estudo da morfologia no início da década de 1990 (Rohlf e Marcus, 1993). A incorporação da geometria para a compreensão da variação morfológica dos organismos é, no entanto, anterior. A título de exemplo,(Dürer, 1524) já propunha o uso de grades de transformação e propriedades geométricas para compreender a variação de forma em humanos, embora com interesse puramente artístico. Ao longo do século XX, diferentes pesquisadores trabalharam pelo desenvolvimento dos métodos que posteriormente formaram a MG, situada entre os campos da geometria e da estatística (Bookstein, 1994; Reyment, 2010).

Bookstein(1991) define variável de forma como aquela cuja medida da configuração de marcos anatômicos não muda quando os comprimentos entres os marcos são multiplicados por um dado valor escalar. A configuração de marcos é proposta para representar então, em um objeto matemático único complexo, a natureza multivariada da forma em questão. Por conta disso, os marcos anatômicos individualmente não apresentam informação sobre essa estrutura complexa (Bookstein, 1991; Mitteroecker e Bookstein, 2007). Embora essa definição tenha permitido que metodologias dotadas de propriedades estatísticas favoráveis ao estudo da variação da forma fossem desenvolvidas (Adams *et al.*, 2013), ela é uma definição matemática, baseada em propriedades geométricas, e desconsidera que em contextos biológicos forma e tamanho são produzidos pelo desenvolvimento e interagem com o meio em conjunto (Atchley e Hall, 1991; Atchley, 1993; Hall, 2003; Zelditch *et al.*, 2008; Marroig *et al.*, 2009; Nogueira *et al.*, 2009).

Dentre as alternativas para a obtenção de variáveis de forma a partir de marcos anatômicos por morfometria geométrica, a superposição generalizada de Procrustes (SGP) é a mais utilizada, sendo incorporada como padrão na maior parte dos softwares (Viscosi e Cardini, 2011; Cardini e Marco, 2022). A preferência pelo uso da SGP é justificada pelo elevado poder estatístico apresentado (Adams *et al.*, 2013), além da topologia de espaços de forma que mantém a forma de distribuições de dados congruente com expectativas teóricas (Monteiro *et al.*, 2000). A superposição de Procrustes utiliza um critério de quadrados mínimos, com três passos: translação, proporcionalização e rotação (Rohlf e Slice, 1990). A translação constitui a transferência das configurações para uma posição comum (ponto médio ou centro de massa) das configurações na origem do sistema de eixos. A proporcionalização modifica a escala das configurações para que elas compartilhem o mesmo tamanho de centroide (raiz quadrada da soma das distâncias quadradas de cada marco até o centro de massa da configuração (Bookstein, 1986; Bookstein, 1991). O tamanho do centroide é considerado a medida de tamanho mais apropriada para configurações de marcos na morfometria geométrica por conta de suas propriedades matemáticas (Bookstein, 1986), que garantem ausência de correlação entre forma e tamanho nas análises, caso não haja alometria (Bookstein, 1991). As configurações de marcos são rotacionadas em relação a

uma configuração referencial, no ângulo ótimo para a redução dos quadrados mínimos entre elas. O objetivo da superposição generalizada de Procrustes é minimizar as diferenças de tamanho isométrico, posição e orientação entre as configurações de marcos anatômicos (Rohlf e Slice, 1990; Monteiro e dos Reis, 1999), de modo que apenas informação sobre forma permaneça nas coordenadas dos marcos, que são utilizadas como variáveis em análises multivariadas.

Há um número de metodologias baseadas em morfometria geométrica para o estudo da integração e da modularidade em estruturas morfológicas (Zelditch *et al.*, 2012; Klingenberg, 2013; Zelditch e Goswami, 2021). Parte desses métodos foi desenvolvida com objetivo de acessar questões específicas com base em diferentes conceitos de integração e modularidade. Por conta disso, muitas vezes, os resultados e interpretações que deles derivam não são compatíveis (Zelditch *et al.*, 2012; Klingenberg, 2013; Zelditch e Goswami, 2021).

Dentre as metodologias disponíveis para a quantificação da intensidade da associação entre as partes de uma estrutura, o coeficiente RV de Escoufier (Klingenberg, 2009) é a mais frequentemente usada no contexto da morfometria geométrica (Adams, 2016; Cardini, 2019). Ele representa uma razão entre a intensidade da correlação entre os conjuntos de variáveis e a covariação dentro desses conjuntos. Esse coeficiente permite avaliar as correlações entre os marcos anatômicos a partir das matrizes de covariância entre as coordenadas desses marcos (Klingenberg, 2009). Valores baixos de RV são esperados na presença de modularidade, isso porque esses valores são indicativos de que a covariação é maior dentro dos conjuntos do que entre os conjuntos de variáveis. Alternativamente, valores altos são indicativos de integração (Klingenberg, 2009; Zelditch *et al.*, 2012).

A forma como as coordenadas dos marcos anatômicos são tratadas na análise morfométrica apresenta impacto relevante sobre os resultados (Klingenberg, 2009; Baab, 2013), podendo inclusive levar a resultados espúrios (Cardini, 2019; Cardini e Marco, 2022). Uma questão importante a ser considerada é: os módulos hipotéticos devem passar pela superposição generalizada individualmente ou em conjunto? Se argumenta na literatura que ambas as alternativas seriam válidas e a escolha depende do objetivo em questão (Zelditch *et al.*, 2012). Essa escolha implica que se todos os marcos são sobrepostos em conjunto e, posteriormente, a configuração de marcos é

seccionada para isolar os módulos teorizados, o tamanho relativo e as diferenças de posição entre os módulos são preservadas (por terem passado pela mesma transformação, todo o conjunto segue no mesmo espaço de forma). Por outro lado, se cada conjunto de marcos correspondente a um módulo passa por uma superposição generalizada de Procrustes separada, as diferenças de tamanho e posição entre os módulos são perdidas, porque cada módulo está em um espaço de forma diferente. Devido a essas diferenças é aconselhado que os autores considerem a relevância da manutenção das relações de tamanho e forma entre os módulos hipotéticos no estudo (Klingenberg, 2009; Baab, 2013). Adicionalmente, os autores devem estar conscientes de que a manutenção da forma e do tamanho relativo pode obscurecer o sinal da modularidade, criando um viés para a observação de integração devido à covariação artificial introduzida entre os marcos no processo de superposição (Mitteroecker e Bookstein, 2007), como discutido abaixo. A divisão da estrutura em configurações de marcos que representem a estrutura modular hipotética pode ter o efeito inverso, criando um viés para o fortalecimento do sinal modular por realçar a covariância apenas dentro dos módulos postulados (Klingenberg, 2009; Baab, 2013).

O uso das coordenadas geométricas dos marcos anatômicos como caracteres na análise de modularidade por meio do coeficiente RV apresenta problemas metodológicos, que emergem das propriedades geométricas envolvidas (Bookstein, 1991; Mitteroecker e Bookstein, 2007; Cardini, 2019; Cardini e Marco, 2022). Correlações arbitrárias são geradas entre os marcos na superposição generalizada de Procrustes. Essa metodologia direta ou indiretamente assume ausência de correlação entre os marcos anatômicos como modelo nulo e por isso irão necessariamente incorrer nesse problema (Mitteroecker e Bookstein, 2007). A esse problema se soma um ainda mais grave, a ausência de sentido biológico da posição individual dos marcos no espaço de formas gerado após a superposição (Bookstein, 1991; Mitteroecker e Bookstein, 2007; Cardini, 2019; Cardini e Marco, 2022).

Os trabalhos formadores da morfometria geométrica, em sua maioria publicados entre os anos de 1980 e 1990 (Reyment, 2010; Adams *et al.*, 2013; Cardini e Marco, 2022), já discutiam as limitações e fontes de erros dos métodos de superposição, como a superposição de Procrustes. Uma parte dos erros na investigação da integração e da modularidade com o uso da morfometria

geométrica na literatura recente possivelmente provém do "esquecimento" da premissa de que os modelos de superposição não são baseados em modelos biológicos (Cardini, 2020; Cardini e Marco, 2022).

A comparação direta entre os valores ou mesmo a magnitude da integração observada com o uso de morfometria tradicional e a geométrica não é possível, porque não se observa validade externa entre os valores obtidos por essas análises, apenas nas tendências (Machado *et al.*, 2019). No entanto, é possível que algumas divergências entre os padrões obtidos em estudos investigando integração e modularidade nos mesmos sistemas biológicos decorram, ao menos em parte, do obscurecimento dos padrões reais por conta da não observação da influência da escolha da superposição generalizada de Procrustes(Garcia, 2016). Por exemplo, Martínez-Abadías *et al.*(2011) observaram forte integração na morfologia craniana em humanos. Esses autores realizaram a sobreposição generalizada de Procrustes na configuração inteira e posteriormente separarem os módulos postulados (procedimento que tende a fortalecer o padrão de integração). Seus resultados contrastam com o observado por de Oliveira *et al.* (2009) e Porto *et al.*(2009), cujos resultados, baseados em morfometria tradicional, indicam que dentre os mamíferos, os humanos estão entre as linhagens com os mais fortes padrões de modularidade morfológica. As dificuldades metodológicas evidenciam a necessidade de uma discussão sobre o que deveria ser considerado a unidade (caráter) no contexto teórico dos estudos de integração/modularidade e o que está sendo medido nos organismos.

Contexto teórico das medições

Os modelos usados em ciência têm como objetivo auxiliar na compreensão dos fenômenos e processos do mundo natural. Esses modelos são simplificações e como tal apresentam limitações (Godfrey-Smith, 2006), seja por conta da necessidade de atender premissas conceituais ou derivadas de propriedades matemáticas. É necessário que os investigadores se mantenham atentos a essas limitações e se preocupem com a garantia da conexão entre o contexto teórico das medições e a realidade das questões empíricas sob investigação (Godfrey-Smith, 2006; Houle *et al.*, 2011).

A morfometria é, ao menos *a priori*, um ramo das análises matemáticas de forma, não da biologia. Por este motivo, a extração das informações dos conjuntos de dados é baseada não em princípios filosóficos ou biológicos, mas em operações matemáticas (Reyment, 2010; Zelditch *et al.*, 2012). Logo, é importante que não sejam negligenciadas questões como: o que está sendo medido? Como? Por que essas medições são feitas? As mudanças de escala embutidas nas superposições envolvem perda de significado biológico? (Houle *et al.*, 2011; Zelditch *et al.*, 2012).

A desconexão entre modelos matemáticos usados e as questões empíricas para a representação das quais eles foram propostos, não é uma exclusividade da investigação dos fenômenos de integração e modularidade. A teoria da medição é, segundo Houle *et al.*(2011), ignorada por muitos na biologia. Algumas transformações são permitidas nos dados originais, mas não devem causar mudança na ordenação (relações empíricas) das observações. Isso garante, por exemplo, que um resultado estatisticamente significativo (baseado em um determinado valor de probabilidade) não seja confundido com um resultado biologicamente relevante (Houle *et al.*, 2011). A atenção ao contexto teórico pode evitar que transformações nos dados sejam feitas puramente para atender às escolhas estatísticas do método escolhido, independentemente do efeito dessas transformações para a interpretação das relações sob avaliação (Hansen e Houle, 2008; Houle *et al.*, 2011).

Ao contrário dos aspectos metodológicos, que são alvo de ampla discussão nos estudos de integração e modularidade—*e.g.*, (Baab, 2013; Adams, 2016; Cardini, 2019; Machado *et al.*, 2019; Zelditch e Goswami, 2021; Cardini e Marco, 2022), questões conceituais teóricas não recebem a mesma atenção. A definição dos caracteres usados nas análises, por exemplo, carece de discussão, dado que o objetivo dessas análises é investigar o padrão de associação entre as partes que compõem as estruturas (Esteve-Altava, 2017; Zelditch e Goswami, 2021) e que essas estruturas podem ser decompostas de diferentes formas (Roth, 2001). Por uma perspectiva evolutiva, Houle(2001) defende que um caractere deve ser delimitado com base nas relações bioquímicas, de desenvolvimento, na fisiologia e na função apresentadas pelo sistema. Essas relações são dependentes de um número grande de genes, fatores epigenéticos, interação com o meio e propriedades emergentes (Houle, 2001; Hall, 2003). Logo, basear a delimitação

dos caracteres nessas relações implicaria dimensionalidade proibitivamente alta no conjunto de caracteres de qualquer análise evolutiva (Houle, 2001). A delimitação dos caracteres evolutivos deve portanto ser baseada nas vias de desenvolvimento, que conectam o genótipo ao fenótipo (Houle, 2001; Melo *et al.*, 2016). Esta constatação nos leva a uma proposta de delimitação de caracteres cuja discussão foi relativamente negligenciada nas discussões sobre integração e modularidade: as condensações celulares como unidades físicas onde concentrar os esforços de medição.

Condensações celulares como unidades morfogenéticas em estudos de integração

Estrutura morfológicas complexas podem compartilhar origem embriológica e estar sob a influência dos mesmos processos seletivos. Os componentes morfogenéticos derivados das condensações celulares, que formam regiões específicas do crânio e da mandíbula em vertebrados, são exemplos de unidades, segundo essa definição (Atchley e Hall, 1991). Os processos da demografia celular (divisão, migração, morte) e mecanismos epigenéticos derivados de interações célula a célula durante o desenvolvimento embriológico são, portanto, importantes para a compreensão da associação entre esses componentes que formam a estrutura complexa final (Hall e Miyake, 2000; Hall, 2003). A compreensão da estrutura de variação entre componentes morfogenéticos permite inferências sobre a hierarquia dos processos emergentes do desenvolvimento, por ser derivada das vias que ligam o genótipo ao fenótipo (Hall, 2003).

A mandíbula de mamíferos é considerada um paradigma para o estudo do desenvolvimento e é também um bom exemplo de estrutura morfológica complexa (Hall, 2003). Ela pode ser decomposta nas seguintes partes: ramo, o osso alveolar (associado aos dentes), e três processos ósseos. Cada uma dessas partes representa uma unidade morfogenética derivada de uma condensação mesenquimal específica (Figura 1) (Atchley e Hall, 1991; Hall e Miyake, 2000; Hall, 2003).

A análise dos padrões de covariação entre as regiões da mandíbula de espécies de roedores (com base em distâncias lineares e áreas, determinadas

segundo as diferentes unidades morfogenéticas que a compõem), associada a um modelo quantitativo de desenvolvimento controlando diferenças de tamanho e variabilidade genética, mostraram que a variação da forma e do tamanho nessa estrutura complexa deriva da variabilidade das unidades morfogenéticas (Atchley, 1993). Isso indica que a evolução de estruturas complexas reflete os processos de desenvolvimento subjacentes. Dado que o desenvolvimento é o responsável por traduzir o mapa genotípico em fenótipo, as vias que o organizam são uma alternativa para a delimitação de caracteres evolutivos sensu (Houle, 2001).
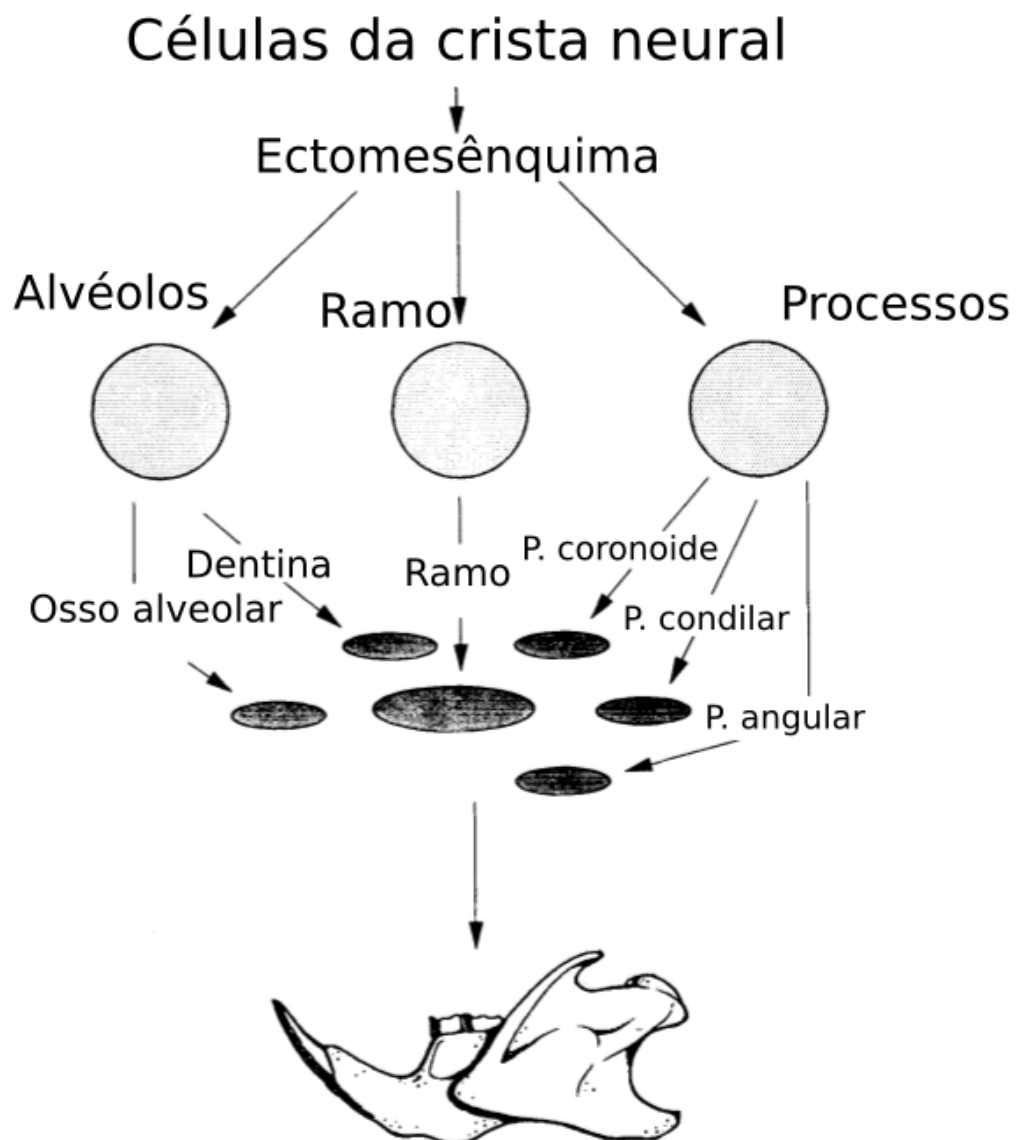
Figura 1: Representação esquemática do desenvolvimento embriológico da mandíbula em roedores. Os círculos representam as condensações mesenquimais que se diferenciam nos componentes morfogenéticos. A associação entre esses componentes origina a mandíbula enquanto estrutura complexa. (figura adaptada de Atchley et al. (1992).

Associações entre unidades morfogenéticas e o estudo da integração

Monteiro *et al.*(2005) propuseram uma combinação de metodologias para a investigação dos processos de integração e modularidade baseado nas matrizes de distâncias de Procrustes (distância de corda dentro do espaço de forma criado após a superposição (Monteiro e dos Reis, 1999). Essas matrizes são calculadas entre as observações, para as unidades morfológicas que componham a estrutura sob análise. Essa é uma abordagem similar à implementada por Atchley (1993), que usou a área dos componentes morfogenéticos para analisar seus padrões de covariação, com base no modelo de desenvolvimento da mandíbula proposto por Atchley e Hall (1991).

A escolha dos conjuntos de marcos anatômicos que sofreram a superposição é necessariamente baseada em informações disponíveis sobre a biologia do desenvolvimento acerca da estrutura morfológica em questão. Deste modo, cada conjunto de marcos corresponde a uma unidade morfogenética e cada caráter em questão é a forma multivariada descrita pelo conjunto, não a coordenada cartesiana de um marco. O delineamento experimental deve partir de dois passos fundamentais: a delimitação das unidades morfogenéticas que serão usadas como caracteres no estudo e a proposição das hipóteses de integração e modularidade a serem testadas (Monteiro *et al.*, 2005; Monteiro e Nogueira, 2010). Uma superposição generalizada de Procrustes é então realizada individualmente para cada unidade morfogenética. Essa divisão permite que a forma do componente, enquanto unidade de desenvolvimento, seja tratada como um objeto matemático único (a ser usado como caractere). Dessa forma, o método respeita o caráter multivariado da forma dos componentes, mantendo a conexão das medições com o contexto teórico e com sentido biológico das interpretações sobre integração (Monteiro *et al.*, 2005). É importante ressaltar que as unidades morfogenéticas não representam necessariamente os módulos nessa análise (Monteiro *et al.*, 2005; Monteiro e Nogueira, 2010), como interpretado por alguns autores — *e.g.* (Márquez *et al.*, 2012; Zelditch *et al.*, 2012; Zelditch e Goswami, 2021). As condensações representam as unidades fundamentais do

desenvolvimento. Qualquer propriedade desta condensação, sejam distâncias entre pontos extremos, área ou forma, será uma medição dos processos demográficos celulares mediando as interações entre genótipo e fenótipo. Por conta disso, correlações artificiais ou a ausência de sentido biológico nas posições relativas entre os marcos anatômicos (Bookstein, 1991; Mitteroecker e Bookstein, 2007) no contorno das unidades morfogenéticas não reflete problema sobre o teste das hipóteses de integração e modularidade, já que a estrutura de correlação dentro da unidade morfogenética não tem relevância biológica (Monteiro *et al.*, 2005).

Distâncias de Procrustes entre as formas dos componentes morfogenéticos em diferentes indivíduos (ou médias de populações ou espécies), são salvas em matrizes quadradas simétricas nas quais os elementos fora da diagonal correspondem à distância entre pares de observações para o dado componente morfogenético. A intensidade da associação (integração) é medida pelo valor das correlações entre distâncias de forma obtidas a partir de diferentes componentes morfogenéticos (figura 2) (Monteiro *et al.*, 2005).
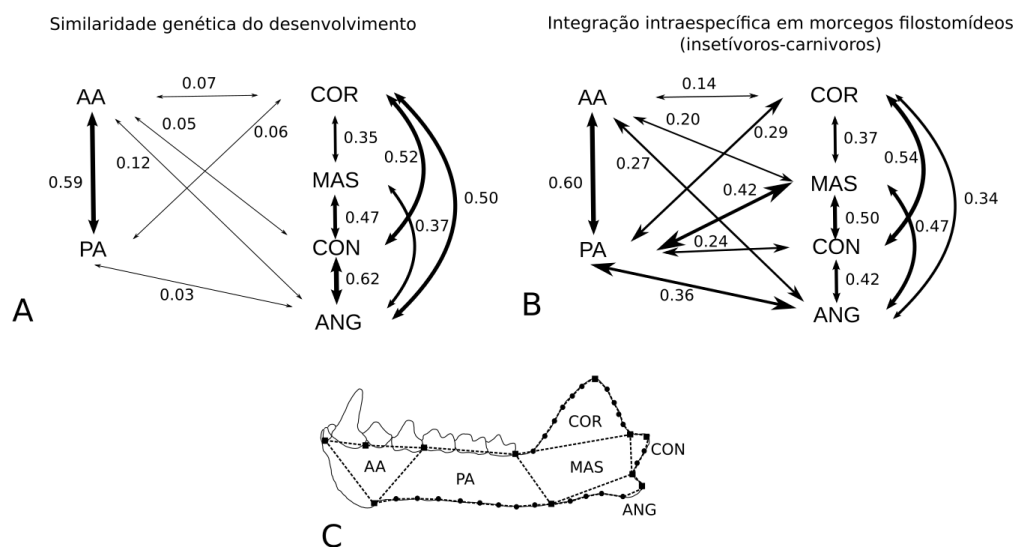
Figura 2: Integração entre unidades morfogenéticas na mandíbula de morcegos filostomídeos. (A) Modelo teórico da integração do desenvolvimento baseado na proporção de genes de desenvolvimento com efeitos pleiotrópicos. (B) Padrões observados de integração em morcegos animalívoros (insetívoros e carnívoros). (C) Mandíbula de um morcego filostomídeo mostrando a delimitação componentes morfogenéticos que compõe essa estrutura (AA, região anterior alveolar; PA, região posterior alveolar; MAS, masseter; COR, processo coronoide; CON, processo condilar; ANG, processo angular). Figura adaptada de Monteiro e Nogueira (2010).

As matrizes de correlação entre as unidades de desenvolvimento são usadas para a construção das matrizes de integração. Outras métricas de integração, como o índice de Cheverud *et al.* (1983) podem adicionalmente ser utilizadas—desde que o índice em questão use a estrutura de correlação, por conta da arbitrariedade da escala nas distâncias de Procrustes (Monteiro *et al.*, 2005).

Para o teste dos módulos postulados, as matrizes de correlação entre componentes morfogenéticos devem ser associadas a matrizes teóricas que representem as hipóteses de modularidade, sejam elas de desenvolvimento e/ou funcionais. Componentes morfogenéticos dentro de um mesmo módulo hipotético devem apresentar maior associação entre si do que com aqueles de outros módulos (Bookstein *et al.*, 2003; Monteiro *et al.*, 2005; Houle *et al.*, 2011).

Ao incorporar as trajetórias de desenvolvimento embrionário como parâmetro para a subdivisão da estrutura morfológica complexa em caracteres que podem ser usados para testar hipóteses de integração e modularidade, o método introduzido por (Monteiro *et al.*, 2005) utiliza estratégias de mensuração adequadas ao contexto teórico da investigação dos processos de integração e modularidade em estruturas morfológicas complexas, como preconizado pela teoria da medição (Houle, 2001; Monteiro *et al.*, 2005; Monteiro e Nogueira, 2010; Houle *et al.*, 2011). O método não se limita a análises geométricas de forma em coordenadas de marcos anatômicos. É possível, como em Atchley (1993), medir propriedades relativas ao tamanho das unidades morfogenéticas, como a área, ou mesmo incorporar o tamanho dos componentes às coordenadas superpostas para a obtenção de distâncias entre observações que incorporam forma e tamanho (Bookstein, 2021), de acordo com questões biológicas específicas, tendo em vista que, em análises ontogenéticas ou funcionais não é possível ignorar a variação de escala (Santana *et al.*, 2010; Cardini e Polly, 2013).

Considerações finais

O estudo dos fenômenos de integração e modularidade em estruturas morfológicas complexas é importante para a compreensão da evolução da complexidade biológica. Isso porque a quase-independência entre os módulos

permite que partes de uma estrutura possam ser modificadas durante processos evolutivos sem que a estrutura completa seja alterada. Esses fenômenos têm recebido crescente atenção e diferentes metodologias têm sido propostas para sua investigação. É primordial que essas investigações, independentemente da metodologia adotada, sejam realizadas mantendo a conexão com o contexto teórico da análise e que não sejam desconsideradas as limitações apresentadas pelas metodologias empregadas.

Referências Bibliográficas

Adams, D.C. (2016). Evaluating modularity in morphometric data: challenges with the RV coefficient and a new test measure. *Methods in Ecology and Evolution* 7:565–572.

Adams, D.C., Rohlf, F.J., Slice, D.E. (2013). A field comes of age: geometric morphometrics in the 21st century. *Hystrix, the Italian Journal of Mammalogy* 24:7–14.

Atchley, W.R. (1993). Genetic and developmental aspects of variability in the mammalian mandible. *In*: Hanken, J.; Hall, B.K. (eds.) *The skull*. Chicago: University of Chicago Press, Chicago. p. 207–247.

Atchley, W.R., Cowley, D.E., Vogl, C., McLellan, T. (1992). Evolutionary Divergence, Shape Change, and Genetic Correlation Structure in the Rodent Mandible. *Systematic Biology* 41:196–221.

Atchley, W.R., Hall, B.K. (1991). A model for development and evolution of complex morphological structures. *Biological Reviews* 66:101–157.

Atkinson, E.G., Rogers, J., Mahaney, M.C., Cox, L.A., Cheverud, J.M. (2015). Cortical folding of the primate brain: an interdisciplinary examination of the genetic architecture, modularity, and evolvability of a significant neurological trait in pedigreed baboons (Genus Papio). *Genetics* 200:651–665.

Baab, K.L. (2013). The impact of superimposition choice in geometric morphometric approaches to morphological integration. *Journal of Human Evolution* 65:689–692.

Berg, R.L. (1960). The ecological significance of correlation pleiades. *Evolution* 14:171–180.

Bonner, J.T. (1988). *The evolution of complexity by means of natural selection*. Princeton, New Jersey: Princeton University Press. 272 p.

Bookstein, F.L. (1986). Size and shape spaces for landmark data in two dimensions. *Statistical Science* 1:181–242.

Bookstein, F.L. (1991). *Morphometric tools for landmark data: geometry and biology*. Cambridge, UK: Cambridge University Press. 435 p.

Bookstein, F.L. (1994). The Morphometric Synthesis: A Brief Intellectual History. *In*: Levin, S.A. (eds.) *Frontiers in Mathematical Biology*. Berlin: Springer-Verlag. p. 212–237.

Bookstein, F.L. (1996). Biometrics, biomathematics and the morphometric synthesis. *Bulletin of Mathematical Biology* 58:313–365.

Bookstein, F.L. (2021). Centric allometry: Studying growth using landmark data. *Evolutionary Biology* 48:129–159.

Bookstein, F.L., Gunz, P., Mitteroecker, P., Prossinger, H., Schaefer, K., Seidler, H. (2003). Cranial integration in Homo: singular warps analysis of the midsagittal plane in ontogeny and evolution. *Journal of human evolution* 44:167–187.

Brown, R.L. (2014). What evolvability really is. *The British Journal for the Philosophy of Science* 65:1–24.

Callebaut, W. (2005). The ubiquity of modularity. *In*: Rasskin-Gutman, W.C. (eds.) *Modularity understanding the development and evolutionof natural complex systems*. Cambridge, MA: MIT Press Cambridge, MA. p. 3–28.

Cardini, A. (2019). Integration and modularity in Procrustes shape data: is there a risk of spurious results?. *Evolutionary Biology* 46:90–105.

Cardini, A. (2020). Less tautology, more biology? A comment on "high-density" morphometrics. *Zoomorphology* 139:513–529.

Cardini, A., Marco, V.A. (2022). Procrustes shape cannot be analyzed, interpreted or visualized one landmark at a time. *Evolutionary Biology* :No Prelo.

Cardini, A., Polly, P.D. (2013). Larger mammals have longer faces because of size-related constraints on skull form. *Nature communications* 4:1–7.

Cheverud, J.M. (1982). Phenotypic, genetic, and environmental morphological integration in the cranium. *Evolution* 36:499.

Cheverud, J.M. (1995). Morphological integration in the saddle-back tamarin (Saguinus fuscicollis) cranium. *The American Naturalist* 145:63–89.

Cheverud, J.M., Rutledge, J.J., Atchley, W.R. (1983). Quantitative genetics of development: genetic correlations among age-specific trait values and the evolution of ontogeny. *Evolution* 37:895–905.

Cheverud, J.M., Wagner, G.P., Dow, M.M. (1989). Methods for the comparative analysis of variation patterns. *Systematic Zoology* 38:201.

Deline, B., Greenwood, J.M., Clark, J.W., Puttick, M.N., Peterson, K.J., Donoghue, P.C.J. (2018). Evolution of metazoan morphological disparity. *Proceedings of the National Academy of Sciences* 115:E8909-E8918.

Dürer, A. (1524). *Vier Bücher von menschlicher Proportion*. Nuremberg: Hieronymus Andreae. 264 p.

Esteve-Altava, B. (2017). In search of morphological modules: a systematic review. *Biological Reviews* 92:1332–1347.

Ferrarini, L. et al. (2009). Hierarchical functional modularity in the resting-state human brain. *Human Brain Mapping* 30:2220–2231.

Garcia, G. (2016). *Perspectivas sobre o reconhecimento de padrões de modularidade e suas implicações para a evolução de morfologias*

complexas. Tese de Doutorado (Instituto de Biociências da Universidade de São Paulo), , 160 p. .

Godfrey-Smith, P. (2006). The strategy of model-based science. *Biology & Philosophy* 21:725–740.

Gutiérrez-Ibáñez, C. et al. (2014). Mosaic and concerted evolution in the visual system of birds. *PLoS ONE* 9:e90102.

Hall, B.K. (2003). Unlocking the black box between genotype and phenotype: cell condensations as morphogenetic (modular) units. *Biology and Philosophy* 18:219–247.

Hall, B.K., Miyake, T. (2000). All for one and one for all: condensations and the initiation of skeletal development. *BioEssays* 22:138–147.

Hansen, T.F., Houle, D. (2008). Measuring and comparing evolvability and constraint in multivariate characters. *Journal of Evolutionary Biology* 21:1201–1219.

Hendrikse, J.L., Parsons, T.E., Hallgrimsson, B. (2007). Evolvability as the proper focus of evolutionary developmental biology. *Evolution & development* 9:393–401.

Houle, D. (2001). Characters as the units of evolutionary change. *In*: Wagner, G.P. (eds.) *The Character Concept in Evolutionary Biology*. San Diego, Califórnia: Academic Press. p. 109–140.

Houle, D., Pélabon, C., Wagner, G., Hansen, T. (2011). Measurement and meaning in biology. *The Quarterly Review of Biology* 86:3–34.

Jensen, R.J. (2003). The conundrum of morphometrics. *Taxon* 52:663.

Jolicoeur Pierre, Mosimann, J.E. (1960). Size and shape variation in the painted turtle. A principal component analysis. *Growth* 24:339–354.

Krebs, D.E. (1987). Measurement theory. *Physical Therapy*, 67:1834-1839.

Klingenberg, C.P. (2005). Developmental constraints, modules, and evolvability. *In*: Hallgrímsson, B.; Hall, B.K. (eds.) *Variation*. Amsterdam, Netherlands: Elsevier. p. 219–247.

Klingenberg, C.P. (2009). Morphometric integration and modularity in configurations of landmarks: tools for evaluating a priori hypotheses. *Evolution & Development* 11:405–421.

Klingenberg, C.P. (2013). Cranial integration and modularity: insights into evolution and development from morphometric data. *Hystrix, the Italian Journal of Mammalogy* 24:43-58.

Klingenberg, C.P. (2014). Studying morphological integration and modularity at multiple levels: concepts and analysis. *Philosophical Transactions of the Royal Society B: Biological Sciences* 369:20130249.

Konuma, J., Yamamoto, S., Sota, T. (2014). Morphological integration and pleiotropy in the adaptive body shape of the snail-feeding carabid beetle Damaster blaptoides. *Molecular Ecology* 23:5843–5854.

López-Guerrero, P., Álvarez-Sierra, M., Garca-Paredes, I., Peláez-Campomanes, P. (2014). New Cricetodontini from the middle Miocene of Europe: an example of mosaic evolution. *Bulletin of Geosciences* 89:573–592.

Machado, F.A., Hubbe, A., Melo, D., Porto, A., Marroig, G. (2019). Measuring the magnitude of morphological integration: The effect of differences in morphometric representations and the inclusion of size. *Evolution* 73:2518–2528.

Marcus, L. (1990). Traditional morphometrics. *In*: Rohlf, F.J.; Bookstein, F.L. (eds.) *Proceedings of the Michigan Morphometrics Workshop, Special Publication no. 2*. Ann Arbor, MI: The University of Michigan Museum of Zoology. p. 77–122.

Márquez, E.J., Cabeen, R., Woods, R.P., Houle, D. (2012). The measurement of local variation in shape. *Evolutionary biology* 39:419–439.

Marroig, G., Cheverud, J. (2010). Size as a line of least resistance II: direct selection on size or correlated response due to constraints?. *Evolution* 64:1470–1488.

Marroig, G., Cheverud, J.M. (2005). Size as a line of least evolutionary resistance: diet and adaptive morphological radiation in new world monkeys. *Evolution* 59:1128–1142.

Marroig, G., Shirai, L.T., Porto, A., de Oliveira, F.B., Conto, V.D. (2009). The Evolution of Modularity in the Mammalian Skull II: Evolutionary Consequences. *Evolutionary Biology* 36:136–148.

Martínez-Abadías, N. et al. (2011). Pervasive genetic integration directs the evolution of human skullshape. *Evolution* 66:1010–1023.

Melo, D., Porto, A., Cheverud, J.M., Marroig, G. (2016). Modularity: genes, development, and evolution. *Annual Review of Ecology, Evolution, and Systematics* 47:463–486.

Mitteroecker, P., Bookstein, F. (2007). The conceptual and statistical relationship between modularity and morphological integration. *Systematic Biology* 56:818–836.

Monteiro, L.R., Bonato, V., dos Reis, S.F. (2005). Evolutionary integration and morphological diversification in complex morphological structures: mandible shape divergence in spiny rats (Rodentia, Echimyidae). *Evolution & Development* 7:429–439.

Monteiro, L.R., Bordin, B., Reis, S.F. (2000). Shape distances, shape spaces and the comparison of morphometric methods. *Trends in Ecology and Evolution* 15:217–220.

Monteiro, L.R., Nogueira, M.R. (2010). Adaptive radiations, ecological specialization, and the evolutionary integration of complex morphological structures. *Evolution: International Journal of Organic Evolution* 64:724–744.

Monteiro, L.R., dos Reis, S.F. (1999). *Princípios de morfometria geométrica*. Ribeirão Preto: Holos. 198 p.

Nogueira, M.R., Peracchi, A.L., Monteiro, L.R. (2009). Morphological correlates of bite force and diet in the skull and mandible of phyllostomid bats. *Functional Ecology* 23:715–723.

de Oliveira, F.B., Porto, A., Marroig, G. (2009). Covariance structure in the skull of Catarrhini: a case of pattern stasis and magnitude evolution. *Journal of Human Evolution* 56:417–430.

Olson, E.C., Miller, R.L. (1958). *Morphological integration.*. Chicago, Illinois: University of Chicago Press. 317 p.

Olson, M.E. (2019). Spandrels and trait delimitation: No such thing as "architectural constraint". *Evolution & Development* 21:59–71.

Payne, J.L., Wagner, A. (2019). The causes of evolvability and their evolution. *Nature Reviews Genetics* 20:24–38.

Pearson, K., Davin, A.G. (1924). On the biometric constants of the human skull. *Biometrika* 16:328.

Peres-Neto, P.R., Jackson, D.A. (2001). How well do multivariate data sets match? The advantages of a Procrustean superimposition approach over the Mantel test. *Oecologia* 129:169–178.

Porto, A., de Oliveira, F.B., Shirai, L.T., Conto, V.D., Marroig, G. (2009). The Evolution of Modularity in the Mammalian Skull I: Morphological Integration Patterns and Magnitudes. *Evolutionary Biology* 36:118–135.

Porto, A., Schmelter, R., VandeBerg, J.L., Marroig, G., Cheverud, J.M. (2016). Evolution of the genotype-to-phenotype map and the cost of pleiotropy in mammals. *Genetics* 204:1601–1612.

Reaney, A.M., Bouchenak-Khelladi, Y., Tobias, J.A., Abzhanov, A. (2020). Ecological and morphological determinants of evolutionary diversification in Darwin's finches and their relatives. *Ecology and evolution* 10:14020–14032.

Reyment, R.A. (2010). Morphometrics: An Historical Essay. *In*: Elewa Ashraf MT; Elewa, A.M. (eds.) *Morphometrics for Nonmorphometricians*. Berlin: Springer Berlin Heidelberg. p. 9–24.

Rohlf, F.J., Marcus, L.F. (1993). A revolution in morphometrics. *Trends in Ecology & Evolution* 8:129–132.

Rohlf, F.J., Slice, D. (1990). Extensions of the Procrustes method for the optimal superimposition of landmarks. *Systematic biology* 39:40–59.

Rossoni, D.M., Costa, B.M.A., Giannini, N.P., Marroig, G. (2019). A multiple peak adaptive landscape based on feeding strategies and roosting ecology shaped the evolution of cranial covariance structure and morphological differentiation in phyllostomid bats. *Evolution* 73:961–981.

Roth, V.L. (2001). Character replication. *In*: Wagner, G.P. (eds.) *The Character Concept in Evolutionary Biology*. San Diego, California: Academic Press. p. 81–107.

Santana, S.E., Dumont, E.R., Davis, J.L. (2010). Mechanics of bite force production and its relationship to diet in bats. *Functional Ecology* 24:776–784.

Schwarz, A.J., Gozzi, A., Bifone, A. (2008). Community structure and modularity in networks of correlated brain activity. *Magnetic Resonance Imaging* 26:914–920.

Soyer, O.S., Bonhoeffer, S. (2006). Evolution of complexity in signaling pathways. *Proceedings of the National Academy of Sciences* 103:16337–16342.

Sundberg, P. (1989). Shape and size-constrained principal components analysis. *Systematic Zoology* 38:166–168.

Terentjev, P.V. (1931). Biometrische Untersuchungen Uber Die MorphoLogischen Merkmale Von Rana Ridibunda Pall: (Amphibia, Salientia). *Biometrika* 23:23–51.

Verd, B., Monk, N.A., Jaeger, J. (2019). Modularity, criticality, and evolvability of a developmental gene regulatory network. *eLife* 8:e42832.

Vinciguerra, N.T., Burns, K.J. (2021). Species diversification and ecomorphological evolution in the radiation of tanagers (Passeriformes: Thraupidae). *Biological Journal of the Linnean Society* 133:920–930.

Viscosi, V., Cardini, A. (2011). Leaf morphology, taxonomy and geometric morphometrics: a simplified protocol for beginners. *PLoS ONE* 6:e25630.

Wagner, G.P., Altenberg, L. (1996). Perspective: complex adaptations and the evolution of evolvability. *Evolution* 50:967–976.

Zelditch, M.L. (2022). Extending microevolutionary theory to a macroevolutionary theory of complex adaptations. *Evolution* :No prelo.

Zelditch, M.L., Goswami, A. (2021). What does modularity mean?. *Evolution & Development* 23:377–403.

Zelditch, M.L., Swiderski, D.L., Sheets, H.D. (2012). *Geometric morphometrics for biologists: a primer*. San Diego, California: Academic Press. 478 p.

Zelditch, M.L., Wood, A.R., Bonett, R.M., Swiderski, D.L. (2008). Modularity of the rodent mandible: Integrating bones, muscles, and teeth. *Evolution & Development* 10:756–768.

Capítulo 2: Is developmental instability a property of the individual? Fluctuating asymmetry in developmental and functional trait sets in short-tailed bats (*Carollia perspicillata*)

Lucas Carneiro[a,b], Bruce D. Patterson[b], Marcelo R. Nogueira[a], Leandro R. Monteiro[a]

(a) Laboratório de Ciências Ambientais, Universidade Estadual do Norte Fluminense Darcy Ribeiro, Campos dos Goytacazes, Brasil; (b) Negaunee Integrative Research Center, Field Museum of Natural History, Chicago, USA.

Abstract

The inability of a genotype to buffer deviations that arise during development in order to generate the optimal phenotype is called developmental instability (DI). There is evidence showing that DI is inversely associated with regulatory performance and fitness. Developmental instability generates imprecision in development, which can be measured, in bilateral organisms, by differences between the right and left sides (fluctuating asymmetry – FA). At the population level, asymmetry can be considered a tool for environmental monitoring, as populations would present greater asymmetry in more disturbed environments. Few studies, however, have been carried out with a large number of characters to show the existence of a systemic (throughout the organism) effect of DI. The bat *Carollia perspicillata* is considered an emerging model for biological studies. There is robust evidence that forearm asymmetry is a good indicator of immunological response and fitness in the species. We measured size-corrected right-left differences in 18 traits (skull, forelimbs and hindlimbs) in museum specimens from populations across the species' range. We examined whether DI presents a systemic effect (correlated asymmetries in a large set of characters), what is the influence of trait functional importance in the level of DI, and the effects of naturally caused environmental stress in DI levels. The correlations among traits in FA were overall low, but a low dimensionality was observed (2 main axes of variation). Hierarchical mixed models were fitted to size-corrected FA responses, indicating a

fixed effect of lower FA in traits associated with flight. In the random effect component, most FA variation was concentrated at the level of individuals within traits. Dry environments seem to impose more developmental stress than rainforests to *C. perpsicillata*, but the evidence is still uncertain. The effect of DI was not homogeneously nor randomly distributed among traits. Traits associated with flight were more symmetric, traits associated with mastication were intermediate, and traits associated with perching were more asymmetrical. Differential buffering of functionally important traits might reduce the FA correlations resulting from DI systemic effects.

Keywords: fluctuating asymmetry; developmental impression; developmental stress; functional performance.

Introduction

The ontogenetic development is a process composed of successive and complementary stages, capable of altering the course of modifications and producing phenotypic variation. Different mechanisms responsible for the development of morphological structures, such as cell migration, adhesion, differentiation and proliferation, are under the control of different regulatory genes or transcription factors (Hall, 2015; Albertson, 2018) and can be altered by random disturbances (Woods, 2014). The exposure of organisms to environmental stress tends to generate phenotypic variation on a small scale, but with potentially relevant evolutionary consequences (Woods, 2014). The development period (pre- or post-natal) in which a certain disturbance happens, potentially determines the magnitude and location of the disruption, which can generate a response that might be systemic or restricted to a specific area, tissue or morphological structure (Møller, 1989; Van Dongen and Lens, 2000; Van Dongen, 2006; Klingenberg, 2022).

The inability of a genotype to buffer disruptions on during its ontogenetic development is called developmental instability (DI). Combined with developmental noise, generated by environmental stresses, DI can lead to inaccuracy in development that can be measured by variability in repeated

phenotypic structures—*e.g.* left and right sides (Gangestad and Thornhill, 1999; Leamy and Klingenberg, 2005; Klingenberg, 2022). This type of difference between sides is known as fluctuating asymmetry (FA). A kind of asymmetry produced by incidence of random variation on molecular regulators that buffer and stabilize development. These include molecular chaperones—proteins that assist the synthesis and proper folding of other proteins (Leamy *et al.*, 2015; Irvine, 2020)—as well as the Hippo pathway—a signaling chain that regulates cellular processes as proliferation, and apoptosis. These regulators may promote developmental precision through growth regulation (Juarez-Carreño *et al.*, 2018; Zheng and Pan, 2019).

Developmental instability is negatively related to important components of the fitness of organisms such as growth, survival, reproduction and maintenance of general physiological processes (Møller, 1997; Lens *et al.*, 2002a; Van Dongen, 2006; Monteiro *et al.*, 2019; Longman *et al.*, 2021; Mundahl and Hoffmann, 2023; Mellado *et al.*, 2024a). Thus, DI is considered a measure of general quality of a genotype (Voigt *et al.*, 2005; Monteiro *et al.*, 2019; Mundahl and Hoffmann, 2023). This relationship can be explained by the fact that individuals with higher DI are expected to have lower metabolic and functional efficiency, which leads to less energy availability for highly demanding activities such as growth, reproduction and parental care (Møller, 1997; Longman *et al.*, 2021).

The ability to acquire resources, escape from predators, prevent parasitism, compete are factors that determine the survival of an organism (Hendry *et al.*, 2018). Greater asymmetry may be related to worse performance of these functions. Swaddle(1997) observed, under controlled conditions, that more symmetrical flies (*Musca domestica* and *Scathophaga stercoraria*) are also those that achieve the greatest success during foraging. Analysis of the relationship between asymmetry and predation risk in species of Diptera and in the lizard *Lacerta monticola* indicate that more asymmetrical individuals are more susceptible to predation (Swaddle, 1997; López and Martin, 2002). The incidence of parasitism also tends to present a positive correlation with asymmetry (Bergstrom and Reimchen, 2005; Arundell *et al.*, 2019). Lens *et al.*(2002b) also showed that the negative association between asymmetry and survival in the bird *Turdus helleri* is enhanced by environmental disturbances.

Studies have shown a negative association between the functional relevance of trait and its level of developmental instability—measured as FA (Gummer and Brigham, 1995; Crespi and Vanderkist, 1997; Didde and Rivera, 2019), in agreement with the hypothesis that the development of functionally relevant characters is more stable (Palmer and Strobeck, 1986; Graham, 2021). Evidence from analysis of vestigial characters indicated that the relaxation of natural selection on this kind of morphological structure leads to an increase in FA (Crespi and Vanderkist, 1997; Garnier *et al.*, 2006; Tague, 2020; Barlow and Ledbetter, 2024). Emus (*Dromaius novaehollandiae*) present a high level of FA in their rudimentary forelimb—even though there is no information on other morphological complexes for comparison (Maxwell and Larsson, 2007). Comparisons between the 10 metapodial bones in coyotes (*Canis latrans*), indicate that differences between sides is larger in the Mt1 (which is nonfunctional) then the observed in the nine functional ones (Tague, 2020). Forelimbs present higher levels of AF than hindlimbs in anurans (Bufonidae and Ranidae) (Didde and Rivera, 2019), and aquatic species of emydid turtles (Emydidae) (Rivera and Neely, 2020)—in both cases the hindlimb is more relevant for locomotor performance. The bat *Myotis lucifugus* presents lower FA in the forearm than in the tibia (Gummer and Brigham, 1995). Martín and López (2001) showed that femoral asymmetry is negatively associated to the escape performance in the lizard *Psammodromus algirus*. Natural selection may favor those individuals that are more symmetric since this lizards rely on fast escape to avoid predators.

Single-trait asymmetry is a limited estimate of the individual DI for two main reasons: first, the magnitude of the measured FA is sometimes similar to the sampling error. Second, single-trait asymmetry seeks to estimate intra-individual variance with one degree of freedom (Palmer and Strobeck, 2003; Van Dongen, 2006; Graham, 2020), which reduces statistical power and generates biases in the estimation of correlations between DI and ecologically relevant attributes (Palmer and Strobeck, 2003; Van Dongen, 2006; Graham, 2020). Considering that DI is a property of the organism as a whole, it can be expected to manifest in a correlated way in different characters bilaterally arranged in the organism, due to the low capacity of genotypes to buffer the noise of development in the entire body (Klingenberg, 2003; Leamy and Klingenberg, 2005).

The correlation of asymmetric patterns in different characters of an organism can be used both for the inference of the existence of DI influencing the entire organism (organism-wide DI), versus the alternative hypothesis of independent patterns of asymmetry in different traits (Leamy and Klingenberg, 2005; Van Dongen, 2006). By indicating the existence of a systemic effect, the inference of organismic DI is critical for understanding FA as an indicator of stress environmental and fitness (Lens *et al.*, 2002a; Lens and Eggermont, 2008). Correlations between characters can be produced by direct interaction between shared developmental pathways in the components of complex morphological structures or due to parallel variation in separate pathways (Klingenberg, 2008). The use of asymmetry patterns of bilateral structures, in motile organisms, in analyses of development patterns, potentially excludes the effect of genetic and environmental variation on development. Thus, the existence of positive correlations between asymmetries of morphological characters can also be considered evidence of shared developmental stages (Klingenberg, 2008; Klingenberg, 2014).

Seba's short-tailed bat *Carollia perspicillata* is one of the most studied species of bat (Fleming, 1988) and is widely distributed throughout the Neotropics (Cloutier and Thomas, 1992). It consumes mainly fruits of pioneer shrubs (Piperaceae and Solanaceae), which it finds flying inside cluttered forest understories (Mello *et al.*, 2004). Previous studies have shown a negative association between forearm length asymmetry, survival probability, potential reproduction, and immunological response in *C. perspicillata* (Monteiro *et al.*, 2019; Mellado *et al.*, 2024a). This suggests a role for DI to influence measures of regulatory performance (Husak *et al.*, 2009), which are physiological components that maintain organismal homeostasis. On the other hand, no association of forearm asymmetry was observed with dynamic measures of performance (those associated with movement of body parts), such as bite force and flight cost (L. R. Monteiro, umpublished data). Therefore, a question is posed as to whether forearm asymmetry in *C. perspicillata* is associated with asymmetry in other traits, as predicted by the individual-level DI hypothesis.

A more detailed study of asymmetry at the level of individuals and populations of *C. perpicillata*, with a larger number of morphological characters will have the potential to elucidate important questions about the existence of

heterogeneity in DI, whether the DI effect is systemic or restricted to specific traits according to their development and function, as well as their consequences for morphological evolution and adaptation. The main objective of the chapter is to assess the patterns of development instability across trait sets in the bat *Carollia perspicillata*. To achieve this objective, we examined the correlations between fluctuating asymmetry measures of different morphological complexes (forelimbs, hindlimbs and skull), in populations of this bat species throughout its geographic distribution. We evaluated the hypotheses that functionally relevant trait sets will present lower FA, and that individuals from geographic regions with more suitable habitats will present lower FA.

Material and methods

Data collection

We examined a sample of 208 adult specimens of *Carolllia perspicillata*, available in collections from 23 localities distributed along the species' geographic range, for which both skull and mandible were in good condition, as well as the body fixed in fluid from 23 localities distributed along the species' geographic range, available in collections (see Introduction chapter). Four linear measurements were taken from images of the ventral view of the skull (Figure 1): Distance between the third upper molar and the posterior nasal spine (M3PNS); distance between coronoid and mastoid process (GlenoidFossa); distance between the mastoid processes and the posterior end of the occipital (MastoidOccipital), and the width across the tympanic bulla (Bulla). Two linear measurements were taken from photos of each side of the mandible: mandibular length (ManL) and height of mandibular body (ManB) (Figure 1).
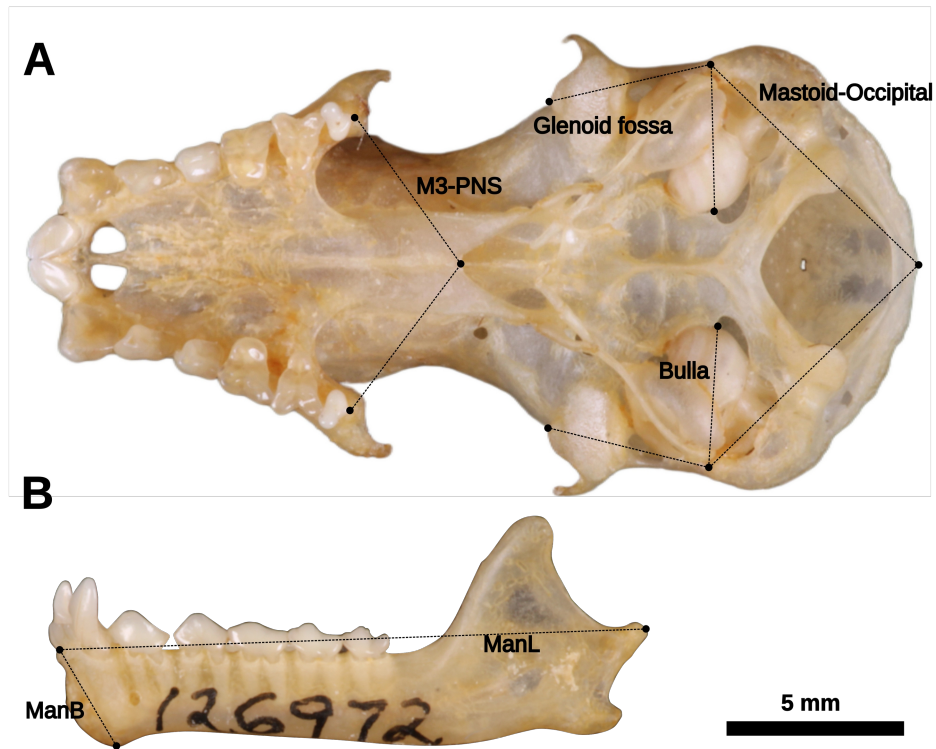
Figure 1*:* Linear measurements taken in the skull and mandible of *Carollia perspicillata.* Variable descriptions: M3-PNS: distance between the third upper molar and the posterior nasal spine, Glenoid fossa: distance across the glenoid fossa, Mastoid-Occipital: distance between the anterior point of mastoid process to the posterior point of the occipital, Bulla: breadth of tympanic bulla, ManL: mandibular length, ManB: height of mandibular body.

We also obtained measurements of forelimb and hindlimb elements from specimens preserved in fluid (Figure 2). The distal phalanges were not included in the sampling due to their low bone density (Cleland *et al.*, 2021), making it difficult to obtain precise measurements. The foot was measured as a composite unit between their proximal joint (the ankle) and their distal end (tips of the digital claws), due to the difficulty in accurately taking measurements of bony elements such as the metatarsals and phalanges of the feet. All measurements were taken on both right and left sides of each individual.
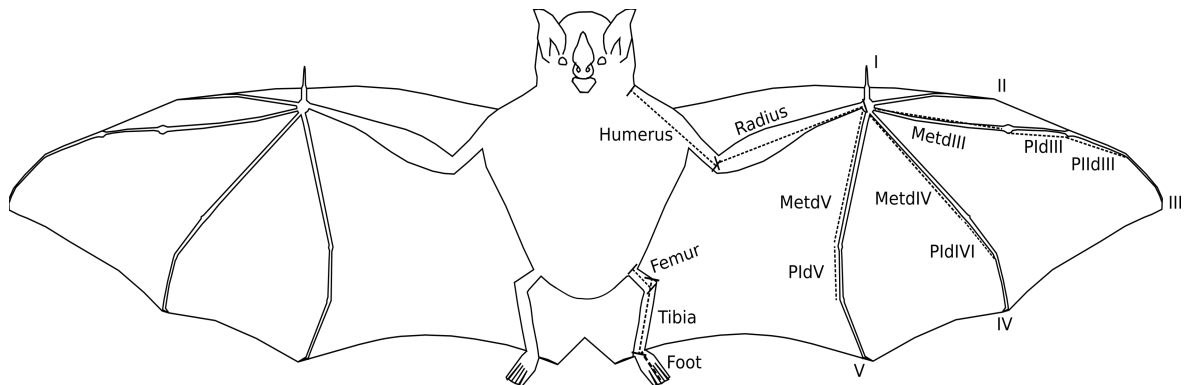
Figure 2: Linear measurements taken in the forelimbs and hindlimbs of *Carollia perspicillata*. Variable descriptions: . From the forelimbs: humerus; radius; metacarpals (Metd) of digits II, IV and V; phalanges (P) I and II of digit (d) III; phalanx I of digit IV and phalanx I of digit V. From the hindlimbs: femur, tibia and foot (see text for explanations on measurement. All variables were measured on both sides. Figure modified from Carneiro et al. (2023).

Validation of asymmetry measurements

Asymmetry is measured as absolute right-left (|R-L|) differences for each trait in the same individual. It can be used as a proxy for developmental instability (Leamy and Klingenberg, 2005; Van Dongen, 2006), but asymmetry measurements need to be validated by comparisons with measurement error (ME) and checked for other types of asymmetry. Asymmetry measures are normally small, and an assessment of the signal-to-noise ratio (FA vs ME) is an essential step of the study (Palmer and Strobeck, 2003).

Repeated measurements of each trait were obtained for the skull (n = 39) and mandible (n = 32). Triplicate measurements were obtained for the limb measurements (n = 71). Replicate measurements were used to validate the asymmetry in the linear mixed model:

$$Measurement = Side + Individual + Side : Individual + error .$$

This model has the linear measurement as predictor, side as fixed effect, and individual as random effect (Palmer and Strobeck, 2003; Montévil, 2019). The occurrence of directional asymmetry is expressed by the difference between sides, the interaction between side and individual represents the fluctuating asymmetry (FA), and its mean square can be compared to the mean square of the residual of the ANOVA, as a measure of the magnitude of FA compared to measurement error (ME) (Palmer and Strobeck, 2003). The square root of the residual mean squares in the ANOVA table is a descriptor of measurement error—ME2 of Palmer and Strobeck (2003). It can be used to calculate the expected value of mean(|R-L|)—

FA1 of Palmer and Strobeck (2003) in the absence of developmental instability as

$$FA1 = \left(0,798\sqrt{(2/n)}\right) \times ME2$$ (Palmer and Strobeck, 2003). This is an important step because the measurement error can be confused with the signal of developmental instability, measured by FA, since it also tends to be small in magnitude, independent and have a mean close to zero (Palmer and Strobeck, 2003). The repeatability of asymmetry measurements for each variable was also evaluated by intraclass correlation coefficients (R_{IC}) from a model with the individual asymmetry |R-L| as the response and the individual as the random factor (Nakagawa and Schielzeth, 2010). Confidence intervals for the intraclass correlation coefficients were estimated by bootstrap with 5000 samples. Repeatability analyses were performed using the package rptR (Stoffel *et al.*, 2017) in the R environment (R Core Team, 2024).

Fluctuating asymmetry in character sets and multivariate assessment of DI.

The measurements analyzed vary widely (*e.g.* the length of radius is 14 times longer than the mandibular body height). Therefore, we used a size-scaled index of fluctuating asymmetry (FA2 = Mean[|R-L|/(R+L)/2]) to account for scale differences among traits (Palmer and Strobeck, 2003) and make the estimates comparable. If DI is a property of the individual, strong correlations in the unsigned FA among different traits at the individual level are expected (Van Dongen, 2006). We also expect to find more FA variation among individuals than among traits or trait sets. We fitted linear hierarchical (nested) mixed models (Galecki and Burzykowski, 2013) to estimate FA differences among postulated trait sets (as fixed effects), traits within sets, and individuals within traits (both as random effects). Four models were fitted, according to the postulated trait sets as fixed effects (Figure 3). One set (developmental) divided traits by body region (head, forelimb, hindlimb). A functional set further divided traits according to their participation in specific functions, braincase, mastication (joining mandibular and maxilary traits), limb (flight), joining forelimb traits and the tibia, which is attached to the wing membrane and might perform relevant tasks in changes of wing shape (Cheney *et al.*, 2014). The two models with fixed effects had different hierarchical structures at the upper level, but had the same random effects, with variation among traits and individuals (nested in traits). Other two models were fitted only

with random effects, one with traits/individuals and one with only random differences among individuals (considered the null model). The models were fitted using package nlme (Pinheiro and Bates, 2000), and compared by Akaike information criteria corrected for small samples (Burnham and Anderson, 2002), using package AICcmodavg (Mazerolle, 2023). Model effects were visualized with package visreg (Breheny and Burchett, 2017). The variance explained by the mixed models was estimated with the coefficients of determination proposed by Nakagawa and Schielzeth (2012), which separate the variance explained into a marginal R^2 (explained by fixed factors) and a conditional R^2 (explained by all factors). These coefficients were calculated with package MuMIn (Bartoń, 2024). All analyses were performed in the R environment (R Core Team, 2024).
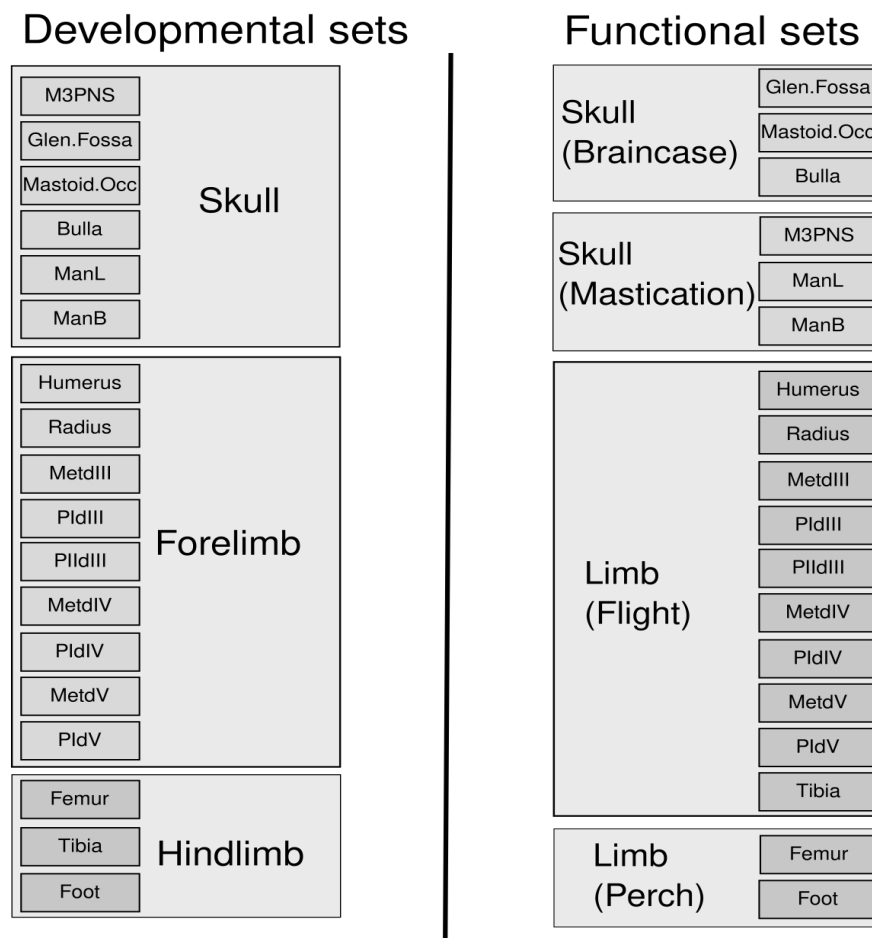
Figure 3: Hierarchical models fitted to fluctuating asymmetry variation in *Carollia perspicillata*. Grouped traits indicate nesting within functional or developmental sets.

Multivariate patterns of asymmetry were evaluated by principal components analysis (PCA) of the matrix with trait FA2. The PCA was calculated with the FactoMineR package (Lê *et al.*, 2008). The dimensionality of the correlation matrix was estimated with parallel analysis (Dinno, 2009). This method compares the eigenvalues obtained from the observed correlation matrix to eigenvalues derived from randomly generated, uncorrelated data with the same number of variables and observations. After correcting for the bias due to sampling error, PCs with eigenvalues > 1 are retained. We used 10000 random data sets to estimate the eigenvalue distributions using package paran (Dinno, 2024). Parallel analysis is considered a method of optimal performance in recovering subjacent dimensionality (Peres-Neto *et al.*, 2005). Correlations among FA estimates are expected to be downward biased in assessing DI correlations (Whitlock, 1998; Van Dongen, 2006). The parallel analysis is used to establish whether the correlation patterns indicate high dimensionality and largely uncorrelated asymmetries.

We calculated a multivariate index of asymmetry (Klingenberg and Monteiro, 2005) by computing PC scores for each observation, standardizing the scores to variance 1, summing the squared scores over all PCs for each observation and computing the square root of the sum. The multivariate FA was used to compare fluctuating asymmetries among sites located in different ecoregions, pooling localities. The regions compared involved three areas with tropical forest: AF – Atlantic Forest (n = 27), AB – Amazon Basin (n = 133), CA – Central America (n = 29), and OA – open areas in the South American dry diagonal (n = 14), mostly Cerrado and Caatinga sites). The average differences in multivariate asymmetry were compared among ecoregions by a linear mixed model, where multivariate FA was the response variable, ecoregion was the fixed factor and site was a random factor within ecorregion. We also compared multivariate FA using a fixed factor contrasting all Forest ecoregions with the Open Areas. We expect the individuals from open areas to be more asymmetric, as *C. perspicillata* is mainly a forest species (Cloutier and Thomas, 1992) and open, drier areas would be less suitable (Maestri *et al.*, 2015). Mark-recapture studies have also shown that extended droughts can reduce body mass and survival in *C. perspicillata*, (Monteiro *et al.*, 2019; Mellado *et al.*, 2024b), corroborating the unsuitability of dry areas.

Results

Validation of DI in asymmetry measurements

The mixed-effect models for all traits indicate that the signal of fluctuating asymmetry is consistently higher than measurement error throughout the whole set of measurements examined (Table 1). We observed statistical support for directional asymmetry (measured by the difference between sides) in the mastoid-occipital, bulla, radius and metacarpal of digit V.

Table 1: Mixed model analysis of variance comparing fixed effect factors (Side – directional asymmetry), random effect (Individual) and Side:individual interaction (fluctuating asymmetry) with measurement error (residuals). Trait descriptions in Figures 1 and 2.

ANOVA	df	Sum Sq	Mean Sq	F	p
M3PNS					
Side	1	0.0210	0.021015	3.552231	0.06713
Individual	38	8.1857	0.215413	52.8166	< 0.0001
Side:Individual	38	0.3568	0.009388	2.3019	0.00102
Residual	76	0.3100	0.004079		
Glenoidfossa					
Side	1	0.0223	0.022261	2.264138	0.14067
Individual	38	7.9325	0.208749	51.6487	< 0.0001
Side:Individual	38	0.3736	0.009832	2.4325	0.00050
Residual	76	0.3072	0.004042		
MastoidOccipital					
Side	1	1.2133	1.21328	20.04759	0.00007
Individual	38	18.4174	0.48467	15.2678	< 0.0001
Side:Individual	38	2.2998	0.06052	1.9065	< 0.0001
Residual	76	2.4126	0.03174		0.00860
Bulla					
Side	1	0.0307	0.030740	5.694702	0.02210

ANOVA	df	Sum Sq	Mean Sq	F	p
Individual	38	3.7995	0.099988	43.2015	< 0.0001
Side:Individual	38	0.2051	0.005398	2.3325	0.00086
Residual	76	0.1759	0.002314		
ManL					
Side	1	0.054	0.05399	0.9644516	0.33367
Individual	31	38.910	1.25516	60.0866	< 0.0001
Side:Individual	31	1.735	0.05598	2.6798	0.00043
Residual	64	1.337	0.02089	0.9644516	
ManB					
Side	1	0.0041	0.004102	0.2905922	0.59369
Individual	31	5.4547	0.175960	26.2362	< 0.00001
Side:Individual	31	0.4376	0.014116	2.1048	0.00606
Residual	64	0.4292	0.006707		
Humerus					
Side	1	0.03	0.0300	0.05523845	0.8148826
Individual	71	449.22	6.3270	210.3153	<0.00001
Side:Individual	69	37.48	0.5431	18.0545	<0.00001
Residuals	278	8.36	0.0301		
Radius					
Side	1	1.80	1.8006	14.96758	0.00024
Individual	71	864.52	12.1763	764.8271	<0.00001
Side:Individual	69	8.30	0.1203	7.6321	<0.00001
Residuals	278	4.43	0.0159		
Metacarpal III					
Side	1	0.70	0.7027	1.765578	0.18813
Individual	71	1348.20	18.9887	658.839	<0.00001
Side:Individual	69	27.46	0.3980	13.810	<0.00001
Residuals	278	8.01	0.0288		
Phalanx I - digit III					
Side	1	0.060	0.0600	1.067616	0.30494
Individual	71	274.750	3.8697	274.9597	<0.00001
Side:Individual	69	3.878	0.0562	3.9937	<0.00001

ANOVA	df	Sum Sq	Mean Sq	*F*	*p*
Residuals	278	3.912	0.0141		
Phalanx II - digit III					
Side	1	0.29	0.2918	1.58587	0.21198
Individual	71	600.26	8.4543	1080.436	<0.00001
Side:Individual	69	12.69	0.1840	23.509	<0.00001
Residuals	278	2.18	0.0078		
Metacarpal IV					
Side	1	0.73	0.7333	2.577504	0.11277
Individual	71	1176.91	16.5762	1431.948	<0.00001
Side:Individual	69	19.63	0.2845	24.577	<0.00001
Residuals	278	3.22	0.0116		
Phalanx I - digit IV					
Side	1	0.002	0.0018	0.01230349	0.91199
Individual	71	249.000	3.5070	485.5239	<0.00001
Side:Individual	69	10.094	0.1463	20.2533	<0.00001
Residuals	278	2.008	0.0072		
Metacarpal V					
Side	1	3.61	3.6103	7.952203	0.00620
Individual	71	1036.41	14.5973	933.602	<0.00001
Side:Individual	69	31.33	0.4540	29.038	<0.00001
Residuals	278	4.35	0.0156		
Phalanx I - digit V					
Side	1	0.655	0.6553	0.04913	0.82521
Individual	71	232.159	3.2698	298.522	<0.00001
Side:Individual	69	10.081	0.1461	13.338	<0.00001
Residuals	278	3.045	0.0110		
Femur					
Side	1	0.85	0.8505	1.489231	0.22632
Individual	71	694.48	9.7815	337.336	<0.00001
Side:Individual	69	39.40	0.5711	19.695	<0.00001

ANOVA	df	Sum Sq	Mean Sq	F	p
Residuals	278	8.06	0.0290		
Tibia					
Side	1	0.08	0.0818	0.280329	0.598114
Individual	71	502.05	7.0711	781.0674	<0.00001
Side:Individual	69	20.13	0.2918	32.2320	<0.00001
Residuals	278	2.52	0.0091		
Foot					
Side	1	1.860	1.8600	2.222488	0.14038
Individual	71	263.599	3.7127	134.168	<0.00001
Side:Individual	69	57.748	0.8369	30.245	<0.00001
Residuals	278	7.693	0.0277		

The intraclass correlation repeatabilities for individual asymmetries were moderate to high (Table 2), with the lowest observed for the ManB (R_{IC} = 0.309), and the highest for the Femur (R_{IC} = 0.934. Most limb trait repeatabilities were > 0.8, whereas cranial and mandible trait repeatabilities were all < 0.7. The observed FA is on average 21.55 times larger (1.95–38.47, SD=9.18) than the expected in the absence of developmental instability for limb traits. For cranial and mandibular traits, the observed FA is on average 7.88 times larger (7.11–8.47, SD=0.41) than the expected in the absence of developmental instability (Table 2). Results indicates a valid biological signal of DI in the asymmetries.

Table 2 Statistics for fluctuating asymmetry (FA) vs measurement error in *C. perspicillata*. Repeatability is the within-individual intraclass correlation coefficient. 95% confidence intervals are shown in parentheses. Expected FA is the magnitude of fluctuating asymmetry expected from measurement error (ME2 of Palmer and Strobeck, 2003), in the absence of developmental instability. Observed FA is the mean of unsigned asymmetries (FA1 of Palmer and Strobeck, 2003).

Trait	Repeatability of FA	Expected FA	Observed FA
M3-PNS	0.648 (0.42–0.799)	0,012	0,082
Glenoid fossa	0.516 (0.250–0.714)	0,011	0,088
Mastoid-Occipital	0.488 (0.206–0.698)	0,032	0,273

Trait	Repeatability of FA	Expected FA	Observed FA
Bulla	0.586 (0.337–0.761)	0,009	0,069
ManLth	0.414 (0.0886–0.659)	0,026	0,208
ManB	0.309 (0–0.592)	0,015	0,119
Humerus	0.850 (0.783–0.897)	0.023	0.466
Radius	0.706 (0.594–0.79)	0.017	0.260
Metacarpal III	0.839 (0.763–0.889)	0.022	0.423
Phalanx I - digit III	0.628 (0.498–0.729)	0.011	0.179
Phalanx II - digit III	0.930 (0.895–0.952)	0.12	0.234
Metacarpal IV	0.908 (0.863–0.938)	0.014	0.337
Phalanx I - digit IV	0.888 (0.834–0.922)	0.011	0.242
Metacarpal V	0.91 (0.867–0.938)	0.017	0.441
Phalanx I - digit V	0.863 (0.798–0.905)	0.014	0.267
Femur	0.934 (0.902–0.955)	0.023	0.511
Tibia	0.890 (0.839–0.924)	0.013	0.440
Foot	0.923 (0.0157–0.947)	0.015	0.577

Trait	Repeatability of FA	Expected FA	Observed FA

Fluctuating asymmetry in trait sets

The distribution of size-corrected asymmetries (FA2) indicates considerable variation among traits (Figure 4). Unsigned asymmetry distributions are normally asymmetric with a long tail and 95% of observations (considering all traits) are below FA2 = 0.06 (*i.e.* less than 6% of trait size). A few traits, such as the foot, femur, and mandible body height (ManB) spread over a longer interval, but even in these traits, FA2 is mostly < 0.1.
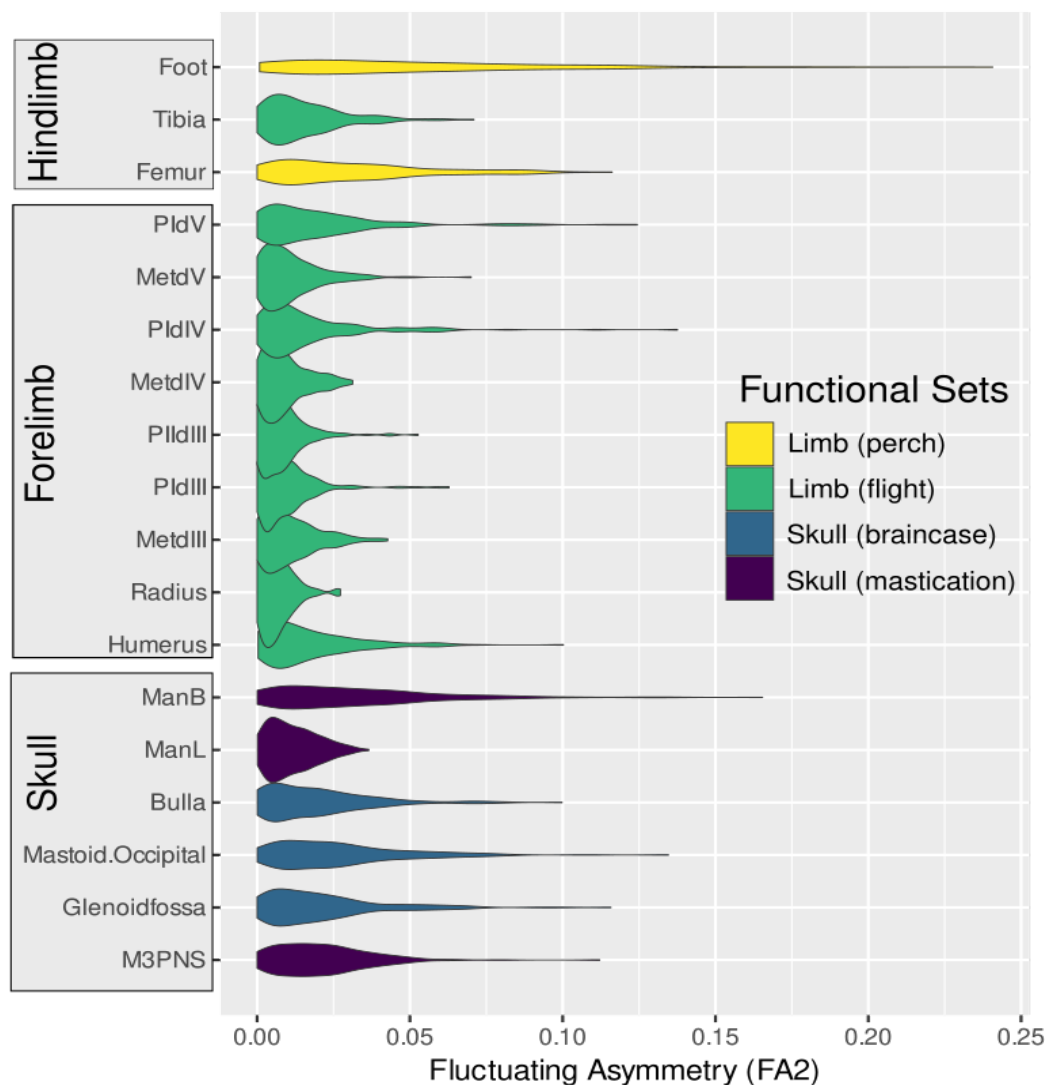
Figure 4: Violin plots of size-corrected fluctuating asymmetry index FA2 (|R-L|/mean(R,L)). Each trait shows a representation of distribution density, where width is proportional to the number of observations along the FA2 axis.

Table 3: Hierarchical mixed-model comparison using Akaike information criteria corrected for small sample sizes (AICc). K is the number of parameters in the model, ΔAICc is the AICc difference from the best fitting model and wAICc are Akaike weights.

Model	K	AICc	ΔAICc	wAICc
Functional Set	7	-18923.93	0.00	0.98
Developmental Set	6	-18916.52	7.41	0.02
Individuals within Traits (random effects)	4	-18908.35	15.59	0.00
Individuals (random effect)	3	-17941.78	982.16	0.00

The best fitting hierarchical mixed model (Table 3) had functional sets as fixed effects and traits/individuals as random effects nested within the functional sets (individuals nested within traits). The conditional R^2 (variance explained by the model) was 0.904, and the marginal R^2 (variance explained by the fixed factor) was 0.173. Therefore, most FA variation was allocated among traits and individuals. Between random effect levels, the intraclass correlation coefficients (variance components as proportions) were 0.086 among traits, 0.798 among individuals, and 0.116 for residuals. Therefore, the largest proportion of FA variance is observed among individuals nested within traits.

The fixed effects obtained from the best fitting model (functional sets) indicate that limb bones associated with perching are by far the most asymmetric traits, whereas limb bones associated with flight are the least asymmetric (Figure 5). Skull elements presented intermediate asymmetries and are not different between functional groups.
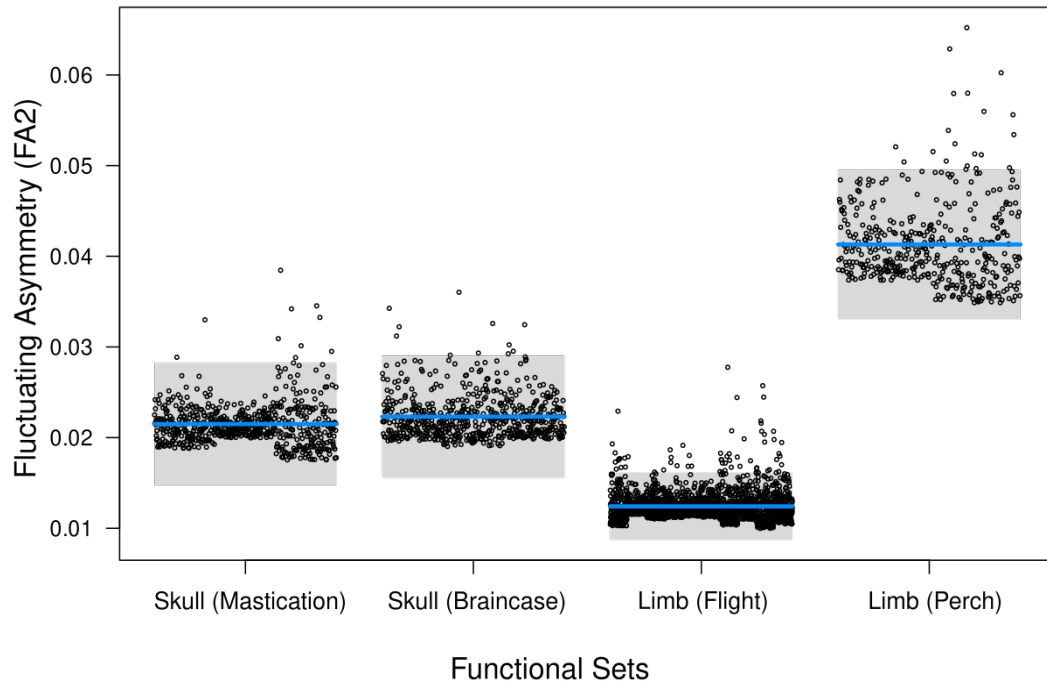
Figure 5: Effect plot of the hierarchical mixed model with functional trait sets as a fixed effect and traits/individuals as random effects nested below the functional trait set. Blue lines indicate group averages, gray boxes depict 95% confidence intervals for group means, and points are partial residuals (independent of trait and individual variation).

The multivariate set of 18 size-corrected trait asymmetries was estimated by parallel analysis to have two dimensions (two adjusted eigenvalues > 1). The first two principal components of the correlation matrix explained 16.8% of total variation in FA2 (figure 6). The patterns of observed association were mostly among traits belonging to the same limb pair. PC1 contrasted forelimb traits plus the tibia associated with positive PC scores, with hindlimb elements and cranial traits presenting negative associations. PC2 contrasted hindlimb and forelimb elements. Cranial traits did present a clear pattern of associations. Some phalanges and metacarpals were also associated with elements from other limb pairs.
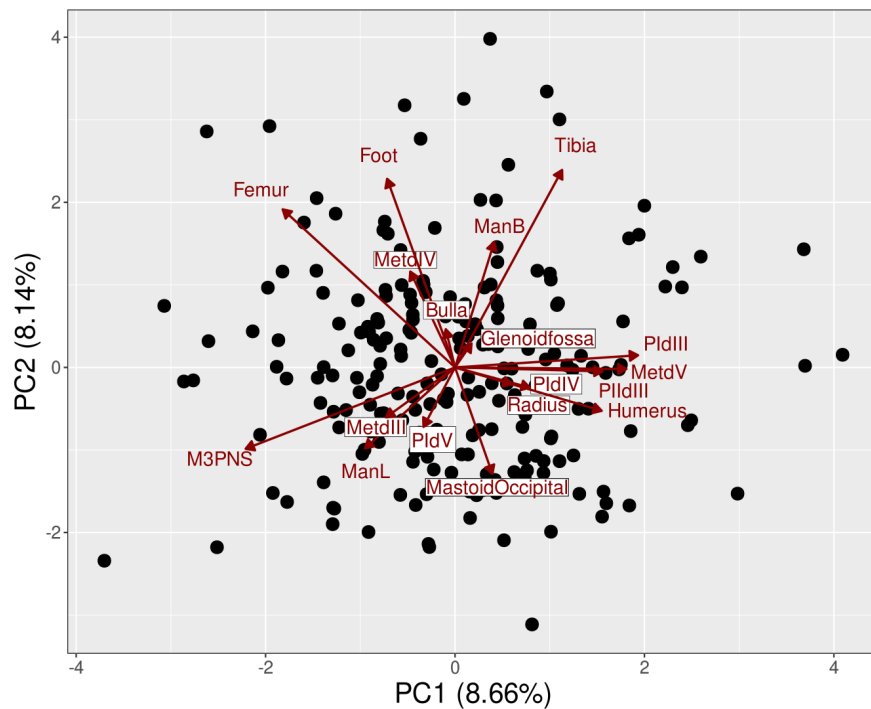
Figure 6: Principal component ordination biplot of unsigned trait asymmetries (FA2). Phalanx names abbreviated as "P" followed by Roman numerals (I, II) and digit "d" followed by Roman numerals. Same pattern used for metacarpals, using "Met". M3-PNS: distance between the third upper molar, ManL: mandibular length, ManB: height of mandibular body.

Geographic variation in multivariate FA

The distribution of multivariate FA indicated an increased density of high FA in sites located at open areas (Figure 7). The mixed effects model comparing multivariate FA among forested and open areas with site as a random factor indicated a trend of increasing asymmetry in individuals from open areas (Figure 8). A null model only with sites as a random effect was a worse fit than the forest/open area model but the two models might be considered statistically equivalent ($\Delta AICc = 1.48$), possibly due to the small sample from open areas. Nevertheless, there is little overlap in effects associated with the environmental differences (Figure 8). The model separating all four ecoregions fitted worse than the null ($\Delta AICc = 2.76$).
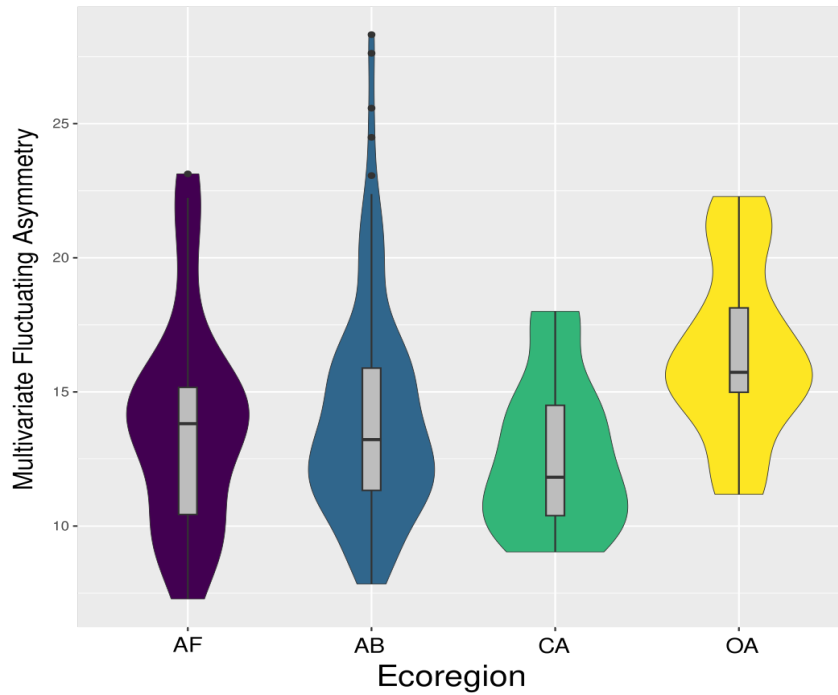
Figure 7: Violin plots of multivariate fluctuating asymmetry (sum of squared PC scores). The plot shows a representation of distribution density, where width is proportional to the number of observations along the multivariate FA axis. Plotted ecoregions are AF: Atlantic forest, AB: Amazon basin, CA: Central America, and OA: South American dry diagonal.
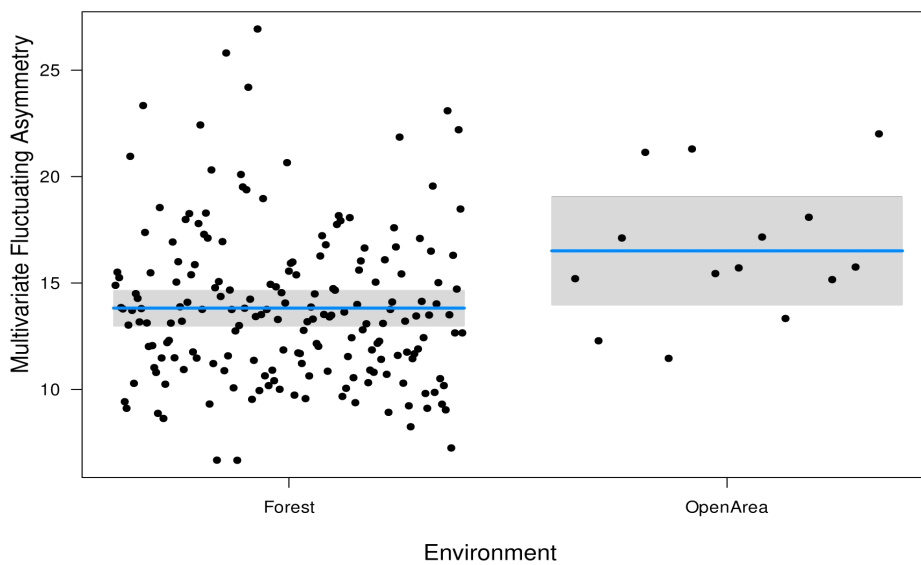
Figure 8: Effect plot of the mixed model with forest/open areas as fixed effect and sites as random effects. Blue lines indicate group averages, gray boxes depict 95% confidence intervals for group means, and points are partial residuals (independent of site variation).

Discussion

Results showed that fluctuating asymmetry was not uniformly nor randomly distributed throughout the body in *C. perspicillata*. The correlations among unsigned asymmetries were low, as expected due to the low repeatability of DI in FA measures (Whitlock, 1998), but the multivariate pattern of correlations supported a low dimensionality (no evidence of largely independent trait FAs). The hierarchical mixed models indicated that most variation of size-corrected asymmetries was concentrated at the level of individuals within traits. This provides support for a small effect of DI as a property of the individual. On other hand, the lower levels of FA in traits associated with flight and higher levels of FA in traits associated with other functions suggest that flight is a function that requires more symmetric traits and that localized buffering of functionally relevant traits might be operational (Polak *et al.*, 2003).

Validation of FA as a measure of DI

The assessment of measurement error indicated that FA measures were repeatable across all traits, and considerably larger than ME. The lower repeatability observed in skull variables might be related to how traits were measured. All skulls traits were measured as distances between landmarks taken from photographs for a geometric morphometrics study (see chapter on skull integration). On the other hand, all limb measurements were taken directly from specimens using calipers. Differences in measurement technique and lower sample sizes might explain the lower repeatability observed in cranial data (Fruciano, 2016). Directional asymmetry was observed in four out of 18 traits (~20%). We considered that these might be related to measurement artifacts rather than a biological property of these traits (Palmer and Strobeck, 2003; Klingenberg, 2015; Monteiro *et al.*, 2019). Error due to DA is then expected to add to noise, but not generate trends in FA that could cause problems of misinterpretation. Hypothetical DI repeatabilities estimated for the traits using the (Whitlock, 1998) formula with the coefficient of variation (results not shown), varied between 0.04 and 0.34, suggesting that all correlations of DI between traits might have been underestimated by the use of FA as a proxy (Van Dongen, 2006).

Fluctuating asymmetry is considered an imprecise measure of DI (Van Dongen and Gangestad, 2011) so that the small effect of DI in biologically relevant characteristics of organisms may not be recognized—see (Van Dongen and Gangestad, 2011; Beasley *et al.*, 2013; Coda *et al.*, 2017) for examples and further discussion. Our results add to previous literature that indicates the need for large sample sizes so that the individual effects of DI can be identified (Gangestad and Thornhill, 1999; Van Dongen, 2006; Van Dongen and Gangestad, 2011; Graham, 2020; Graham, 2021).

Is DI a property of the individual?

Although small and difficult to measure through FA, the effect of DI on regulatory performance and important aspects of the life history of organisms has been repeatedly observed. For example, in gazelle species FA is associated with different health parameters related with regulatory performance suggesting that FA reflects as individual property (Cuervo *et al.*, 2011); in male guppies (*Gyrodactylus turnbulli*) the fluctuating asymmetry is negatively associated to the resistance to parasites and chances of mate (Stephenson *et al.*, 2020); mate choice in humans is also consistently inversely associated with FA (Hill *et al.*, 2017). The low correlations of FA among traits in *C. perspicillata* suggests that the systemic effect of DI is weak in this species. However, the observable effect is clearly underestimated, due to low repeatability of DI in FA and to differential buffering of functional trait sets. A more pervasive effect of DI can be also inferred from the negative associations of FA with survival and reproduction (Monteiro *et al.*, 2019), and immune response—as a measure of the organism's regulatory performance (Mellado *et al.*, 2024a).

Fluctuating asymmetry levels in functional and developmental trait sets

Lower FA in traits associated with flight, partially corroborate the hypothesis of negative association between functional importance of a character and its developmental control (Gummer and Brigham, 1995; Crespi and Vanderkist, 1997; Garnier *et al.*, 2006; Rivera and Neely, 2020; Tague, 2020). To the best of our knowledge, this was the first time a large set of limb characters was used to

compare the level of developmental instability across functionally divergent limbs in Tetrapoda. Previous investigations of this issue have compared serial homologous bones between the sets of limbs, with one bone per limb (Didde and Rivera, 2019; Rivera and Neely, 2020).

Gummer and Brigham (1995) found that the variance of signed FA in the tibia is two times larger than the variance observed in the forearm (radius) in the bat *Myotis lucifugus*. The authors predicted that the tibia would be less functionally relevant than the forearm because it would be only associated with perching in roosts. Because Gummer and Brigham (1995) used an FA measure that is more difficult to interpret (variance of signed asymmetry), and provided no estimate of error, their study is not directly comparable. We found that radius mean asymmetry is the smallest in the entire trait set, but the distribution of FA for the tibia is not similar to other leg bones, as average FA for the femur and the foot are two and three times that observed for the tibia, respectively. The tibia was the only leg trait with a FA level similar to that observed in the wing traits. We consider that this bone is relevant to flight because of its attachment to both wing membrane and uropatagium because its potential role in changing camber during flight (Cheney *et al.*, 2014; Carneiro, L. O. and Monteiro, L. R., pers. Obs.).

According to the hypothesis that there is a greater buffering of the development of functionally relevant structures (Polak *et al.*, 2003), the characters analyzed here might present a gradient of developmental control following the functional demand to which they are subjected (flight > mastication and protection of the central nervous system and sensory organs (brain case) > perch). This result is consistent with the expected for bats since their biology relays on flight (Neuweiler, 2000) and skull characters are demonstrably also important from a functional point of view (Nogueira *et al.*, 2009; Monteiro and Nogueira, 2010; Monteiro and Nogueira, 2011; Rossoni *et al.*, 2017; Arbour *et al.*, 2019; Rossoni *et al.*, 2019). It remains to be examined whether flight traits are more buffered than skull traits within individuals because the fine tuning of wing symmetry is functionally more relevant than that of skull dimensions.

Geographic variation in multivariate FA

Fluctuating asymmetry is, in general, considered a reliable indicator of environmental stress in small mammal populations (Coda *et al.*, 2017). Lower environmental suitability across species distributions (Maestri *et al.*, 2015), as well as anthropogenic factors like habitat fragmentation and changes in land use (Teixeira *et al.*, 2006; Castilheiro *et al.*, 2022) are associated with increased FA levels.

In spite of the statistical equivalence between the model comparing multivariate FA between forest/open areas and the null model, the tendency for higher FA levels in the open formations (Cerrado and Caatinga) seems to be biologically relevant. This is indicated by the small overlap in FA distributions between OA and the other ecoregions. The lack of statistical support in the model is probably result of a small sample size for OA in our study. It is noteworthy that, despite being a widely distributed species, generally present at high abundance, and tolerant of disturbances, *C. perspicillata* has a greater affinity with rain forests (Cloutier and Thomas, 1992; Solari *et al.*, 2019), and experiences decreased survival and body mass during extended droughts (Monteiro *et al.*, 2019; Mellado *et al.*, 2024b).

Across the Cerrado and Caatinga, *C. perspicillata* is found in variable abundance, but never with numbers similar to the rain forest closer to the Atlantic coast (Lapenta and Bueno, 2015). Climate change is predicted to cause the species to lose some of its potential distribution in the Cerrado (Aguiar *et al.*, 2016). It is noteworthy that among Caatinga subregions, the species was not captured in areas such as the Dunes of São Francisco, characterized by low rainfall and high temperatures (de Carvalho-Neto *et al.*, 2016). The higher abundance in the Caatinga is observed in humid forest enclaves (Vargas-Mena *et al.*, 2023), that might not even be a proper Caatinga formation rainforest enclaves (Lima *et al.*, 2023). It reinforces the idea that dry areas are less suitable for the species. Further research, increasing the number of samples from open, dry areas is required to assess this relationship with more certainty.

Final remarks

We demonstrated both the presence of a small to moderate systemic effect of DI, measured by FA, and that the DI magnitude in a trait is associated with

functional relevance. Wing traits and the tibia, which are involved with flight were less asymmetric than skull traits, which were in turn less asymmetric than leg traits associated with perching. As most of the literature about the relationship between DI and survival, reproduction, performance and environmental stress focuses on the DI of functionally important traits. Future research should investigate the influence of character choice and the probability of finding associations, considering the potential for developmental buffering to shade patterns between DI and fitness or performance. One relevant applied question is the suitability of traits for ecological monitoring using FA, given their functional relevance. If functional traits are more buffered against developmental perturbations, they might have more DI signal in the FA measurements, whereas if a trait is less functionally relevant, it might be more developmentally noisy and have high FA even in less disturbed populations. We also showed that challenging environments might increase the level of DI in populations of *C. perspicillata*. We highlight the importance of carrying out assessments of the impact of environmental stress caused by anthropogenic factors with caution and carefully considering the ecology of the species and the traits chosen for the study.

References

Aguiar, L.M., Bernard, E., Ribeiro, V., Machado, R.B., Jones, G. (2016). Should I stay or should I go? Climate change effects on the future of Neotropical savannah bats. *Global Ecology and Conservation* 5:22–33.

Albertson, R.C. (2018). Cellular basis of evolution in animals. *In*: Brian K. Hall, Sally A. Moody. (eds.) *Cells in Evolutionary Biology*. Boca Raton, Florida: CRC Press. p. 213–234.

Arbour, J.H., Curtis, A.A., Santana, S.E. (2019). Signatures of echolocation and dietary ecology in the adaptive evolution of skull shape in bats. *Nature Communications* 10:1–13.

Arundell, K.L., Bojko, J., Wedell, N., Dunn, A.M. (2019). Fluctuating asymmetry, parasitism and reproductive fitness in two species of gammarid crustacean. *Diseases of Aquatic Organisms* 136:37–49.

Barlow, G.M., Ledbetter, N.M. (2024). Carpal variability and asymmetry in limb reduced Western lesser sirens (*Siren nettingi*). *Journal of Morphology* 285:1–8.

Bartoń, K. (2024). MuMIn: Multi-Model Inference. . . https://CRAN.R-project.org/package=MuMIn.

Beasley, D.A.E., Bonisoli-Alquati, A., Mousseau, T.A. (2013). The use of fluctuating asymmetry as a measure of environmentally induced developmental instability: A meta-analysis. *Ecological Indicators* 30:218–226.

Bergstrom, C., Reimchen, T. (2005). Habitat dependent associations between parasitism and fluctuating asymmetry among endemic stickleback populations. *Journal of Evolutionary Biology* 18:939–948.

Breheny, P., Burchett, W. (2017). Visualization of regression models using visreg. *The R Journal* 9:56–71.

Burnham, K.P., Anderson, D.R. (2002). *Model selection and multimodel inference: a practical information-theoretic approach*. New York: Springer. 488 p.

Carneiro, L.O., Mellado, B., Nogueira, M.R., Cruz-Neto, A.P.d., Monteiro, L.R. (2023). Flight performance and wing morphology in the bat *Carollia perspicillata*: biophysical models and energetics. *Integrative Zoology* 18:876–890.

de Carvalho-Neto, F.G., da Silva, J.R., Santos, N., Rohde, C., Garcia, A.C.L., Montes, M.A. (2016). The heterogeneity of Caatinga biome: an overview of the bat fauna. *Mammalia* 81:257–264.

Castilheiro, W.F.F., Muñoz-Muñoz, F., Ventura, J., dos Santos-Filho, M., Mathias, M.d.L., Gabriel, S.I. (2022). Differential impact of forest fragmentation on fluctuating asymmetry in South Amazonian small mammals. *Symmetry* 14:981.

Cheney, J.A., Ton, D., Konow, N., Riskin, D.K., Breuer, K.S., Swartz, S.M. (2014). Hindlimb motion during steady flight of the lesser dog-faced fruit bat, *Cynopterus brachyotis*. *PLoS ONE* 9:e98093.

Cleland, T.P., Wang, Z., Wang, B., Picu, C.R., Vashishth, D. (2021). Mechano-chemical regulation of bat wing bones for flight. *Journal of the Mechanical Behavior of Biomedical Materials* 124:104809.

Cloutier, D., Thomas, D.W. (1992). *Carollia perspicillata*. *Mammalian species* :1–9.

Coda, J.A., Martínez, J.J., Steinmann, A.R., Priotto, J.W., Gomez, M.D. (2017). Fluctuating asymmetry as an indicator of environmental stress in small mammals. *Mastozoologia Neotropical* 24:313–321.

Crespi, B.J., Vanderkist, B.A. (1997). Fluctuating asymmetry in vestigial and functional traits of a haplodiploid insect. *Heredity* 79:624–630.

Cuervo, J.J., Dhaoui, M., Espeso, G. (2011). Fluctuating asymmetry and blood parameters in three endangered gazelle species. *Mammalian Biology* 76:498–505.

Didde, R.D., Rivera, G. (2019). Patterns of fluctuating asymmetry in the limbs of anurans. *Journal of Morphology* 280:587–592.

Dinno, A. (2009). Exploring the sensitivity of Horn's parallel analysis to the distributional form of random data. *Multivariate Behavioral Research* 44:362–388.

Dinno, A. (2024). paran: Horn's test of principal components/factors. https://CRAN.R-project.org/package=paran.

Fleming, T. (1988). *The short-tailed fruit bat: a study in plant-animal interactions*. Chicago, USA: Chicago University Press. 365 p.

Fruciano, C. (2016). Measurement error in geometric morphometrics. *Development Genes and Evolution* 226:139–158.

Galecki, A., Burzykowski, T. (2013). *Linear mixed-effects models using R*. New York: Springer. 542 p.

Gangestad, S.W., Thornhill, R. (1999). Individual differences in developmental precision and fluctuating asymmetry: a model and its implications. *Journal of evolutionary Biology* 12:402–416.

Garnier, S., Gidaszewski, N., Charlot, M., Rasplus, J.-Y., Alibert, P. (2006). Hybridization, developmental stability, and functionality of morphological traits in the ground beetle *Carabus solieri* (Coleoptera, Carabidae). *Biological Journal of the Linnean Society* 89:151–158.

Graham, J.H. (2020). Fluctuating asymmetry and developmental instability, a guide to best practice. *Symmetry* 13:9.

Graham, J.H. (2021). Nature, nurture, and noise: developmental instability, fluctuating asymmetry, and the causes of phenotypic variation. *Symmetry* 13:1204.

Gummer, D.L., Brigham, R.M. (1995). Does fluctuating asymmetry reflect the importance of traits in little brown bats (*Myotis lucifugus*)?. *Canadian Journal of Zoology* 73:990–992.

Hall, B.K. (2015). *Bones and cartilage: developmental and evolutionary skeletal biology*. New York: Elsevier. 892 p.

Hendry, A.P., Schoen, D.J., Wolak, M.E., Reid, J.M. (2018). The Contemporary evolution of fitness. *Annual Review of Ecology, Evolution, and Systematics* 49:457–476.

Hill, A.K. et al. (2017). Are there vocal cues to human developmental stability? Relationships between facial fluctuating asymmetry and voice attractiveness. *Evolution and Human Behavior* 38:249–258.

Husak, J.F., Irschick, D.J., McCormick, S.D., Moore, I.T. (2009). Hormonal regulation of whole-animal performance: Implications for selection. *Integrative and Comparative Biology* 49:349–353.

Irvine, S.Q. (2020). Embryonic canalization and its limits—A view from temperature. *Journal of Experimental Zoology Part B: Molecular and Developmental Evolution* 334:128–144.

Juarez-Carreño, S., Morante, J., Dominguez, M. (2018). Systemic signalling and local effectors in developmental stability, body symmetry, and size. *Cell Stress* 2:340–361.

Klingenberg, C.P. (2003). A developmental perspective on developmental instability: theory, models and mechanisms. *In*: Polak, M. (eds.) *Developmental instability: causes and consequences*. New York: Oxford University Press. p. 14–34.

Klingenberg, C.P. (2008). Morphological integration and developmental modularity. *Annual Review of Ecology, Evolution, and Systematics* 39:115–132.

Klingenberg, C.P. (2014). Studying morphological integration and modularity at multiple levels: concepts and analysis. *Philosophical Transactions of the Royal Society B: Biological Sciences* 369:20130249.

Klingenberg, C.P. (2015). Analyzing fluctuating asymmetry with geometric morphometrics: concepts, methods, and applications. *Symmetry* 7:843–934.

Klingenberg, C.P. (2022). Shape asymmetry — what's new?. *Emerging Topics in Life Sciences* 6:285–294.

Klingenberg, C.P., Monteiro, L.R. (2005). Distances and directions in multidimensional shape spaces: implications for morphometric applications. *Systematic Biology* 54:678–688.

Lapenta, M.J., Bueno, A.D.A. (2015). Checklist of bats (Mammalia, Chiroptera) from Tocantins and Bahia, Brazil: a gradient from Cerrado, Caatinga and Atlantic Forest. *Check List* 11:1673.

Lê, S., Josse, J., Husson, F. (2008). FactoMineR: A Package for Multivariate Analysis. *Journal of Statistical Software* 25:1–18.

Leamy, L., Klingenberg, C., Sherratt, E., Wolf, J., Cheverud, J. (2015). The genetic architecture of fluctuating asymmetry of mandible size and shape in a population of mice: another look. *Symmetry* 7:146–163.

Leamy, L.J., Klingenberg, C.P. (2005). The genetics and evolution of fluctuating asymmetry. *Annual Review of Ecology, Evolution and Systematics* 36:1-21.

Lens, L., Eggermont, H. (2008). Fluctuating asymmetry as a putative marker of human-induced stress in avian conservation. *Bird Conservation International* 18:S125–S143.

Lens, L., Van Dongen, S., Kark, S., Matthysen, E. (2002a). Fluctuating asymmetry as an indicator of fitness: can we bridge the gap between studies?. *Biological Review* 77:27-38.

Lens, L., Van Dongen, S., Matthysen, E. (2002b). Fluctuating asymmetry as an early warning system in the critically endangered Taita thrush. *Conservation Biology* 16:479-487.

Lima, R.D., Fernandes, M.F., Ferreira de Vasconcelos, M., Cardoso, D., de Queiroz, L.P. (2023). Disparate biomes within the Caatinga region are not part of the same evolutionary community: A reply to Araujo et al. (2022). *Journal of Arid Environments* 209:104901.

Longman, D.P. et al. (2021). Fluctuating asymmetry, a marker of poor growth quality, is associated with adult male metabolic rate. *American Journal of Physical Anthropology* 175:646–655.

López, P., Martin, J. (2002). Locomotor capacity and dominance in male lizards *Lacerta monticola*: a trade-off between survival and reproductive success?. *Biological Journal of the Linnean Society* 77:201–209.

Maestri, R., Fornel, R., Galiano, D., de Freitas, T.R.O. (2015). Niche suitability affects development: skull asymmetry increases in less suitable areas. *PLOS ONE* 10:e0122412.

Martín, J., López, P. (2001). Hindlimb asymmetry reduces escape performance in the lizard *Psammodromus algirus*. *Physiological and Biochemical Zoology*, 74:619-624.

Maxwell, E.E., Larsson, H.C. (2007). Osteology and myology of the wing of the Emu (*Dromaius novaehollandiae*), and its bearing on the evolution of vestigial structures. *Journal of Morphology* 268:423–441.

Mazerolle, M.J. (2023). AICcmodavg: Model selection and multimodel inference based on (Q)AIC(c). https://cran.r-project.org/package=AICcmodavg.

Mellado, B., Carneiro, L.d.O., Nogueira, M.R., Herrera M, L.G., Cruz-Neto, A.P., Monteiro, L.R. (2024a). Developmental instability, body mass, and reproduction predict immunological response in short-tailed bats. *Current Zoology* In Press:zoae034.

Mellado, B., de Oliveira Carneiro, L., Nogueira, M.R., Monteiro, L.R. (2024b). Not all size measures are created equal: different body size proxies are not equivalent fitness predictors in the bat *Carollia perspicillata*. *Journal of Mammalian Evolution* 31:9.

Mello, M.A.R., Schittini, G.M., Selig, P., Bergallo, H.G. (2004). Seasonal variation in the diet of the bat *Carollia perspicillata* (Chiroptera: Phyllostomidae) in an Atlantic Forest area in southeastern Brazil. *Mammalia* 68:49–55.

Monteiro, L.R., Mellado, B., Nogueira, M.R., Morais-Jr, M.M. (2019). Individual asymmetry as a predictor of fitness in the bat *Carollia perspicillata*. *Journal of Evolutionary Biology* 32:1207–1229.

Monteiro, L.R., Nogueira, M.R. (2010). Adaptive radiations, ecological specialization, and the evolutionary integration of complex morphological structures. *Evolution* 64:724–744.

Monteiro, L.R., Nogueira, M.R. (2011). Evolutionary patterns and processes in the radiation of phyllostomid bats. *BMC Evolutionary Biology* 11:1–23.

Montévil, M. (2019). Measurement in biology is methodized by theory. *Biology & Philosophy* 34:35.

Mundahl, N.D., Hoffmann, K.A. (2023). Condition, Reproductive Fitness, and Fluctuating Asymmetry in Brook Stickleback: Responses to Anthropogenic Runoff. *Fishes* 8:557.

Møller, A. (1989). Ejaculate quality, testes size and sperm production in mammals. *Functional Ecology* :91–96.

Møller, A.P. (1997). Developmental stability and fitness: a review. *The American Naturalist* 149:916–932.

Nakagawa, S., Schielzeth, H. (2010). Repeatability for Gaussian and non-Gaussian data: a practical guide for biologists. *Biological Reviews* 85:935–956.

Nakagawa, S., Schielzeth, H. (2012). A general and simple method for obtaining R2 from generalized linear mixed-effects models. *Methods in Ecology and Evolution* 4:133–142.

Neuweiler, G. (2000). *The biology of bats*. Oxford, United Kingdom: Oxford University Press. 320 p.

Nogueira, M.R., Peracchi, A.L., Monteiro, L.R. (2009). Morphological correlates of bite force and diet in the skull and mandible of phyllostomid bats. *Functional Ecology* 23:715–723.

Palmer, A.R., Strobeck, C. (1986). Fluctuating asymmetry: Measurement, Analysis, Patterns. *Annual Review of Ecology and Systematics* 17:391–421.

Palmer, A.R., Strobeck, C. (2003). Fluctuating asymmetry analyses revisited. *In*: Polak, M. (eds.) *Developmental instability: causes and consequences*. New York: Oxford University Press. p. 279–319.

Peres-Neto, P.R., Jackson, D.A., Somers, K.M. (2005). How many principal components? stopping rules for determining the number of non-trivial axes revisited. *Computational Statistics & Data Analysis* 49:974–997.

Pinheiro, J., Bates, D. (2000). *Mixed-Effects Models in S and S-PLUS*. New York: Springer. 528 p.

Polak, M., Møller, A., Gangestad, S., Kroeger, D., Manning, J., Thornhill, R. (2003). Does an individual asymmetry parameter exist? A meta-analysis. *In*: Polak, M. (eds.) *Developmental instability: causes and consequences*. Oxford: Oxford University Press. p. 81–96.

Rivera, G., Neely, C.M.D. (2020). Patterns of fluctuating asymmetry in the limbs of freshwater turtles: Are more functionally important limbs more symmetrical?. *Evolution* 74:660–670.

Rossoni, D.M., Assis, A.P.A., Giannini, N.P., Marroig, G. (2017). Intense natural selection preceded the invasion of new adaptive zones during the radiation of New World leaf-nosed bats. *Scientific Reports* 7:11076.

Rossoni, D.M., Costa, B.M.A., Giannini, N.P., Marroig, G. (2019). A multiple peak adaptive landscape based on feeding strategies and roosting ecology shaped the evolution of cranial covariance structure and morphological differentiation in phyllostomid bats. *Evolution* 73:961–981.

Solari, S. et al. (2019). Family Phyllostomidae (New World Leaf-nosed Bats). *In*: Wilson, D.; Mittermeier, R.A. (eds.) *Handbook of the Mammals of the World*. Barcelona, Spain: Lynx. p. 444–583.

Stephenson, J.F., Stevens, M., Troscianko, J., Jokela, J. (2020). The Size, Symmetry, and Color Saturation of a Male Guppy's Ornaments Forecast His Resistance to Parasites. *The American Naturalist* 196:597–608.

Stoffel, M.A., Nakagawa, S., Schielzeth, H. (2017). rptR: repeatability estimation and variance decomposition by generalized linear mixed-effects models. *Methods in Ecology and Evolution* 8:1639–1644.

Swaddle, J.P. (1997). Developmental stability and predation success in an insect predator-prey system. *Behavioral Ecology* 8:433–436.

Tague, R.G. (2020). Rudimentary, "functionless" first metapodials of *Canis latrans*: Variation and association in length with longer, functional metapodials. *Evolution* 74:2465–2482.

R Core Team (2024). R: A Language and Environment for Statistical Computing. R Foundation for Statistical Computing. Vienna, Austria. https://www.R-project.org/.

Teixeira, C.P., Hirsch, A., Perini, H., Young, R.J. (2006). Marsupials from space: fluctuating asymmetry, geographical information systems and animal conservation. *Proceedings of the Royal Society B: Biological Sciences* 273:1007–1012.

Van Dongen, S. (2006). Fluctuating asymmetry and developmental instability in evolutionary biology: past, present and future. *Journal of Evolutionary Biology* 19:1727–1743.

Van Dongen, S., Gangestad, S.W. (2011). Human fluctuating asymmetry in relation to health and quality: a meta-analysis. *Evolution and Human Behavior* 32:380–398.

Van Dongen, S., Lens, L. (2000). The evolutionary potential of developmental instability. *Journal of Evolutionary Biology* 13:326–335.

Vargas-Mena, J.C., Cordero-Schmidt, E., Rodríguez-Herrera, B., Venticinque, E.M. (2023). Differences in the structure of bat assemblages among habitats in the Caatinga dry forest. *Journal of Tropical Ecology* 39:e42.

Voigt, C.C., Heckel, G., Mayer, F. (2005). Sexual selection favours small and symmetric males in the polygynous greater sac-winged bat *Saccopteryx bilineata* (Emballonuridae, Chiroptera). *Behavioral Ecology and Sociobiology* 57:457–464.

Whitlock, M. (1998). The repeatability of fluctuating asymmetry: a revision and extension. *Proceedings of the Royal Society B: Biological Sciences* 265:1429–1431.

Woods, H.A. (2014). Mosaic physiology from developmental noise: within-organism physiological diversity as an alternative to phenotypic plasticity and phenotypic flexibility. *Journal of Experimental Biology* 217:35–45.

Zheng, Y., Pan, D. (2019). The Hippo Signaling Pathway in Development and Disease. *Developmental Cell* 50:264–282.

Capítulo 3: Developmental architecture and morphological evolution in the wings of the bat *Carollia perspicillata*

Lucas Carneiro[a,b], Bruce D. Patterson[b], Leandro R. Monteiro[a]

(a) Laboratório de Ciências Ambientais, Universidade Estadual do Norte Fluminense Darcy Ribeiro, Campos dos Goytacazes, Brasil; (b) Negaunee Integrative Research Center, Field Museum of Natural History, Chicago, USA.

Abstract

Forelimbs and hind limbs of tetrapods are composed of serially homologous segments (which share the same developmental pathways): stylopodium (humerus or femur), zeugopodium (radius and ulna or tibia and fibula) and autopodium (bones of the hands and feet). Given their shared genetic architecture, these structures typically show greater correlation with each other, compared to other bones that belong to the same limb—forming developmental modules. In lineages whose limb morphology has evolved divergently, the pattern of modularity is reduced and an increased correlation is observed between elements belonging to the same limb. The objective of this work is to investigate the patterns of intraspecific association between the elements that make up the limbs in bats, using *Carollia perspicillata* as a model. Partial correlation patterns of linear measurements of 12 bones from the three limb segments in 276 specimens (139 ♀ and 137 ♂) from 25 locations throughout the Neotropical region were analyzed. The developmental architecture of the anterior and posterior limbs is relatively independent of each other. Morphological divergence between members implies a lower level of integration between developmental homologs. For the first time in bats, two distinct modules were identified in the autopodium of the forelimb: metacarpals and phalanges. Considering that these modules integrate functionally divergent structures with respect to flight, the differences in integration and modularity patterns between the static and evolutionary levels indicate that natural

selection have reduce the similarity between homologous developmental structures in the wing.

Keywords: Morphological integration; modularity; developmental instability; serial homology; flight.

Introduction

Morphological integration is defined by patterns of association between elements of a morphological structure that share developmental pathways, gene regulation, or constraints from natural selection (Hall and Miyake, 2000; Klingenberg, 2014; Melo *et al.*, 2016). The modularity of a complex structure can be inferred by groups of components that are more associated within groups (modules) than between groups (Klingenberg, 2014; Zelditch and Goswami, 2021). The developmental processes can constrain evolutionary change, because selection acts on the variation produced during development (Cheverud, 1996a; Hendrikse *et al.*, 2007; Olson, 2019). Thus, the association between genotype and phenotype through development can be understood by the predisposition in the directions of phenotypic variation (Hendrikse *et al.*, 2007; Klingenberg, 2015).

Patterns of integration and modularity can be comprehended in different levels, according to the processes acting on a given set of characters (Klingenberg, 2014; Duclos *et al.*, 2019). The intra-individual patterns, known as developmental integration/modularity, emerge from pleiotropic effects of genes or developmental processes (Klingenberg, 2014; Duclos *et al.*, 2019). Patterns inferred at the individual level, in the same population and developmental stage, are termedstatic integration/modularity—sensu Klingenberg (2014). At the level of populations, or lineages, the evolutionary association among parts of a structure will determine its integration/modularity patterns (Zelditch and Goswami, 2021). Despite being relatively uncommon (Klingenberg, 2014), studies analyzing integration and modularity at different levels of biological complexity can clarify the connections between these levels—*e.g.* the effects of the developmental program on the evolvability of a complex structure (Zelditch and Goswami, 2021).

The limbs of vertebrates is composed of serially homologous segments—stylopodium (humerus in the forelimb and femur in the hindlimb), zeugopodium

(radius and ulna in the forelimb and the tibia and fibula in the hindlimb), and autopodium—bone structures that form the *manus* and *pes*; figure 1 (Hall, 2015; Sears *et al.*, 2015a; Adachi *et al.*, 2016). Although there are still open questions regarding the determination of the development of limbs (Cooper and Sears, 2013; Sears *et al.*, 2015b; Huang and Mackem, 2021; Tsutsumi and Eiraku, 2023), it is established that shared or homologous pathways pervade the development of its homologous structures (Sears *et al.*, 2015b; Tickle, 2015; Eckalbar *et al.*, 2016; Boer *et al.*, 2019).
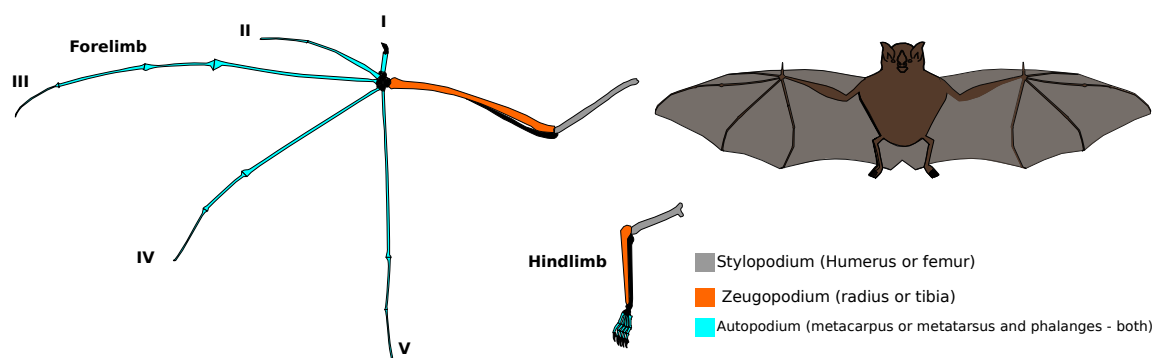
Figure 1: Schematic representation of the fore- and hindlimbs of the bat *Carollia perspicillata* indicating the the homologous structures among them.

Limb morphology is also associated with the functional demands to which they are subjected (Maher *et al.*, 2022). Quadrupedalism—with diagonal limbs moving simultaneously (seen in animals such as salamanders and some lizards)—is the ancestral condition in Tetrapoda (Wimberly *et al.*, 2021). This locomotion type keeps the limbs under similar functional demands and selective effects (Ashley-Ross and Bechtel, 2004). With the diversification of the group, different locomotion types evolved (such as other forms of quadrupedalism, bipedalism, swimming, and flight), each associated with a range of specific functional demands that might differ between limb pairs (Ashley-Ross and Bechtel, 2004; Irschick and Higham, 2015; Maher *et al.*, 2022).

A wide variation in the degree of functional divergence between limbs is observed in mammals (Ashley-Ross and Bechtel, 2004; Irschick and Higham, 2015; Maher *et al.*, 2022). The patterns of integration and modularity of these structures are associated with the level of functional independence observed between them (Young and Hallgrímsson, 2005; Young *et al.*, 2010; Bell *et al.*,

2011; Martín-Serra *et al.*, 2015). Cursorial species, such as *Lophuromys flavopunctatus* and *Canis lupus* have highly integrated limbs (with strong correlations between elements belonging to the same limbs and between serially homologous elements from different limbs; Young and Hallgrímsson, 2005; Martín-Serra *et al.*, 2015). This strong association is linked to the fact that, in these animals, the structures present similar functional demands imposed by locomotion (Young and Hallgrímsson, 2005; Martín-Serra *et al.*, 2015). Conversely, reduced functional association among limbs leads to a decrease in the integration level (Young and Hallgrímsson, 2005; Young *et al.*, 2009; Martín-Serra *et al.*, 2015).

Mammals whose forelimbs and hindlimbs differ in morphology and function, reflecting specific adaptations, may show greater association between elements belonging to the same limb than that shown with their homologous elements in the other limb (Young *et al.*, 2010; Bell *et al.*, 2011). In primates, adaptations to bipedalism, running, and tool handling (Lieberman, 2013) are associated with the dissociation between the proportions of homologs between the limbs conversely, integration within each limb is increased, when compared to patterns in quadrupedal primates (Young *et al.*, 2010).

Along with selection, developmental processes play a role structuring patterns of limb integration and modularity (Young and Hallgrímsson, 2005; Klingenberg, 2008; Klingenberg, 2014). Lineages with a moderate level of functional divergence (such as hypercarnivorous feliforms, in which there is a trade off between cursoriality and prey apprehension) present a relative dissociation between developmental patterns and functional demands (Michaud *et al.*, 2020). Also, there is no relation between the integration and modularity and the level of physical activity between individuals (Young *et al.*, 2009).

An extreme case of modification in the pattern of association between limbs comes from the advent of the evolution of active flight in vertebrates (Bell *et al.*, 2011). Birds, pterosaurs, and bats each present a reduction in the modular structure of serially homologous elements of fore- and hindlimb (Young and Hallgrímsson, 2005; Bell *et al.*, 2011; Sears *et al.*, 2015b). This reduction is thought to originate from the greater independence between the development of the fore- and hindlimbs in these lineages (Hallgrimsson *et al.*, 2002; Young *et al.*, 2009; Boer *et al.*, 2019).

Functional demands are related to the diversification of the morphology of the tetrapod autopodium (Huang and Mackem, 2021), but their influence on the pattern of integration and modularity in the bones of this segment is still poor explored (Kavanagh *et al.*, 2013). Reno *et al.*(2007), analyzing the pattern of integration between bones in the hand of different species of primates, observed greater correlations between metacarpals of different digits than between metacarpals and phalanges of a given digit. The same pattern has been observed previously in humans (Kimura, 1973; Arlegi *et al.*, 2023) where partial correlations were higher between serially homologous bones than between adjacent elements on the same digit. Rothier *et al.*(2022) investigate alternative hypothesis between development and function structuring the autopodium modularity pattern in geckos. Some species in this group present adhesive toepads that generate hyperextension of distal phalanges. They observed that function does not play a major role and the general pattern of metacarpals and phalanges as separate modules is observed.

Bat wings constitute an interesting model for the investigation of the patterns of integration and modularity, given that they constitute an extreme in the diversification of the autopodium (Cooper and Sears, 2013), growth factors act differently on the development of their digits compared to other mammals (Sears *et al.*, 2006; Howenstine *et al.*, 2021), and that their digits are functionally divergent from each other—bones along digit III being functionality associated to flight speed and hovering ability while those along digit V are more related to maneuverability and to the wing's capacity to camber during slow flight (Norberg, 1990; Stockwell, 2001; Carneiro *et al.*, 2023).

This investigates the pattern of modularity and integration of the segments of the fore- and hindlimbs using the bat *Carollia perspicillata* as a model. Here, we present a multilevel analysis, focused on the developmental, static, and evolutionary levels of variation—based on the variability of the symmetric and asymmetric components of bone lengths belonging to the stylopodium, zeugopodium, and autopodium—to examine the general patterns of integration and modularity within and among populations, as well as those that emerge from developmetnal interactions (developmental integration and modularity).

Material and methods

Data collection and validation of asymmetry measurements

We examined 276 specimens (139 females and 137 males) of *Carollia perspicillata* from 26 localities, deposited in fluid in the following zoological collections: Adriano Lúcio Peracchi collection – Universidade Federal Rural do Rio de Janeiro (ALP); American Museum of Natural History (AMNH); Field Museum of Natural History (FMNH) and Mastozoological Collection of the Universidade Estadual do Norte Fluminense (UENFMZ); Descriptions of limb measuremens and the validation of asymmetry measurements (based in a subsample of 71 specimens measured independently three times) are provided in chapter two.

Developmental, static, and evolutionary integration patterns

Developmental integration patterns were estimated from correlations among signed individual asymmetries (Klingenberg, 2008; Klingenberg, 2015). Because asymmetries result from random disturbances during development, traits that share developmental pathways are expected to present correlated asymmetries (they will be smaller or larger on one side). The right-left differences measure within-individual variation and this approach has been successfully applied in several animal systems (Klingenberg, 2014).

To estimate static integration patterns, we adjusted a linear model with the measurement matrices as dependent variables and with sex and geography as independent variables, in order to account for secondary sexual dimorphism (Carneiro *et al.*, 2023) and geographic variation (McLellan and Koopman, 2007) in the sample. Correlation matrices among variables were calculated from the residuals of the linear model. These represent the among-individual, within-population level. A size-corrected version of the static integration pattern was estimated by projecting the variable space into a space that is orthogonal to a within-population size vector, known as a Burnaby projection (Claude, 2008; Klingenberg, 2016). The size vector used was the first principal component of the residuals of the linear model described above. Evolutionary integration patterns were estimated from the correlations of measurement averages for each locality sampled.

Partial correlations were also used to measure the strength of the relationships among each pair of skeletal elements conditioned on the other traits (Magwene, 2001). This allows for a separation of direct trait associations from those that depend on more comprehensive changes in the entire variable set or parts of it (Shipley, 2016), such as changes in body or limb size. Partial correlations were estimated with the ppcor package (Kim, 2015).

Analyses of integration patterns

We used principal component analyses (PCA) to visualize the main axes of variation of the correlation matrices and to explore the association of the traits with each axis (Husson *et al.*, 2017). The PCAs were calculated with the FactoMineR package (Lê *et al.*, 2008). The dimensionality of correlation matrices was estimated with parallel analysis (Dinno, 2009). This method compares the eigenvalues obtained from the observed correlation matrices to eigenvalues derived from randomly generated, uncorrelated data with the same number of variables and observations. After correcting for the bias due to sampling error, PCs with eigenvalues > 1 are retained. We used 10,000 random data sets to estimate the eigenvalue distributions using package paran (Dinno, 2024). Parallel analysis is considered a method of optimal performance in recovering subjacent dimensionality (Peres-Neto *et al.*, 2005). For each integration level, we also calculated the index of integration of Cheverud *et al.*(1983), defined as a standardized variance of the eigenvalues (Monteiro *et al.*, 2005). This index is a measure of eigenvalue variance and has an expected value of zero for a matrix of uncorrelated traits and one if the correlation matrix rank is less than *p.* Therefore, larger I values indicate more integration.

Integration matrices for different levels were compared by matrix correlations and Mantel tests (Legendre and Legendre, 2012). Confidence intervals for matrix correlations were obtained by 5000 bootstrap samples in package ecodist (Goslee and Urban, 2007). Maximum matrix correlations (R_{max}) approach one for large samples, but can be biased downwards for smaller samples. Adjusted matrix correlations were estimated as $R_{adj} = R_{obs}/R_{max}$. (Cheverud, 1996b; Marroig and Cheverud, 2001), where R_{obs} is the observed correlation. The maximum correlation was estimated as $R_{max} = (t_A \, t_B)^{0.5}$., where t_A

and t_B are repeatabilities of integration matrices **A** and **B**, respectively. Repeatabilities were calculated for each integration level using a Monte Carlo procedure, where 1000 random samples were generated using the same sample sizes, trait means, and covariance structures observed in each integration level. A correlation matrix for each random sample was calculated and R_{max} was estimated as the average matrix correlation between the random sample integration matrices and the observed integration matrix.

Independence graphs were built for each integration level (Magwene, 2001), where the edges connecting traits were determined by the edge exclusion deviance statistic, calculated as EED = n * ln(1 − $\rho^2_{ij\{p\}}$), where *n* is the sample size, and $\rho^2_{ij\{p\}}$ is the partial correlation coefficient between traits *i* and *j* with all other *p* elements held constant. This deviance is distributed as a Chi-squared statistic, with one degree of freedom, so a value of 2.7 (the 10% threshold of the distribution) or 3.84 (5%) was used as a reference for the inclusion of edges in the diagram. Because this is an exploratory study, we decided to use a less conservative frequentist approach (P < 0.1), but also keeping in mind that distribution thresholds have no special significance in statistics and other types of evidence should be considered when deciding about the biological relevance of a finding (Wasserstein *et al.*, 2019). Graphs were built using package igraph (Csárdi *et al.*, 2024).

Theoretical correlation matrices were built with zeros and ones for different models of development, to be associated with the integration matrices for each level. The hypotheses were based on the (Hallgrimsson *et al.*, 2002) model where covariation is structured between limbs, between serially homologous limb elements (stylopod, zeugopod, autopod), and within limb elements. In the limb model, the matrix elements were zero for pairs of bones in different limbs and one if they belonged to the same limb. In the serial model, pairs of homologous elements from different limbs received ones and the pairs of bones in different serial positions received zeros. Because most elements had one single measurement (bone lengths), the within-element model differed from the limb model by separating the autopodial elements (phalanges and metacarpals) from other forelimb elements (see Supplementary Material Table S1). The within-elements model is nested in the limb model. Matrix correlations and Mantel tests

were used to determine the association of integration matrices from each level with the theoretical matrices.

Results

Asymmetry and developmental integration patterns

The asymmetries of limb measurements presented similar and low correlations and partial correlations (Supplementary Table S2), with an integration index I = 0.078. The parallel analysis found 4 axes with eigenvalues larger than expected from a random distribution of uncorrelated variables. The general pattern of asymmetry correlations is shown for the first 2 principal components, which account for 22% of the total variation. The forelimb asymmetries are mostly associated with positive scores in PC1 and PC2, whereas hindlimb asymmetries were associated with negative scores in PC1 (Figure 2). The remaining PCs (3 and 4) retained by parallel analysis explained 18.99% of asymmetry variation and depicted contrasts mainly between phalanges + metacarpals against the other elements (not shown).
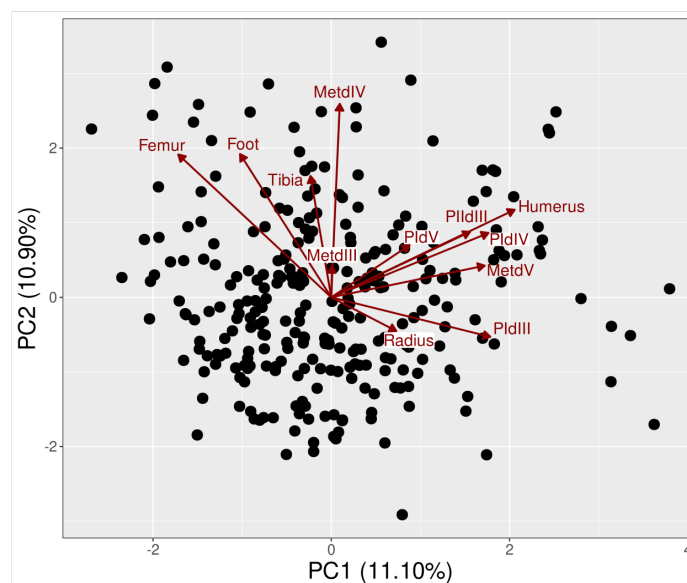
Figure 2: Principal component biplot for individual asymmetries of limb measurements of *Carollia perspicillata*. Phalanx names abbreviated as "P" followed by Roman numerals (I, II) and digit "d" followed by Roman numerals. Same pattern used for metacarpals, using "Met".
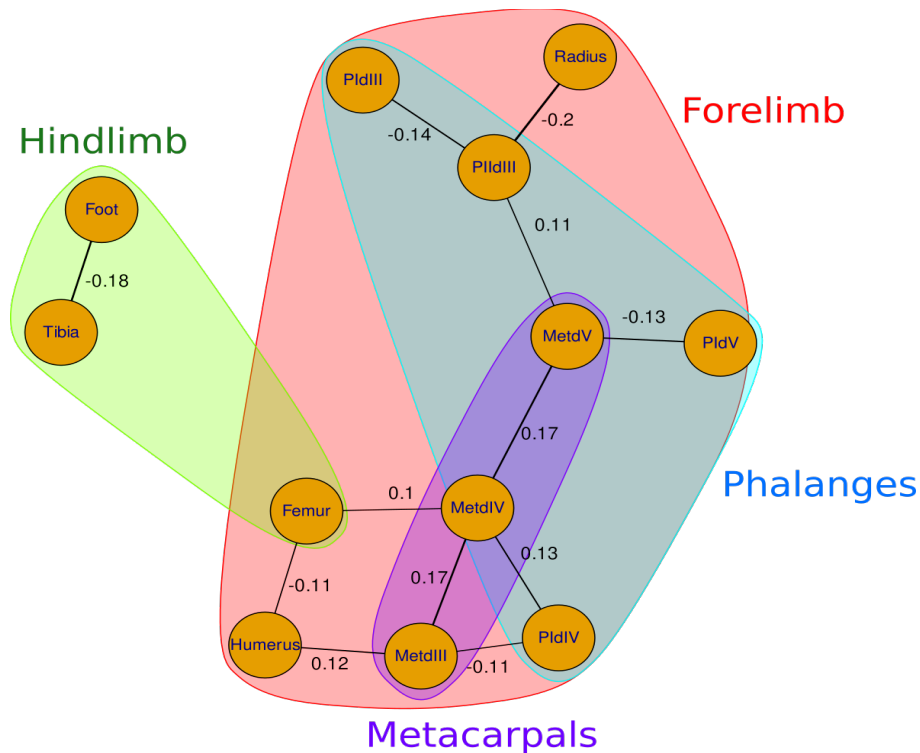
Figure 3: Independence graph showing partial correlations of length asymmetries among limb elements with edge exclusion deviances above the 10% Chi-squared threshold. Phalanx names abbreviated as "P" followed by Roman numerals (I, II) and digit "d" followed by Roman numerals. Same pattern used for metacarpals, using "Met".

Partial correlations of limb element asymmetries were low, with only a few presenting edge exclusion deviances above the 10% threshold (Figure 3, Supplementary Table S2). Most associations were observed within forelimb autopod elements (metacarpals and phalanges). The metacarpal asymmetries are associated with asymmetries in bones from all other elements (phalanges, humerus, and the femur). A few negative partial correlations were observed, where one element might have increased asymmetry in one direction (*e.g.* right side larger) and the other has more asymmetry in the other direction (left side larger).

Static integration patterns

The static within-population patterns were more integrated than the developmental level. The Integration index was I = 0.670 for the non projected data and I = 0.267 for the size-adjusted data. For the non projected data, parallel analysis recovered a single PC with an eigenvalue larger than expected from random independent data. This PC is interpreted as a general size variable because all eigenvectors had the same signal and similar magnitudes. For the

size-adjusted data, parallel analysis recovered three PCs, as variation was more spread along the different dimensions once size was removed. The first 2 PCs of the non projected data accounted for 76.7% of total variation, with all variables associated with the positive direction of PC1 (size variation) (Figure 4A). The first 2 PCs of the size-adjusted data accounted for 46.87% of the total variation, and it is possible to observe the clustering of three groups of variables (Figure 5B): The phalanges (with positive scores in the PC 2), the metacarpal measurements (negative scores on PC1) and a group consisting of the bones belonging to stylopodium, zeugopodium, and the feet (positive scores on PC1). Bones presented higher correlations with those adjacent to them and belonging to the same limb, compared to their homologies in the other limb.
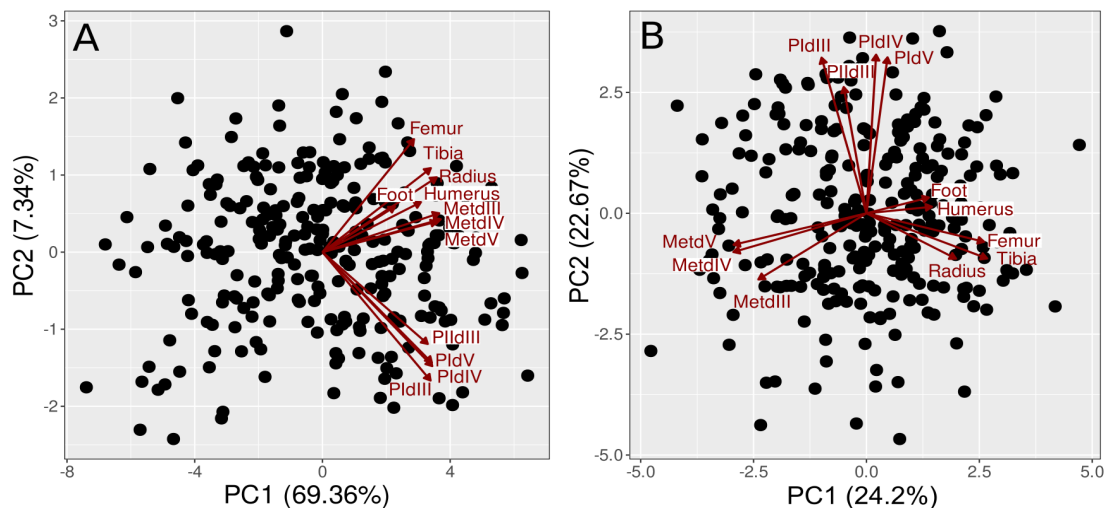
Figure 4: Principal component biplot for within-population limb measurement variation of *Carollia perspicillata*. (A) without size adjustment and (B) with size adjustment (Burnaby projection). Phalanx names abbreviated as "P" followed by Roman numerals (I, II) and digit "d" followed by Roman numerals. Same pattern used for metacarpals, using "Met".

The independence graphs based on partial correlations at the static integration level did provide statistical support for integration within limbs specifically involving elements of the forelimb autopod (metacarpals and phalanges) (Figure 5; Supplementary Tables S3 and S4). The higher correlations were observed among elements within these groups. The only correlation between serially homologous elements was observed between Tibia and Radius. Size adjustment did not change the partial correlations appreciably. Some correlations became slightly larger whereas others became slightly smaller. This is expected

since partial correlations from non projected data were already performing an adjustment for general size variation.
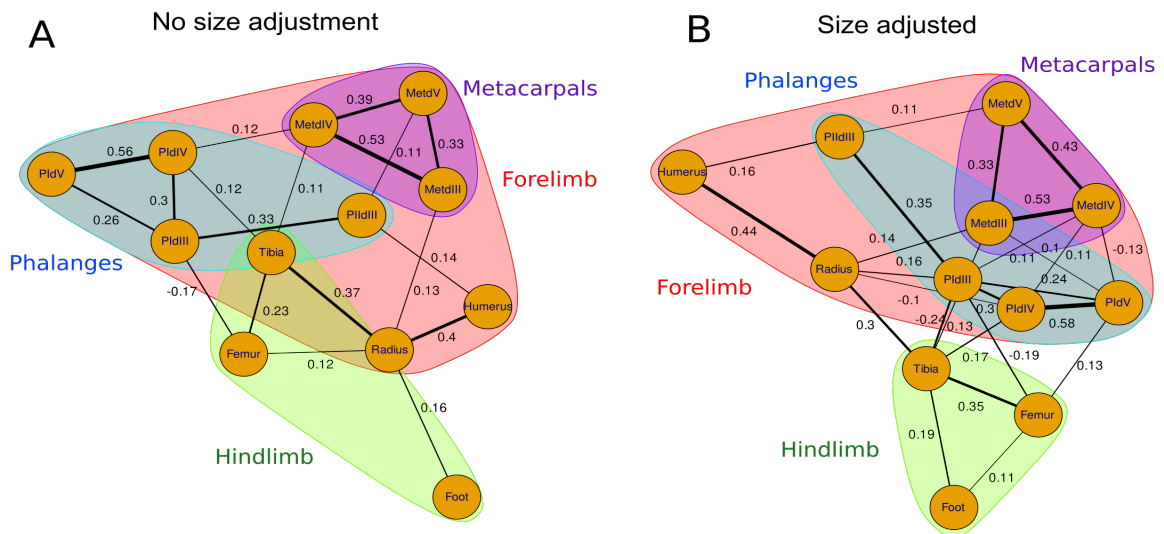
Figure 5: Independence graphs showing partial correlations among within-population limb element lengths with edge exclusion deviances above the 5% Chi-squared threshold. (A) without size adjustment and (B) with size adjustment (Burnaby projection). Phalanx names abbreviated as "P" followed by Roman numerals (I, II) and digit "d" followed by Roman numerals. Same pattern used for metacarpals, using "Met".

Evolutionary integration patterns

The evolutionary among-population patterns were more integrated than both the developmental and the static level. The Integration index was I = 0.769 for the non projected data and I = 0.360 for the size-adjusted data. For the non projected data, parallel analysis recovered a single PC (again, a general size variable). For the size-adjusted data, parallel analysis recovered three PCs. The first 2 PCs of the non projected data accounted for 87.69% of total variation among populations, with all variables associated with the positive direction of PC1 (size variation) (Figure 6A). The first 2 PCs of the size-adjusted data accounted for 56.17% of the total variation (Figure 6B): The first PC contrasts groups with a relatively larger forelimb autopodium and smaller stylopodium and zeugopodium (with positive association) versus groups with smaller forelimb autopodium and larger stylopodium and zeugopodium. The second size-adjusted PC contrasts forelimb and hindlimb, with the exception of one phalanx (PIdIV) that clusters with the hindlimb.
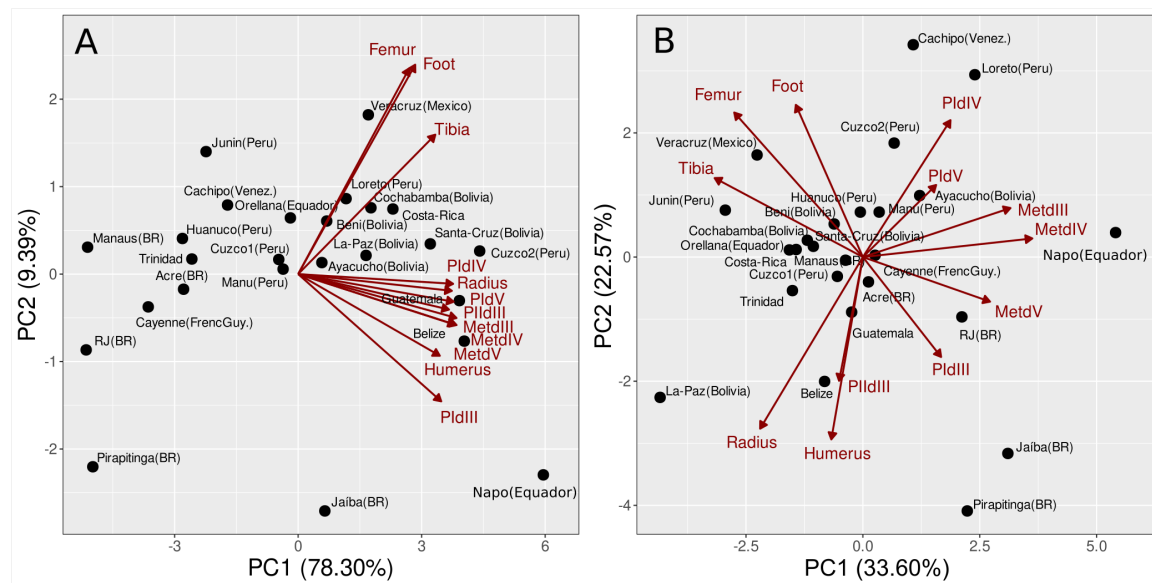
Figure 6: Principal component biplot for among-population limb measurement variation of *Carollia perspicillata*. (A) without size adjustment and (B) with size adjustment (Burnaby projection). Phalanx names abbreviated as "P" followed by Roman numerals (I, II) and digit "d" followed by Roman numerals. Same pattern used for metacarpals, using "Met".

The ordination of localities shows considerable overlap among geographically distant localities. The PC2 of non projected data and the PC1 of size-adjusted means contrast a large group of localities (Figure 7), belonging to different Neotropical Rain Forests, to two open environments (Estação ecológica de Pirapitinga, a savanna in the Cerrado; and Jaíba, a xeric woodland in the Caatinga) and Napo (North center of Ecuador; a locality represented by a single specimen in our sample, which makes it difficult to draw any interpretation). The specimens in open formations presents relatively shorter hindlimbs and longer handwings.

The independence graphs for among-population partial correlations indicate a high level of integration and, no clear modules were recovered (Figure 7A,B, Supplementary Tables S5 and S6). The correlations were moderate to high, and more uniform than at the static level. Again, no relevant differences were observed between the non projected and the size-adjusted data.
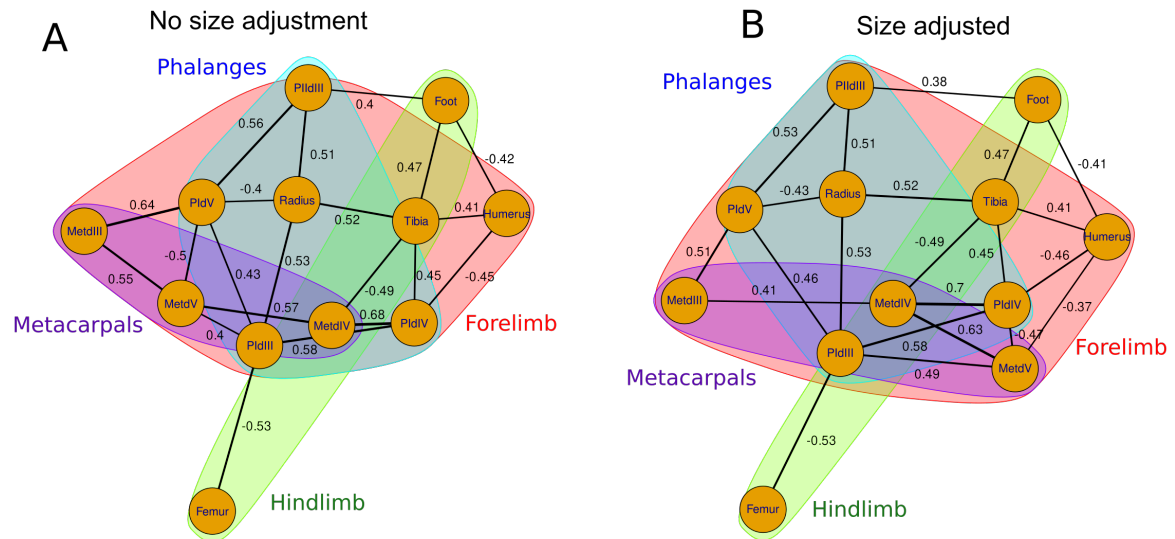
Figure 7: Independence graphs showing partial correlations for among-population limb element lengths with edge exclusion deviances above the 5% Chi-squared threshold. (A) without size adjustment and (B) with size adjustment (Burnaby projection). Phalanx names abbreviated as "P" followed by Roman numerals (I, II) and digit "d" followed by Roman numerals. Same pattern used for metacarpals, using "Met".

Levels of integration and development models

The repeatabilities based on partial correlation matrices ranged from 0.666 (developmental integration) to 0.934 (static integration) (Table 1). Matrix correlations among integration levels indicated stronger associations between adjacent levels. Developmental integration based on signed asymmetry was more closely associated with the static than with the evolutionary level of integration, even though there was some overlap between confidence intervals (Table 1). Evolutionary integration was more associated with the static level. Integration matrices based on size-adjusted data were highly similar to those based on non projected data at the same level, as expected with partial correlations.

Table 1: Matrix correlations between integration levels and theoretical models. Boldface diagonal numbers are matrix repeatabilities. Original correlations are below the diagonal, whereas correlations adjusted by Rmax are shown above the diagonal. Numbers within parentheses are 95% confidence intervals obtained by bootstrapping.

	Development	Static	Static size-adj	Evol.	Evol. size-adj.	Limb sodel	Serial sodel	Within-elements model
Development	**0.666**	0.371	0.342	0.201	0.226	0.185	0.031	0.229
		(0.153, 0.515)	(0.153, 0.481)	(0.001, 0.392)	(0.031, 0.414)	(0.047, 0.305)	(-0.113, 0.224)	(0.067, 0.435)
Static	0.291	**0.925**	1	0.387	0.408	0.257	0.115	0.695
	(0.120, 0.404)			(0.271, 0.517)	(0.286, 0.53)	(0.155, 0.368)	(0.012, 0.216)	(0.583, 0.781)
Static size-adjusted	0.270	0.959	**0.934**	0.444	0.47	0.315	0.094	0.732
	(0.121, 0.391)	(0.937, 0.983)		(0.337, 0.557)	(0.377, 0.585)	(0.219, 0.435)	(-0.007, 0.178)	(0.638, 0.788)
Evolutionary	0.147	0.334	0.385	**0.805**	1	0.171	-0.003	0.342
	(0.001, 0.287)	(0.234, 0.446)	(0.292, 0.483)			(0.03, 0.288)	(-0.191, 0.152)	(0.226, 0.379)
Evolutionary Size-adjusted	0.166	0.353	0.409	0.984	**0.811**	0.16	0.003	0.343
	(0.023, 0.304)	(0.248, 0.459)	(0.328, 0.509)	(0.975, 0.995)		(-0.038, 0.298)	(-0.185, 0.152)	(0.239, 0.445)
Limb model	0.151	0.247	0.304	0.153	0.144	1	*	*
	(0.038, 0.249)	(0.149, 0.354)	(0.212, 0.420)	(0.027, 0.258)	(-0.034, 0.268)			
Serial model	0.025	0.111	0.091	-0.003	0.003	*	1	*
	(-0.092, 0.183)	(0.012, 0.208)	(-0.007, 0.172)	(-0.171, 0.136)	(-0.167, 0.137)			
Within-elements model	0.187	0.668	0.707	0.307	0.309	*	*	1
	(0.055, 0.355)	(0.561, 0.781)	(0.638, 0.788)	(0.203, 0.340)	(0.215, 0.401)			

The within-elements model (which separates the phalanges and metacarpals from other forelimb elements) was the most correlated theoretical integration matrix with all levels, with the highest association observed at the static level (Table 1). The limb model was also associated with all integration levels, but with lower matrix correlations. The serial model was not associated with the development and evolutionary levels, and was weakly correlated with the static level.

Discussion

The appendicular skeleton of short-tailed bats becomes more integrated when moving from the developmental level to the evolutionary. This is expected, since at the evolutionary level, increased integration among elements belonging to different modules can happen due to them being jointly selected (Cheverud, 1996a), and even rearrangements of integration patterns would not be surprising (Monteiro *et al.*, 2005; Monteiro and Nogueira, 2010). Nevertheless, some modular structure is still retained and evident in the patterns of correlations. To the best of our knowledge, we describe for the first time the modular structure in serially homologous elements belonging to the extreme forelimb autopodium of bats (evident in the strong associations between integration patterns and the within-element model). Metacarpal bones are integrated among themselves, as are phalanges of digits III–V. We corroborate previous research that indicated that, in bats, the functional divergence between hind- and forelimb is associated with the reduction in the degree of integration between serially homologous limb bones (Young and Hallgrímsson, 2005; Bell *et al.*, 2011). The lack of partial correlations among fluctuating asymmetry values of homologous bones in the stilopodium and zeugopodium corroborates the hypothesis that the dissociation between fore- and hindlimb reflects a greater degree of developmental independence between them (Young *et al.*, 2009). On the other hand, the clustering of phalangeal asymmetries indicates that these bones are developed under a shared genetic architecture, even if the metacarpals are not (Kavanagh *et al.*, 2013; Parada *et al.*, 2022). The differences between the associations observed at the static and evolutionary levels suggest that selection coefficients overcome the development architecture in bat limbs.

Developmental integration and modularity

The segregation of asymmetries belonging to each limb set, indicates that the development of forelimb and hindlimb bones is relatively independent according to the rationale that fluctuating asymmetry correlations among traits arise from shared developmental pathways (Klingenberg, 2014). This result is a

morphological counterpart to a growing body of knowledge from a molecular point of view that indicates that, compared to the general pattern presented by mammals, bats present differential expression of regularly genes and transcriptomes associated with the development of each set of limbs (Sears *et al.*, 2006; Cooper and Sears, 2013; Eckalbar *et al.*, 2016; Petit *et al.*, 2017; Saxena and Cooper, 2021).

Static integration and modularity

The general pattern of within-population variation in limb measurements is strongly influenced by general size. Once size variation is statistically controlled, the clustering of variables indicates three main groups of variables aligned with different PCs, also evident in the independence graphs. Two autopodial modules were observed in the forelimb, one integrating the metacarpal measurements and one integrating the phalangeal ones (acropodium), and a third group, more loosely associated, is composed by stylopodium and zeugopodium elements of both limbs and the feet. Within the third group, the stronger correlations were observed within limbs. The tibia is the hindlimb bone most closely associated with forelimb elements. Radius and tibia share a large part of their genetic architecture as serial homologous elements (Sears *et al.*, 2015b; Eckalbar *et al.*, 2016); they were as strongly correlated as radius and humerus that, together with digit III bones, make up the wing's length and consequently are functionally associated through flight (Norberg, 1990). Because the tibia is not associated with forelimb elements in the developmental matrix, integration at higher levels might have to do with components being selected together.

A similar pattern of association between stylopodium and zeugopodium elements was observed by Young and Hallgrímsson(2005) with the congeneric species *Carollia brevicauda*. Stronger partial correlations were observed between elements belonging to the limb serial homologies (even though a relevant correlation had also been found between humerus and femur by the authors). Bell *et al.*(2011) analyzing five species of bats suggested that it is a general pattern in the order, as well as for Aves and Pterosauria, even thought they found some divergent results that cannot be biologically interpreted due to their small sample size (number of variables close to the number of specimens, especially for bats

and pterosaurs). This broad congruence in the pattern of association of limb parts among flying vertebrates indicates that the conquest of the air by vertebrates was allowed by the reduction in the degree of association between limb homologous structures of the limb (Young and Hallgrímsson, 2005; Bell *et al.*, 2011).

The autopodium has generally received less attention in previous research on patterns of integration and modularity of limbs. Instead, comparisons between the fore- and hind limbs predominate. (*e.g.* (Hallgrimsson *et al.*, 2002; Young and Hallgrímsson, 2005; Young *et al.*, 2009; Bell *et al.*, 2011; Martín-Serra *et al.*, 2015). The aim in these studies led to sampling designs that either did not include the limb segment (Young and Hallgrímsson, 2005; Martín-Serra *et al.*, 2015), did not include multiple digits (Hallgrimsson *et al.*, 2002; Young and Hallgrímsson, 2005), or faced sample-size limitations (Bell *et al.*, 2011). It prevented these studies from identifying modules integrating metacarpals and phalanges as observed here, compatible with what is expected according to the developmental genetics of these structures (Kavanagh *et al.*, 2013).

The studies that focused on the association patterns among autopodial bones *e.g.* primate hands (Kimura, 1973; Reno *et al.*, 2007), human feet (Arlegi *et al.*, 2023), and the gecko autopodium (Rothier *et al.*, 2022) found results similar to ours (recovered metacarpals and phalanges as part of discrete modules). Even for the extremely modified hand of bats, our results suggest that the adaptation for flight did not change this pattern.

Evolutionary integration and modularity

The evolutionary correlations of forelimb bones reveal a complex pattern of integration. These associations indicate that, in addition to developmental factors, selection coefficients act on patterns of integration between these bones (Monteiro *et al.*, 2005; Marroig *et al.*, 2009; Monteiro and Nogueira, 2010; Arlegi *et al.*, 2019). The difference from the modular pattern in phalanges and metacarpals, observed at the static level indicate the functional demands, resulting from flight in different environments, might have changed the covariation patterns among these bones. Functionally, neither metacarpals nor phalanges act as independent units to perform specific demands during flight, while on the other hand, different

structures along the wing control the generation of aerodynamic forces in a coordinated fashion (Norberg, 1990; Stockwell, 2001; Carneiro *et al.*, 2023).

The pattern of geographic variation in *C. perspicillata* previously observed for skull variables (McLellan, 1984) is complex and might be related to local adaptations (Wadgymar *et al.*, 2022). The ordination of localities along the non projected PC1 aligned with previous research on size variation, as we did not observe clear associations to elevational or latitudinal gradients. Populations in eastern Brazil and the Amazon basin present a negative association between size (body mass and forearm length), latitude, and elevation (Barros *et al.*, 2014). Analyses of the effects of environmental variation along the altitudinal gradient of Colombian Andes on forearm length indicates a positive association between size and altitude (Castillo-Figueroa, 2022). When the influence of general size variation is partialled out, it is evident that populations from localities with more cluttered vegetational formations, present relatively longer hindlimbs—which may improve flight performance (manouevering) in this vegetation type by supporting the camber of armwing along with digit V structures (Norberg, 1990). The ability to increase wing camber is directly associated with manoeuverability (Stockwell, 2001) and the cost of flying within cluttered habitat (Carneiro *et al.*, 2023).

It would be speculative and adaptationist to interpret each partial correlation at the evolutionary level as a functional association due to common selection. However, some of the associations are noteworthy due to flight mechanics. The strong association between PIdV and PIIdIII might be related to selection for camber. It is because the PIIdIII is subject to the bending forces from the dactylopatagium minus during the bending of the wings leading edge in downstroke (Norberg, 1990). The position of the joint between the metacarpal and phalange I of digit V (and consequentially the relative size of these two structures) is the main determinant of the capacity of bending the trailing edge of wing. The relatively strong association between radius and the phalanges of digit III may be related to selection acting on the wing span, as these variables are positioned along the longest axis of the wing (Norberg, 1990). The potential role of the hindlimb in bat flight aerodynamics is still poorly comprehended. Even though it is still difficult to measure the aerodynamic effects of hindlimb motion empirically, it is known that leg movements influence wing shape during flight, since the patagium is attached to the joint between femur and tibia (Cheney *et al.*, 2014). In this

context, the correlation between tibia and radius at both evolutionary and static levels may also be the product of selection related with flight performance.

Final remarks

The pattern of integration at the developmental level indicates a relative independence of developmental architecture among limbs in *C. perspicillata*. The dissociation of the modular pattern in the forelimb autopodium, along with other differences between static and evolutionary levels, indicates that selection acting within and among populations exceed developmental constraints on bat limbs. Future research on integration and modularity of bat limbs (using other widespread species as well as species with different flight patterns) may confirm the role of specific aerodynamic demands in the decoupling between the developmental and evolutionary patterns.

References

Adachi, N., Robinson, M., Goolsbee, A., Shubin, N.H. (2016). Regulatory evolution of Tbx5 and the origin of paired appendages. *Proceedings of the National Academy of Sciences* 113:10115–10120.

Arlegi, M., Pablos, A., Lorenzo, C. (2023). Evolutionary selection and morphological integration in the foot of modern humans. *American Journal of Biological Anthropology* 180:655–672.

Arlegi, M., Veschambre-Couture, C., Gómez-Olivencia, A. (2019). Evolutionary selection and morphological integration in the vertebral column of modern humans. *American Journal of Physical Anthropology* 171:17–36.

Ashley-Ross, M.A., Bechtel, B.F. (2004). Kinematics of the transition between aquatic and terrestrial locomotion in the newt *Taricha torosa*. *Journal of Experimental Biology* 207:461–474.

Barros, L.A.V.d., da Rocha Fortes, R., Lorini, M.L. (2014). The application of Bergmann's rule to *Carollia perspicillata* Linnaeus 1758(Mammalia, Chiroptera). *Chiroptera Neotropical* 20:1243–1251.

Bell, E., Andres, B., Goswami, A. (2011). Integration and dissociation of limb elements in flying vertebrates: a comparison of pterosaurs, birds and bats: Integration and dissociation of limb elements in flying vertebrates. *Journal of Evolutionary Biology* 24:2586–2599.

Boer, E.F., Van Hollebeke, H.F., Park, S., Infante, C.R., Menke, D.B., Shapiro, M.D. (2019). Pigeon foot feathering reveals conserved limb identity networks. *Developmental Biology* 454:128–144.

Carneiro, L.d.O., Mellado, B., Nogueira, M.R., Cruz-Neto, A.P.d., Monteiro, L.R. (2023). Flight performance and wing morphology in the bat *Carollia perspicillata*: biophysical models and energetics. *Integrative Zoology* 18:876–890.

Castillo-Figueroa, D. (2022). Does Bergmann's rule apply in bats? Evidence from two Neotropical species. *Neotropical Biodiversity* 8:200–221.

Cheney, J.A., Ton, D., Konow, N., Riskin, D.K., Breuer, K.S., Swartz, S.M. (2014). Hindlimb motion during steady flight of the lesser dog-faced fruit bat, *Cynopterus brachyotis*. *PLoS ONE* 9:e98093.

Cheverud, J.M. (1996a). Developmental integration and the evolution of pleiotropy. *The American Zoologist* 36:44–50.

Cheverud, J.M. (1996b). Quantitative genetic analysis of cranial morphology in the cotton-top (*Saguinus oedipus*) and saddle-back (*S. fuscicollis*) tamarins. *Journal of Evolutionary Biology* 9:5–42.

Cheverud, J.M., Rutledge, J.J., Atchley, W.R. (1983). Quantitative Genetics of development: genetic correlations among age-specific trait values and the evolution of ontogeny. *Evolution* 37:895–905.

Claude, J. (2008). *Morphometrics with R*. New York: Springer. 316 p.

Cooper, L.N., Sears, K.E. (2013). How to grow a bat wing. *In*: Rick A. Adams, S.C.P. (eds.) *Current Trends in Bat Evolution, Ecology, and Conservation*. New York: Springer. p. 3–20.

Csárdi, G. et al. (2024). igraph: Network Analysis and Visualization in R. https://CRAN.R-project.org/package=igraph.

Dinno, A. (2009). Exploring the sensitivity of Horn's parallel analysis to the distributional form of random data. *Multivariate Behavioral Research* 44:362–388.

Dinno, A. (2024). paran: Horn's test of principal components/factors. . . https://CRAN.R-project.org/package=paran.

Duclos, K.K., Hendrikse, J.L., Jamniczky, H.A. (2019). Investigating the evolution and development of biological complexity under the framework of epigenetics. *Evolution & Development* 21:276–293.

Eckalbar, W.L. et al. (2016). Transcriptomic and epigenomic characterization of the developing bat wing. *Nature Genetics* 48:528–536.

Goslee, S.C., Urban, D.L. (2007). The ecodist package for dissimilarity-based analysis of ecological data. *Journal of Statistical Software* 22:1–19.

Hall, B.K. (2015). *Bones and cartilage: developmental and evolutionary skeletal biology*. New York: Elsevier. 892 p.

Hall, B.K., Miyake, T. (2000). All for one and one for all: condensations and the initiation of skeletal development. *Bioessays* 22:138–147.

Hallgrímsson, B., Willmore, K., Hall, B.K. (2002). Canalization, developmental stability, and morphological integration in primate limbs. *American Journal of Physical Anthropology* 119:131–158.

Hendrikse, J.L., Parsons, T.E., Hallgrímsson, B. (2007). Evolvability as the proper focus of evolutionary developmental biology. *Evolution and Development* 9:393–401.

Howenstine, A.O., Sadier, A., Anthwal, N., Lau, C.L., Sears, K.E. (2021). Non-model systems in mammalian forelimb evo-devo. *Current Opinion in Genetics and Development* 69:65–71.

Huang, B., Mackem, S. (2021). Rethinking positional information and digit identity: The role of late interdigit signaling. *Developmental Dynamics* 251:1414–1422.

Husson, F., Le, S., Pagès, J. (2017). *Exploratory multivariate analysis by example using R*. New York: Chapman and Hall/CRC. 262 p.

Irschick, D.J., Higham, T.E. (2015). *Animal Athletes: An Ecological and Evolutionary Approach*. Oxford, United Kingdom: Oxford University Press. 255 p.

Kavanagh, K.D. et al. (2013). Developmental bias in the evolution of phalanges. *Proceedings of the National Academy of Sciences* 110:18190–18195.

Kim, S. (2015). ppcor: An R Package for a Fast Calculation to Semi-partial Correlation Coefficients. *Communications for Statistical Applications and Methods* 22:665–674.

Kimura, K. (1973). On the variability and correlation of the lengths of phalanges and metacarpals. *Journal of the Anthropological Society of Nippon* 81:174–184.

Klingenberg, C.P. (2008). Morphological integration and developmental modularity. *Annual Review of Ecology, Evolution, and Systematics* 39:115–132.

Klingenberg, C.P. (2014). Studying morphological integration and modularity at multiple levels: concepts and analysis. *Philosophical Transactions of the Royal Society B: Biological Sciences* 369:20130249.

Klingenberg, C.P. (2015). Analyzing fluctuating asymmetry with geometric morphometrics: concepts, methods, and applications. *Symmetry* 7:843–934.

Klingenberg, C.P. (2016). Size, shape, and form: concepts of allometry in geometric morphometrics. *Development Genes and Evolution* 226:113–137.

Lê, S., Josse, J., Husson, F. (2008). FactoMineR: A Package for Multivariate Analysis. *Journal of Statistical Software* 25:1–18.

Legendre, P., Legendre, L. (2012). *Numerical Ecology*. New York: Elsevier. 990 p.

Lieberman, D.E. (2013). *Story Of The Human Body*. New York: Knopf Doubleday Publishing Group. 480 p.

Magwene, P.M. (2001). New tools for studying integration and modularity. *Evolution* 55:1734–1745.

Maher, A.E. et al. (2022). Body size, shape and ecology in tetrapods. *Nature Communications* 13:4340.

Marroig, G., Cheverud, J.M. (2001). A comparison of phenotypic variation and covariation patterns and the role of phylogeny, ecology, and ontogeny during cranial evolution of New World monkeys. *Evolution* 55:2576–2600.

Marroig, G., Shirai, L.T., Porto, A., de Oliveira, F.B., De Conto, V. (2009). The Evolution of Modularity in the Mammalian Skull II: Evolutionary Consequences. *Evolutionary Biology* 36:136–148.

Martín-Serra, A., Figueirido, B., Pérez-Claros, J.A., Palmqvist, P. (2015). Patterns of morphological integration in the appendicular skeleton of mammalian carnivores. *Evolution* 69:321–340.

McLellan, L., Koopman, K. (2007). Subfamily Carolliinae Miller, 1924. *In*: (eds.) *Mammals of South America*. : The University of Chicago Press. p. 208–218.

McLellan, L.J. (1984). A morphometric analysis of *Carollia* (Chiroptera, Phyllostomidae). *American Museum novitates* :1–35.

Melo, D., Porto, A., Cheverud, J.M., Marroig, G. (2016). Modularity: genes, development, and evolution. *Annual Review of Ecology, Evolution, and Systematics* 47:463–486.

Michaud, M., Veron, G., Fabre, A. (2020). Phenotypic integration in feliform carnivores: Covariation patterns and disparity in hypercarnivores versus generalists. *Evolution* 74:2681–2702.

Monteiro, L.R., Bonato, V., Reis, S.F. (2005). Evolutionary integration and morphological diversification in complex morphological structures: mandible

shape divergence in spiny rats (Rodentia, Echimyidae). *Evolution & Development* 7:429–439.

Monteiro, L.R., Nogueira, M.R. (2010). Adaptive radiations, ecological specialization, and the evolutionary integration of complex morphological structures. *Evolution* 64:724–744.

Norberg, U.M. (1990). *Vertebrate Flight*. Heidelberg, Germany: Springer Berlin Heidelberg. 291 p.

Olson, M.E. (2019). Spandrels and trait delimitation: No such thing as "architectural constraint". *Evolution and Development* 21:59–71.

Parada, C. et al. (2022). Mechanical feedback defines organizing centers to drive digit emergence. *Developmental Cell* 57:854–866.e6.

Peres-Neto, P.R., Jackson, D.A., Somers, K.M. (2005). How many principal components? stopping rules for determining the number of non-trivial axes revisited. *Computational Statistics & Data Analysis* 49:974–997.

Petit, F., Sears, K.E., Ahituv, N. (2017). Limb development: a paradigm of gene regulation. *Nature Reviews Genetics* 18:245–258.

Reno, P.L., McCollum, M.A., Cohn, M.J., Meindl, R.S., Hamrick, M., Lovejoy, C.O. (2007). Patterns of correlation and covariation of anthropoid distal forelimb segments correspond to Hoxd expression territories. *Journal of Experimental Zoology Part B: Molecular and Developmental Evolution* 310B:240–258.

Rothier, P.S., Simon, M.N., Marroig, G., Herrel, A., Kohlsdorf, T. (2022). Development and function explain the modular evolution of phalanges in gecko lizards. *Proceedings of the Royal Society B: Biological Sciences* 289:.

Saxena, A., Cooper, K.L. (2021). Diversification of the vertebrate limb: sequencing the events. *Current Opinion in Genetics Development* 69:42–47.

Sears, K.E., Behringer, R.R., Rasweiler, J.J., Niswander, L.A. (2006). Development of bat flight: morphologic and molecular evolution of bat wing digits. *Proceedings of the National Academy of Sciences* 103:6581–6586.

Sears, K.E., Capellini, T.D., Diogo, R. (2015b). On the serial homology of the pectoral and pelvic girdles of tetrapods. *Evolution* 69:2543–2555.

Sears, K.E. et al. (2015a). The relationship between gene network structure and expression variation among individuals and species. *PLOS Genetics* 11:e1005398.

Shipley, B. (2016). *Cause and correlation in biology: a user's guide to path analysis, structural equations and causal inference with R*. Cambridge: Cambridge University Press. 299 p.

Stockwell, E.F. (2001). Morphology and flight manoeuvrability in New World leaf-nosed bats (Chiroptera: Phyllostomidae). *Journal of Zoology* 254:505–514.

Tickle, C. (2015). How the embryo makes a limb: determination, polarity and identity. *Journal of Anatomy* 227:418–430.

Tsutsumi, R., Eiraku, M. (2023). How might we build limbs in vitro informed by the modular aspects and tissue-dependency in limb development?. *Frontiers in Cell and Developmental Biology* 11:1135784.

Wadgymar, S.M., DeMarche, M.L., Josephs, E.B., Sheth, S.N., Anderson, J.T. (2022). Local Adaptation: Causal Agents of Selection and Adaptive Trait Divergence. *Annual Review of Ecology, Evolution, and Systematics* 53:87–111.

Wasserstein, R.L., Schirm, A.L., Lazar, N.A. (2019). Moving to a world beyond " p < 0.05". *The American Statistician* 73:1–19.

Wimberly, A.N., Slater, G.J., Granatosky, M.C. (2021). Evolutionary history of quadrupedal walking gaits shows mammalian release from locomotor constraint. *Proceedings of the Royal Society B: Biological Sciences* 288:20210937.

Young, N.M., Hallgrímsson, B. (2005). Serial homology and the evolution of mammalian limb covariation structure. *Evolution* 59:2691.

Young, N.M., Hallgrímsson, B., Garland, T. (2009). Epigenetic effects on integration of limb lengths in a mouse model: selective breeding for high voluntary locomotor activity. *Evolutionary Biology* 36:88–99.

Young, N.M., Wagner, G.P., Hallgrímsson, B. (2010). Development and the evolvability of human limbs. *Proceedings of the National Academy of Sciences* 107:3400–3405.

Zelditch, M.L., Goswami, A. (2021). What does modularity mean?. *Evolution and Development* 23:377–403.

Supplementary Materials for chapter 3:

Developmental architecture and morphological evolution in the wing of bat *Carollia perspicillata*

Lucas Carneiro, Bruce D. Patterson, Leandro R. Monteiro

Supplementary Table S1 – Theoretical matrices for the different models of development (limb homology, serial element homology, and within-limb elements separating phalanges from the metacarpals.

Limb Model											
	Humerus	Radius	MetdIII	PIdIII	PIIdIII	MetdIV	PIdIV	MetdV	PIdV	Femur	Tibia	Foot
Humerus	1											
Radius	1	1										
MetdIII	1	1	1									
PIdIII	1	1	1	1								
PIIdIII	1	1	1	1	1							
MetdIV	1	1	1	1	1	1						
PIdIV	1	1	1	1	1	1	1					
MetdV	1	1	1	1	1	1	1	1				
PIdV	1	1	1	1	1	1	1	1	1			
Femur	0	0	0	0	0	0	0	0	0	1		
Tibia	0	0	0	0	0	0	0	0	0	1	1	
Foot	0	0	0	0	0	0	0	0	0	1	1	1

Serial homology model											
	Humerus	Radius	MetdIII	PIdIII	PIIdIII	MetdIV	PIdIV	MetdV	PIdV	Femur	Tibia	Foot
Humerus	1											
Radius	0	1										
MetdIII	0	0	1									
PIdIII	0	0	1	1								
PIIdIII	0	0	1	1	1							
MetdIV	0	0	1	1	1	1						
PIdIV	0	0	1	1	1	1	1					
MetdV	0	0	1	1	1	1	1	1				
PIdV	0	0	1	1	1	1	1	1	1			
Femur	1	0	1	1	1	1	1	1	1	1		
Tibia	0	1	1	1	1	1	1	1	1	1	1	
Foot	0	0	1	1	1	1	1	1	1	1	0	1

Within-element model

	Humerus	Radius	MetdIII	PIdIII	PIIdIII	MetdIV	PIdIV	MetdV	PIdV	Femur	Tibia	Foot
Humerus	1											
Radius	1	1										
MetdIII	0	1	1									
PIdIII	0	0	0	1								
PIIdIII	0	0	0	1	1							
MetdIV	0	0	1	0	0	1						
PIdIV	0	0	0	1	1	0	1					
MetdV	0	0	1	0	0	1	0	1				
PIdV	0	0	0	1	1	0	1	0	1			
Femur	0	0	0	0	0	0	0	0	0	1		
Tibia	0	0	0	0	0	0	0	0	0	1	1	
Foot	0	0	0	0	0	0	0	0	0	1	1	1

Supplementary Table S2 – Correlations, partial correlations, and edge exclusion deviances calculated for the signed individual trait asymmetries (R - L) (Developmental integration level) of *Carollia perspicillata*. Deviances in boldface are above the 2.7 threshold (10%) of the Chi-squared distribution.

Correlations												
	Humerus	Radius	MetdIII	PIdIII	PIIdIII	MetdIV	PIdIV	MetdV	PIdV	Femur	Tibia	Foot
Humerus	1.000											
Radius	0.050	1.000										
MetdIII	0.116	-0.045	1.000									
PIdIII	-0.066	0.063	0.009	1.000								
PIIdIII	-0.017	-0.210	0.034	-0.132	1.000							
MetdIV	-0.013	0.087	0.155	0.074	-0.009	1.000						
PIdIV	-0.055	0.007	-0.101	0.023	0.067	0.114	1.000					
MetdV	0.059	0.061	0.029	0.067	0.081	0.181	-0.021	1.000				
PIdV	-0.071	0.085	-0.094	0.104	-0.024	-0.007	0.114	-0.123	1.000			
Femur	-0.102	0.096	0.047	0.047	-0.061	0.135	-0.014	0.104	0.021	1.000		
Tibia	0.050	-0.002	-0.065	-0.081	-0.058	-0.010	-0.003	-0.013	-0.073	-0.007	1.000	
Foot	-0.027	0.005	0.050	-0.068	0.009	-0.070	-0.081	0.001	-0.031	0.034	-0.171	1.000

Partial correlations above diagonal, EED below diagonal												
	Humerus	Radius	MetdIII	PIdIII	PIIdIII	MetdIV	PIdIV	MetdV	PIdV	Femur	Tibia	Foot
Humerus	*	0.067	0.123	-0.065	-0.024	-0.028	-0.035	0.069	-0.041	-0.114	0.042	-0.033
Radius	1.219	*	-0.055	0.020	-0.202	0.072	0.004	0.063	0.084	0.075	-0.008	0.017
MetdIII	**4.142**	0.830	*	0.020	0.034	0.171	-0.106	-0.028	-0.077	0.044	-0.064	0.044
PIdIII	1.144	0.107	0.108	*	-0.136	0.042	0.009	0.081	0.096	0.015	-0.089	-0.079
PIIdIII	0.150	**11.292**	0.312	**5.044**	*	-0.010	0.076	0.111	0.010	-0.049	-0.066	-0.006
MetdIV	0.215	1.412	**7.965**	0.487	0.028	*	0.132	0.166	-0.003	0.104	-0.004	-0.072
PIdIV	0.325	0.005	**3.040**	0.024	1.550	**4.724**	*	-0.033	0.096	-0.023	-0.006	-0.064
MetdV	1.278	1.064	0.205	1.786	**3.376**	**7.504**	0.297	*	-0.131	0.090	-0.011	0.009
PIdV	0.458	1.929	1.602	2.502	0.029	0.002	2.496	**4.648**	*	0.025	-0.074	-0.028
Femur	**3.530**	1.508	0.534	0.060	0.659	**2.959**	0.141	2.197	0.166	*	0.011	0.038
Tibia	0.479	0.019	1.124	2.166	1.190	0.005	0.011	0.031	1.484	0.032	*	-0.176
Foot	0.289	0.075	0.528	1.675	0.008	1.420	1.122	0.020	0.219	0.385	**8.479**	*

Supplementary Table S3 – Correlations, partial correlations, and edge exclusion deviances (EED) calculated for the symmetrized traits ((R+L)/2) of *Carollia perspicillata*. Correlated data are residuals from a multivariate linear model with sex and geographic location as independent variables (Static integration level – no size adjustment). Deviances in boldface are above the 3.84 threshold (5%) of the Chi-squared distribution.

Correlations

	Humerus	Radius	MetdIII	PIdIII	PIIdIII	MetdIV	PIdIV	MetdV	PIdV	Femur	Tibia	Foot
Humerus	1.000											
Radius	0.760	1.000										
MetdIII	0.651	0.821	1.000									
PIdIII	0.591	0.669	0.702	1.000								
PIIdIII	0.611	0.654	0.696	0.788	1.000							
MetdIV	0.673	0.823	0.942	0.728	0.717	1.000						
PIdIV	0.575	0.669	0.719	0.844	0.746	0.737	1.000					
MetdV	0.648	0.798	0.915	0.706	0.705	0.923	0.693	1.000				
PIdV	0.599	0.688	0.711	0.834	0.738	0.714	0.889	0.687	1.000			
Femur	0.556	0.668	0.631	0.463	0.512	0.626	0.539	0.582	0.549	1.000		
Tibia	0.640	0.821	0.778	0.608	0.614	0.783	0.658	0.735	0.639	0.678	1.000	
Foot	0.376	0.514	0.450	0.449	0.388	0.476	0.451	0.468	0.442	0.385	0.474	1.000

Partial correlations above diagonal, EED below diagonal

	Humerus	Radius	MetdIII	PIdIII	PIIdIII	MetdIV	PIdIV	MetdV	PIdV	Femur	Tibia	Foot
Humerus	*	0.403	-0.078	0.032	0.141	0.066	-0.040	0.013	0.048	0.080	-0.015	-0.062
Radius	**48.858**	*	0.125	0.061	-0.050	0.040	-0.098	0.083	0.094	0.121	0.367	0.165
MetdIII	1.668	**4.356**	*	-0.047	-0.011	0.529	0.009	0.334	0.089	0.069	0.082	-0.094
PIdIII	0.284	1.040	0.617	*	0.335	0.072	0.303	0.056	0.256	-0.171	-0.061	0.077
PIIdIII	**5.562**	0.689	0.034	**32.849**	*	0.033	0.079	0.110	0.057	0.069	0.026	-0.051
MetdIV	1.212	0.442	**90.469**	1.415	0.299	*	0.119	0.394	-0.099	0.026	0.109	0.034
PIdIV	0.440	2.665	0.021	**26.589**	1.714	**3.924**	*	-0.072	0.563	0.040	0.124	0.048
MetdV	0.047	1.895	**32.693**	0.881	3.366	**46.579**	1.439	*	0.004	-0.060	-0.053	0.073
PIdV	0.624	2.424	2.211	**18.701**	0.894	2.720	**105.011**	0.005	*	0.097	-0.048	0.006
Femur	1.793	**4.095**	1.333	**8.161**	1.336	0.181	0.444	0.987	2.623	*	0.233	0.046
Tibia	0.063	**39.929**	1.853	1.035	0.185	3.303	**4.247**	0.785	0.637	**15.376**	*	0.063
Foot	1.063	**7.596**	2.474	1.629	0.709	0.324	0.645	1.457	0.009	0.572	1.105	*

Supplementary Table S4 – Correlations, partial correlations, and edge exclusion deviances (EED) calculated for the size-adjusted symmetrized traits of *Carollia perspicillata*. Correlated data are projections of original data to a space orthogonal to the within-population size vector (Static integration level – size adjusted). Deviances in boldface are above the 3.84 threshold (5%) of the Chi-squared distribution.

Correlations												
	Humerus	Radius	MetdIII	PIdIII	PIIdIII	MetdIV	PIdIV	MetdV	PIdV	Femur	Tibia	Foot
Humerus	1.000											
Radius	0.277	1.000										
MetdIII	-0.342	-0.337	1.000									
PIdIII	-0.018	-0.163	-0.172	1.000								
PIIdIII	0.031	-0.260	-0.243	0.473	1.000							
MetdIV	-0.264	-0.368	0.362	0.008	-0.104	1.000						
PIdIV	-0.084	-0.240	-0.195	0.536	0.312	-0.140	1.000					
MetdV	-0.268	-0.354	0.252	0.022	-0.052	0.374	-0.209	1.000				
PIdV	-0.033	-0.170	-0.209	0.504	0.286	-0.245	0.705	-0.208	1.000			
Femur	-0.004	-0.020	-0.301	-0.342	-0.184	-0.430	-0.053	-0.458	-0.006	1.000		
Tibia	-0.017	0.123	-0.243	-0.389	-0.259	-0.385	-0.042	-0.466	-0.065	0.389	1.000	
Foot	-0.060	0.002	-0.221	-0.036	-0.067	-0.206	0.087	-0.167	0.089	0.155	0.209	1.000

Partial correlations above diagonal, EED below diagonal												
	Humerus	Radius	MetdIII	PIdIII	PIIdIII	MetdIV	PIdIV	MetdV	PIdV	Femur	Tibia	Foot
Humerus	*	0.435	-0.063	0.016	0.158	0.065	-0.031	-0.008	0.040	0.076	0.015	-0.048
Radius	**57.928**	*	0.143	0.156	-0.072	0.082	-0.100	0.078	0.038	0.077	0.301	0.062
MetdIII	1.088	**5.724**	*	-0.066	-0.012	0.526	0.022	0.325	0.098	0.074	0.128	-0.078
PIdIII	0.072	**6.768**	1.217	*	0.349	0.114	0.304	0.068	0.237	-0.189	-0.239	0.024
PIIdIII	**7.011**	1.454	0.042	**35.781**	*	0.055	0.080	0.108	0.047	0.073	0.022	-0.027
MetdIV	1.170	1.857	**89.273**	3.593	0.824	*	0.114	0.429	-0.134	0.010	0.044	0.006
PIdIV	0.262	2.787	0.138	**26.748**	1.782	3.601	*	-0.088	0.575	0.028	0.173	0.051
MetdV	0.019	1.689	**30.908**	1.297	3.215	**56.178**	**2.125**	*	0.033	-0.052	-0.087	0.072
PIdV	0.444	0.399	2.654	**15.973**	0.615	**4.999**	**110.945**	0.295	*	0.134	0.012	0.050
Femur	1.592	1.652	1.533	**9.994**	1.460	0.026	0.224	0.760	**4.975**	*	0.348	0.108
Tibia	0.060	**26.134**	**4.587**	**16.260**	0.137	0.531	**8.383**	2.107	0.043	**35.621**	*	0.188
Foot	0.626	1.072	1.704	0.163	0.203	0.009	0.732	1.423	0.692	3.212	**9.980**	*

Supplementary Table S5 – Correlations, partial correlations, and edge exclusion deviances (EED) calculated for the symmetrized traits ((R+L)/2) of *Carollia perspicillata*. Correlated data are means for each geographic location (Evolutionary integration level). Deviances in boldface are above the 3.84 threshold (5%) of the Chi-squared distribution.

Correlations												
	Humerus	Radius	MetdIII	PIdIII	PIIdIII	MetdIV	PIdIV	MetdV	PIdV	Femur	Tibia	Foot
Humerus	1.000											
Radius	0.883	1.000										
MetdIII	0.822	0.857	1.000									
PIdIII	0.780	0.827	0.842	1.000								
PIIdIII	0.852	0.897	0.854	0.796	1.000							
MetdIV	0.807	0.870	0.982	0.862	0.867	1.000						
PIdIV	0.708	0.806	0.925	0.870	0.804	0.941	1.000					
MetdV	0.809	0.883	0.975	0.848	0.860	0.983	0.902	1.000				
PIdV	0.786	0.807	0.937	0.859	0.858	0.919	0.938	0.882	1.000			
Femur	0.507	0.653	0.614	0.390	0.564	0.586	0.640	0.592	0.620	1.000		
Tibia	0.695	0.807	0.709	0.609	0.701	0.687	0.747	0.690	0.742	0.829	1.000	
Foot	0.378	0.559	0.585	0.384	0.595	0.600	0.638	0.577	0.595	0.697	0.708	1.000

Partial correlations above diagonal, EED below diagonal

	Humerus	Radius	MetdIII	PIdIII	PIIdIII	MetdIV	PIdIV	MetdV	PIdV	Femur	Tibia	Foot
Humerus	*	0.102	0.275	0.240	0.345	0.309	-0.449	-0.356	-0.066	0.012	0.411	-0.421
Radius	0.261	*	-0.013	0.529	0.509	0.331	-0.312	-0.071	-0.396	0.358	0.517	-0.170
MetdIII	1.963	0.004	*	-0.265	-0.329	0.240	-0.055	0.549	0.638	0.017	-0.060	-0.016
PIdIII	1.480	**8.219**	1.824	*	-0.269	-0.342	0.579	0.403	0.427	-0.532	-0.270	-0.078
PIIdIII	3.164	**7.513**	2.869	1.877	*	-0.107	0.058	0.291	0.555	-0.177	-0.366	0.396
MetdIV	2.516	2.893	1.484	3.105	0.288	*	0.685	0.574	0.080	-0.276	-0.487	0.307
PIdIV	**5.641**	2.562	0.076	**10.196**	0.085	**15.829**	*	-0.338	0.120	0.325	0.446	-0.098
MetdV	3.389	0.125	**8.965**	**4.442**	2.213	**9.986**	3.039	*	-0.495	0.199	0.262	-0.157
PIdV	0.110	**4.265**	**13.040**	**5.042**	**9.225**	0.160	0.360	**7.028**	*	0.186	0.267	-0.101
Femur	0.003	3.420	0.008	**8.324**	0.794	1.978	2.799	1.013	0.881	*	0.180	0.129
Tibia	**4.616**	**7.768**	0.089	1.895	3.590	**6.755**	**5.541**	1.772	1.846	0.820	*	0.471
Foot	**4.880**	0.737	0.007	0.151	**4.261**	2.480	0.242	0.622	0.257	0.420	**6.277**	*

Supplementary Table S6 – Correlations, partial correlations, and edge exclusion deviances (EED) calculated for the size-adjusted symmetrized traits ((R+L)/2) of *Carollia perspicillata*. Correlated data are population means of projections of original data to a space orthogonal to the within-population size vector (Evolutionary integration level – size adjusted). Deviances in boldface are above the 3.84 threshold (5%) of the Chi-squared distribution.

Correlations

	Humerus	Radius	MetdIII	PIdIII	PIIdIII	MetdIV	PIdIV	MetdV	PIdV	Femur	Tibia	Foot
Humerus	1.000											
Radius	0.399	1.000										
MetdIII	-0.101	-0.686	1.000									
PIdIII	0.135	0.184	-0.019	1.000								
PIIdIII	0.321	0.326	-0.277	0.119	1.000							
MetdIV	-0.238	-0.507	0.674	0.217	-0.139	1.000						
PIdIV	-0.490	-0.514	0.251	0.369	-0.244	0.442	1.000					
MetdV	-0.229	-0.228	0.380	0.244	-0.131	0.625	0.007	1.000				
PIdV	-0.078	-0.490	0.360	0.338	0.106	0.195	0.550	-0.167	1.000			
Femur	-0.293	-0.081	-0.396	-0.596	-0.280	-0.605	-0.075	-0.559	-0.157	1.000		
Tibia	-0.036	0.213	-0.603	-0.255	-0.151	-0.758	-0.054	-0.634	-0.069	0.599	1.000	
Foot	-0.478	-0.186	-0.260	-0.398	0.022	-0.173	0.120	-0.244	-0.027	0.430	0.407	1.000

Partial correlations above diagonal, EED below diagonal

	Humerus	Radius	MetdIII	PIdIII	PIIdIII	MetdIV	PIdIV	MetdV	PIdV	Femur	Tibia	Foot
Humerus	*	0.107	0.256	0.236	0.330	0.297	-0.456	-0.374	-0.014	0.005	0.409	-0.412
Radius	0.286	*	-0.040	0.529	0.514	0.329	-0.313	-0.063	-0.430	0.356	0.516	-0.167
MetdIII	1.695	0.040	*	-0.291	-0.259	0.405	-0.047	0.281	0.510	0.060	-0.043	-0.117
PIdIII	1.435	8.192	2.213	*	-0.265	-0.339	0.581	0.495	0.460	-0.531	-0.269	-0.085
PIIdIII	2.880	7.674	1.733	1.826	*	-0.077	0.066	0.205	0.528	-0.169	-0.365	0.379
MetdIV	2.309	2.870	4.489	3.051	0.147	*	0.698	0.633	0.008	-0.271	-0.486	0.292
PIdIV	5.829	2.585	0.056	10.294	0.109	16.706	*	-0.474	0.120	0.328	0.448	-0.103
MetdV	3.760	0.099	2.060	7.011	1.075	12.804	6.347	*	-0.282	0.216	0.310	-0.089
PIdV	0.005	5.108	7.535	5.930	8.166	0.002	0.363	2.065	*	0.182	0.279	-0.042
Femur	0.001	3.396	0.090	8.280	0.726	1.905	2.839	1.197	0.839	*	0.182	0.123
Tibia	4.570	7.743	0.046	1.874	3.581	6.745	5.592	2.518	2.033	0.846	*	0.470
Foot	4.647	0.709	0.342	0.181	3.873	2.233	0.267	0.200	0.044	0.380	6.246	*

Capítulo 4: Multilevel integration analysis of bat skulls: from development to evolutionary patterns in short-tailed bats.

Lucas Carneiro[a,b], Bruce D. Patterson[b], Marcelo R. Nogueira[a], Leandro R. Monteiro[a]

(a) Laboratório de Ciências Ambientais, Universidade Estadual do Norte Fluminense Darcy Ribeiro, Campos dos Goytacazes, Brasil; (b) Negaunee Integrative Research Center, Field Museum of Natural History, Chicago, USA.

Abstract

The mammalian skull is a classic model for the study of morphological evolution. The morphological diversification of cranial structures allowed ecological and sensory diversification of different mammalian lineages. The skull is formed by the cranium and mandible, which are complex structures themselves. The relationships between these components during mammalian diversification has attracted the interest of evolutionary biologists and has been studied under the prism of integration and modularity. A notable case of diversification in this group is the adaptive radiation of phyllostomid bats. The aim of this work is to analyze the patterns of integration and modularity in the skull of the phyllostomid bat *Carollia perspicillata*. We compared the cranial and mandibular integration at the developmental (measured as fluctuating asymmetry correlations), static (within-population correlations), evolutionary level (among-population correlations) and also compared the intraspecific integration patterns those of with phyllostomid clades/guilds at higher levels. At the developmental level, there was integration between adjacent morphogenetic components, which might be result of coordinated signaling and shared developmental pathways during morphogenesis. Cranium and mandible were poorly integrated at this level. The static level presented a similar structure of association, as an indicative that developmental processes prevail at this level. The pattern of integration was stronger and more complex at the evolutionary, indicating of the influence of selection gradients and functional demands at this level of integration. The comparison between the

intraspecific patterns of integration with the macroevolutionary patterns shows similarities between the developmental and the static patterns of *C. perspicillata* with static (within-species) level of nectarivorous bats. The intraspecific static and evolutionary levels were both associated with the evolutionary (among species) matrix of more specialized frugivorous bats (Stenodermatinae). These results indicate that development structures the integration pattern at the static level. At the evolutionary (among populations) level, selection gradients, probably related with diet, might strengthen the integration among components that are not developmentally integrated.

Keywords: Morphological integration; modularity; developmental instability; skull; mandible, diet.

Introduction

The mammalian skull is composed by complex morphological structures—cranium and mandible (Hallgrímsson *et al.*, 2006; Koyabu, 2023). Viscerocranium (originated from cell condensations from the neural crest) and neurocranium—originated from the paraxial mesoderm (Hall, 2015) are the two main components of the cranium. The mandible can be decomposed into different morphogenetic components: ramus, alveolar bone (anterior and posterior associated with the teeth), and three posterior processes. Each of these elements represents a unit derived from a specific cell condensation originated in the neural crest (Hall, 2015). The viscerocranium comprehends the rostrum area and is functionally associated with the acquisition and processing of food, while the neurocranium is responsible for support and protection of sensory structures and the brain (Richtsmeier and Flaherty, 2013; Law *et al.*, 2022). The mandible plays a central role in chewing, since it is the mobile complex of the cranium (Anthwal and Tucker, 2022).

The diversification of mammals is partly attributed to the morphological diversity of cranial structures, as morphological specialization to specific ecological niches promoted diversification in some lineages (Monteiro and Nogueira, 2010; Álvarez *et al.*, 2013; Rossoni *et al.*, 2019; Meloro and Tamagnini, 2021). As selection can organize the association patterns of morphological characters that

comprehend the skull and mandible, the patterns of integration and modularity of those structures are associated with their evolutionary potential (Monteiro and Nogueira, 2010; Rossoni *et al.*, 2019; Rossoni *et al.*, 2024). This is due to modular patterns allowing for greater flexibility in the response to selection and consequently leading to higher evolvability (Zelditch and Goswami, 2021).

The evolution of phyllostomid bats is characterized by a remarkable adaptive radiation (Fleming *et al.*, 2020). The family has at least 230 species (Mammal Diversity Database, 2024) and its taxonomic diversity is characterized by extreme morphologic and ecological diversity (Fleming *et al.*, 2020). In terms of diets, species in this group range from the completely liquid sanguivory (Zepeda Mendoza *et al.*, 2018), to extreme durophagy, like carnivory (Gual-Suárez and Medellín, 2021) or granivory (Nogueira *et al.*, 2005). In terms of roosting, the family is also diverse, compared to other bat lineages. Phyllostomidae bat species use different types of available roosts in the environment (foliage, cavities in standing trees, fallen trees, earth banks, animal burrows, caves or abandoned human structures) or actively built their roosts (tents in the foliage or cavities excavated in arboreal insect nests) (Voss *et al.*, 2016).

The role of major ecological differentiation on phyllostomid morphological diversification in the evolutionary level was successfully demonstrated. This adaptive radiation was preceded by strong selection gradients associated with the major dietary transitions (Monteiro and Nogueira, 2010; Monteiro and Nogueira, 2011; Rossoni *et al.*, 2019; Grossnickle *et al.*, 2024), as well as associated with differences in roosting ecology (Rossoni *et al.*, 2019). Morphological modifications, related to the major ecological differences in this group, were associated with changes in patterns of integration and modularity between cranial structures (Monteiro and Nogueira, 2010; Rossoni *et al.*, 2019).

Effects of ecological shifts on morphological divergence are frequently based on comparative datasets (Esteve-Altava, 2017), even though most literature compares the patterns of variation computed within-populations (static) at the evolutionary level (Klingenberg, 2014). Yet, It is noteworthy that the intraspecific and developmental patterns are the primary source of variation for evolutionary diversification at the macroevolutionary scale (Rolland *et al.*, 2023). On the other hand, it has been shown that evolutionary processes, such as genetic drift, inbreeding depression (Martín-Serra *et al.*, 2019; Loy *et al.*, 2021), and selection

gradients (Milošević-Zlatanović *et al.*, 2022) can lead to modifications in patterns of associations between cranial traits.

In the present study, we analyzed the patterns of integration and modularity in the skull and mandible of the widespread phyllostomid bat, *Carollia perspicillata*, from different localities across its distribution range in the Neotropical region. We compared the association between elements belonging to these complex structures at the developmental (within-individual variation, measured as fluctuation asymmetry), static (within-population variation), and evolutionary level (among populations). We then compared these intraspecific integration patterns with higher levels obtained from the literature (Monteiro and Nogueira, 2010). This multi-level approach is expected to help elucidate the role of different sources of variation and association between morphogenetic components forming the skull.

Material and methods

Data collection and validation of asymmetry measurements

We examined a sample composed by 309 adult specimens of *Carolllia perspicillata* (collected in 35 localities across the specie's distribution) for which both skull and mandible were available in natural history collections—Adriano Lúcio Peracchi Mammal Collection (Universidade Federal Rural do Rio de Janeiro), American Museum of Natural History Mammal Collection, Field Museum of Natural History Mammal Collection, and Universidade Estadual do Norte Fluminense Darcy Ribeiro Mammal Collection.

The shape of biological structures was measured from two-dimensional coordinates of anatomical landmarks located at the ventral view of the skull and both left and right lateral views of the mandible (Figure 1). Information about data collection and asymmetry validations provided in chapter two.
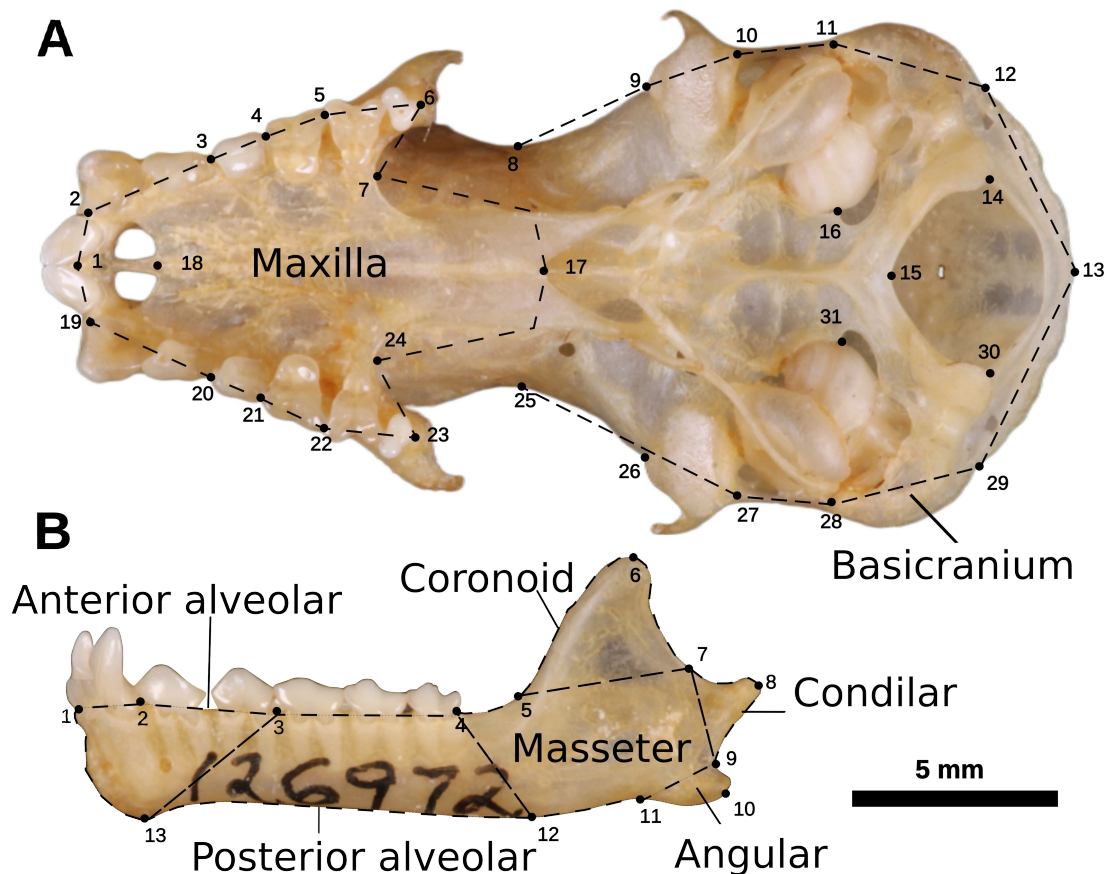
Figure 1: Landmarks digitized in the ventral cranium and lateral view of the mandible of *Carollia perspicillata*. Dashed lines indicate boundaries of morphogenetic components that were used as traits in our analyses.

Associations between morphogenetic units and integration of shape

We used the combination of methodologies proposed by Monteiro *et al.* (2005) and Klingenberg(2003) for investigating integration and modularity patterns (Zelditch *et al.*, 2008a), based on Procrustes distance matrices—the distance within the shape space created after configuration superpositions (Monteiro and Reis, 1999). We delimited eight sets of anatomical landmarks, each of them corresponding to a morphogenetic unit (Figure 1). The cranium was divided into the facial region (maxilla; landmarks 1–7; 17–24), and the basicranium (cranial base; landmarks 8–16; 25–31). The mandible was divided into anterior alveolar (landmarks 1–3; 13); posterior alveolar (landmarks 3–4; 12–13); coronoid (landmarks 5–7); masseter (landmarks 4–5; 7; 9; 12); condylar (landmarks 7–9); and angular (landmarks 9–11) (Monteiro and Nogueira, 2010). Each component was considered as a multivariate shape described by the set of landmarks. A GPA

was performed individually for each morphogenetic unit. This division allowed for the component shape, as a development unit, to be treated as a single mathematical object (used as a character). Integration is then assessed by correlations of Procrustes distance matrices (between observations at different levels) calculated for different components (Monteiro *et al.*, 2005). This approach is different from others reported in the literature, where integration is estimated from the correlations between landmark coordinates (Klingenberg, 2014). The individual landmarks (more specifically their coordinates) do not correspond to biological or developmental structures, so their correlation has no biological meaning (Houle *et al.*, 2011) in the theoretical context of integration and modularity.

Developmental integration was estimated by the asymmetric component (within-individual) of shape variation. Bilateral landmark differences (after superimposition) were used to calculate asymmetry distances between each pair of individuals in the sample, generating an asymmetry distance matrix for each morphogenetic component. Euclidean distances based on superimposed landmarks are one type of Procrustes distances (Dryden and Mardia, 2016). Partial matrix correlations and Mantel tests (Legendre and Legendre, 2012) were used to estimate the association between each pair of components, keeping the influence of other components constant. The asymmetries are expected to originate from random disturbances during development, when the organism is unable to buffer their effect, leading to developmental instability (Van Dongen, 2006). When two morphogenetic components share a developmental pathway, their asymmetries are expected to be correlated (Klingenberg, 2003).

Static integration was estimated by the symmetric component (symmetrized landmark coordinates) as a within-population level of variation (Klingenberg, 2014). The Procrustes distances were calculated between individuals, and geographic distances among individuals (those belonging to the same population had a distance = 0) were included as covariates in the formula when calculating partial matrix correlations among components (Monteiro *et al.*, 2005; Monteiro and Nogueira, 2010).

Evolutionary integration was estimated by the symmetric component, averaged by locality. Procrustes distances were calculated between population means (not individuals) and the distance matrices for different morphogenetic

components were correlated to estimate evolutionary integration matrices (Monteiro *et al.*, 2005; Monteiro and Nogueira, 2010). All matrix correlations were calculated with the package ecodist (Goslee and Urban, 2007). All analyses were performed in the R environment (R Core Team, 2024).

Analyses of integration matrices

The integration matrices for each level were compared to each other by matrix correlations. Independence graphs were also built for each integration level (Magwene, 2001), where edges connecting traits were determined by the level of statistical support provided by *p*-values of Mantel tests (based on 10000 permutations). Because this is an exploratory study, we were flexible regarding the acceptable level of support ($p < 0.1$) (Wasserstein *et al.*, 2019). Independence graphs were built using package igraph (Csárdi *et al.*, 2024) in the R environment. We calculated integration indices for each level using a standardized variance of the eigenvalues (Cheverud, 1996; Monteiro *et al.*, 2005). This index is a ratio of the observed eigenvalue variance to the maximum possible eigenvalue variance and approaches one as integration increases.

We compared the integration matrices estimated for different levels of integration in *C. perspicillata* to matrices for levels of developmental (theoretical), static, and evolutionary integration for different lineages of phyllostomid bats, available from the study of (Monteiro and Nogueira, 2010). These analyses were carried out with the mandibular components only, because the integration matrices available in the literature did not include the cranial components. The theoretical integration matrices were assembled from the developmental history of cell condensations (sequential partitioning of cell populations; Atchley and Hall, 1991; Hall, 2015), and the joint effect of developmental genes inferred from knockout studies (Monteiro and Nogueira, 2010). The developmental matrix based on cell condensations assigned four arbitrary levels of correlations to pairs of morphogenetic components based on their shared developmental history—see Figure 3 in Monteiro and Nogueira(2010). The genetic developmental association matrix was based on 49 genes with knockout effects spreading to more than one component. Presence or absence was attributed where the effect of a gene was observed or not in a mandibular component. A Jaccard similarity was then

calculated as the proportion of developmental genes shared by each pair of components (Monteiro and Nogueira, 2010).

Within-group correlations were used to determine phyllostomid static integration patterns, pooling species belonging to the same feeding guild (and lineage). This pattern was estimated for frugivores, insectivores, and nectarivores. (sanguivores were not included due to small sample sizes) (Monteiro and Nogueira, 2010). Evolutionary integration patterns were calculated from distances among species means, comparing insectivores (the postulated ancestral form) with each group of species in a lineage/guild (Monteiro and Nogueira, 2010). Even though *C. perspicillata* is predominantly frugivorous, it was not included in the frugivore integration matrices (static or evolutionary), as most of those species were more specialized stenodermatines.

Monteiro and Nogueira(2010) compared the estimated matrices with a non-metric multidimensional scaling of the reciprocal matrix correlations ($1 - r$) among integration patterns. A minimum spanning tree was also used to infer goodness of fit of the ordination. We correlated the three integration matrices estimated for *C. perspicillata* with the matrices estimated by Monteiro and Nogueira(2010) for higher levels of variation in phyllostomids. The resulting correlation matrix among integration patterns was evaluated by an independence graph (Magwene, 2001), based on correlations with statistical support (generally $P < 0.1$). The correlations were also transformed to reciprocal distances and a multidimensional scaling ordination and minimum spanning trees (Legendre and Legendre, 2012) were estimated using the package vegan (Oksanen *et al.*, 2024) in the R environment (R Core Team, 2024).

Results

Asymmetry and developmental integration

The matrix correlations of asymmetry-based distances varied considerably (0.05 to 0.83). The developmental integration index was 0.253. The strongest associations were observed among adjacent mandibular components, with the exception of the angular, which is as weakly associated to the other mandible components as the mandible is associated with the cranium (Figure 2). One axis

of developmental integration can be observed along the mandibular components from the middle to the posterodorsal processes (coronoid, angular). The cranium is developmentally independent from the mandible, but the two cranial components are associated.

Figure 2: Independence graph showing partial correlations of asymmetry distances (developmental integration) among cranial and mandibular components. Numbers correspond to partial correlations with statistical support and edge thickness are proportional to the correlations. Distances among components are arbitrary, and their positions approximate the anatomical structure.

Static integration

The cranium and mandible were less integrated at the static within-population level than at the developmental within-individual level. The static integration index was 0.205 and the correlations were lower and fewer (Figure 3). The only static correlation that was higher than the developmental was between the alveolar processes. At this level, the cranium and mandible are integrated only by a weak association between basicranium and condylar process. Overall, the

static integration pattern was very similar to the developmental pattern, and the correlation between patterns was 0.953 (95% CI 0.895 to 0.978).
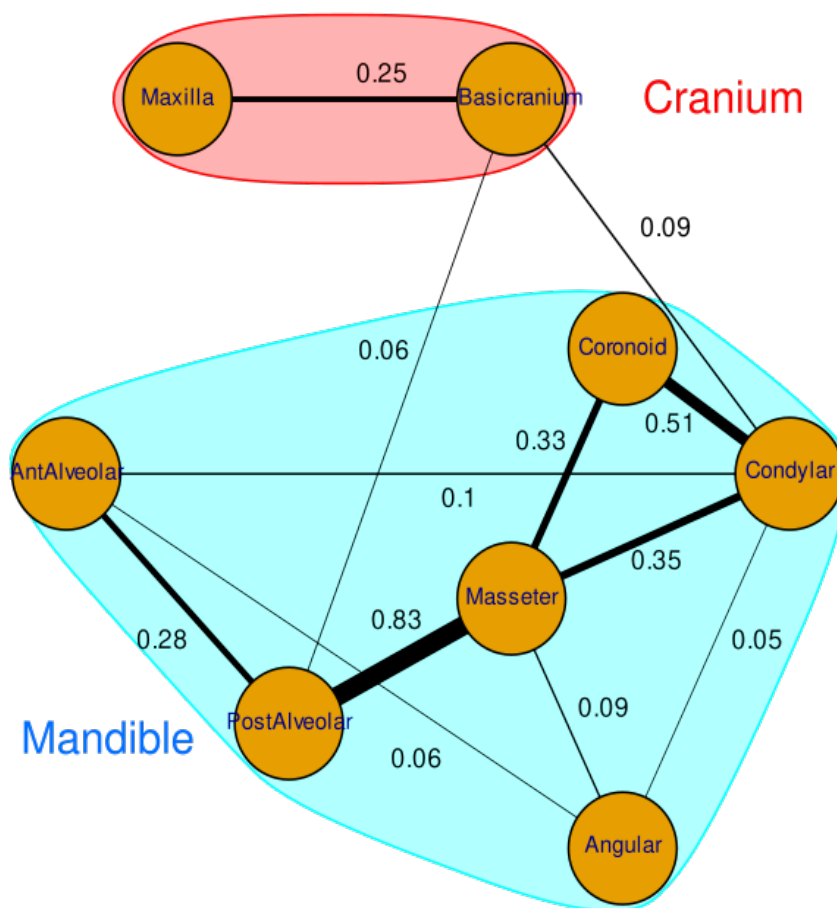

Figure 3: Independence graph showing partial correlations of within-population distances (static integration) among cranial and mandibular components. Numbers correspond to partial correlations with statistical support and edge thickness are proportional to the correlations. Distances among components are arbitrary, and their positions approximate the anatomical structure.

Evolutionary integration

The mandible and cranium become more integrated within and between structures at the evolutionary, among-population level. The evolutionary integration index is 0.273 and correlations are higher and numerous, even among non-adjacent components (Figure 4). The anterior alveolar component is integrated at this level with all mandibular processes and the posterior part of the cranium (basicranium). The anterior part of the cranium (maxilla), on the other hand, is integrated with the posterior components of the mandible (angular and condylar processes), but also with the posterior alveolar. The reorganization of the

integration pattern at the evolutionary level decreases its similarity with the static and developmental levels. The matrix correlation between evolutionary and developmental integration patterns was 0.732 (95%CI 0.428 to 0.852), whereas the correlation between evolutionary and static integration patterns was 0.755 (95%CI 0.419 to 0.844).
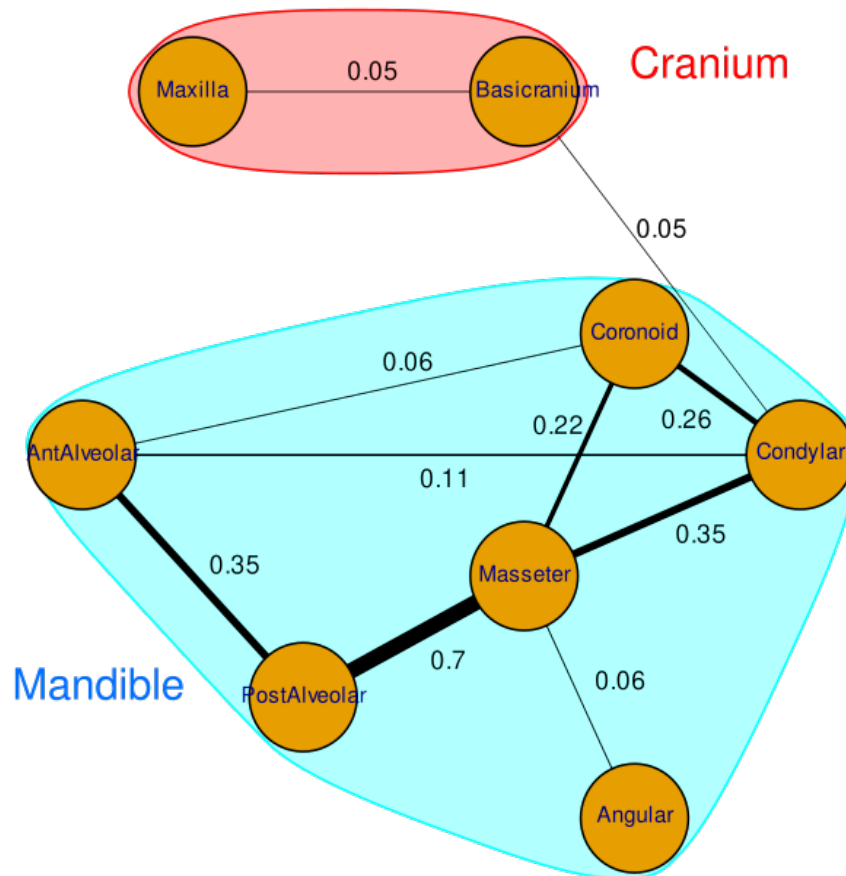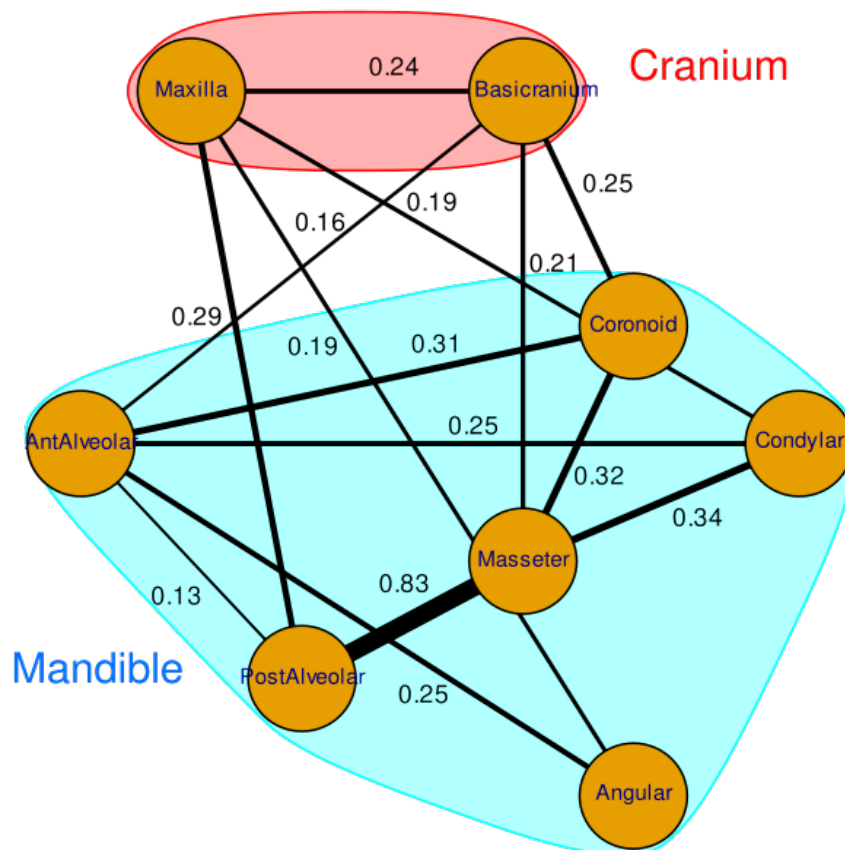

Figure 4: Independence graph showing partial correlations of among-population distances (evolutionary integration) among cranial and mandibular components. Numbers correspond to partial correlations with statistical support and edge thickness are proportional to the correlations. Distances among components are arbitrary, and their positions approximate the anatomical structure.

The principal component ordination of geographic localities based on mean mandible shapes for each site does not indicate a clear geographic structure. On the other hand, all samples but two from Peru, Colombia, and Bolivia have positive scores on the PC1 (Figure 5). The first two PCs explain 40.1% of total shape variation among populations. The shape changes associated with the first PC are concentrated in the mandibular processes and the anterior region. Sites with positive PC1 scores have average shapes with relatively smaller coronoid and

angular, but also with a more vertical angle at the anterior mandibular border (the "chin"). The shape changes associated with the second PC spread over more mandibular regions, with changes in all processes, the anterior and posterior alveolar (Figure 5).

Figure 5: Principal components for mandible shape variation among geographic sites in this study. The grid diagrams below the ordination plot depict shape changes associated with the PCs. The dashed line corresponds to the wireframe of the overall mean shape (the reference, with a score of 0 in all axes), and the solid line corresponds to the shape change associated with positive scores in each axis.

The principal component ordination of geographic localities based on mean cranial shapes for each site again does not indicate a clear geographic structure (Figure 6). The first two PCs explain 46.7% of total shape variation among

populations. The shape changes associated with the first PC are concentrated in the posterior region, where positive scores are associated with a relatively wider basicranium at the level of the (more anteriorly positioned) mastoid process. The shape changes associated with positive scores along the second PC indicate an overall wider and shorter cranium (Figure 6).

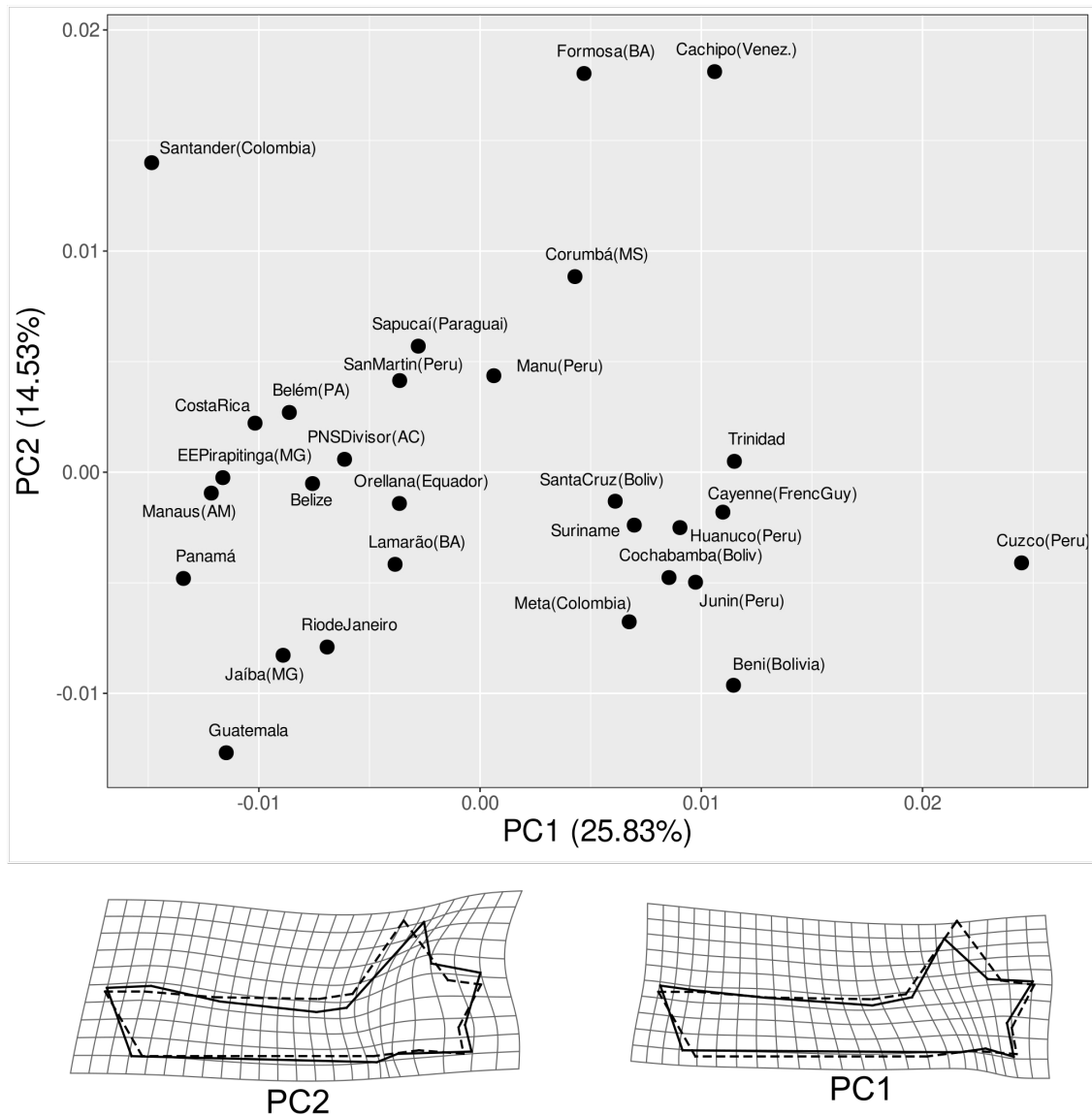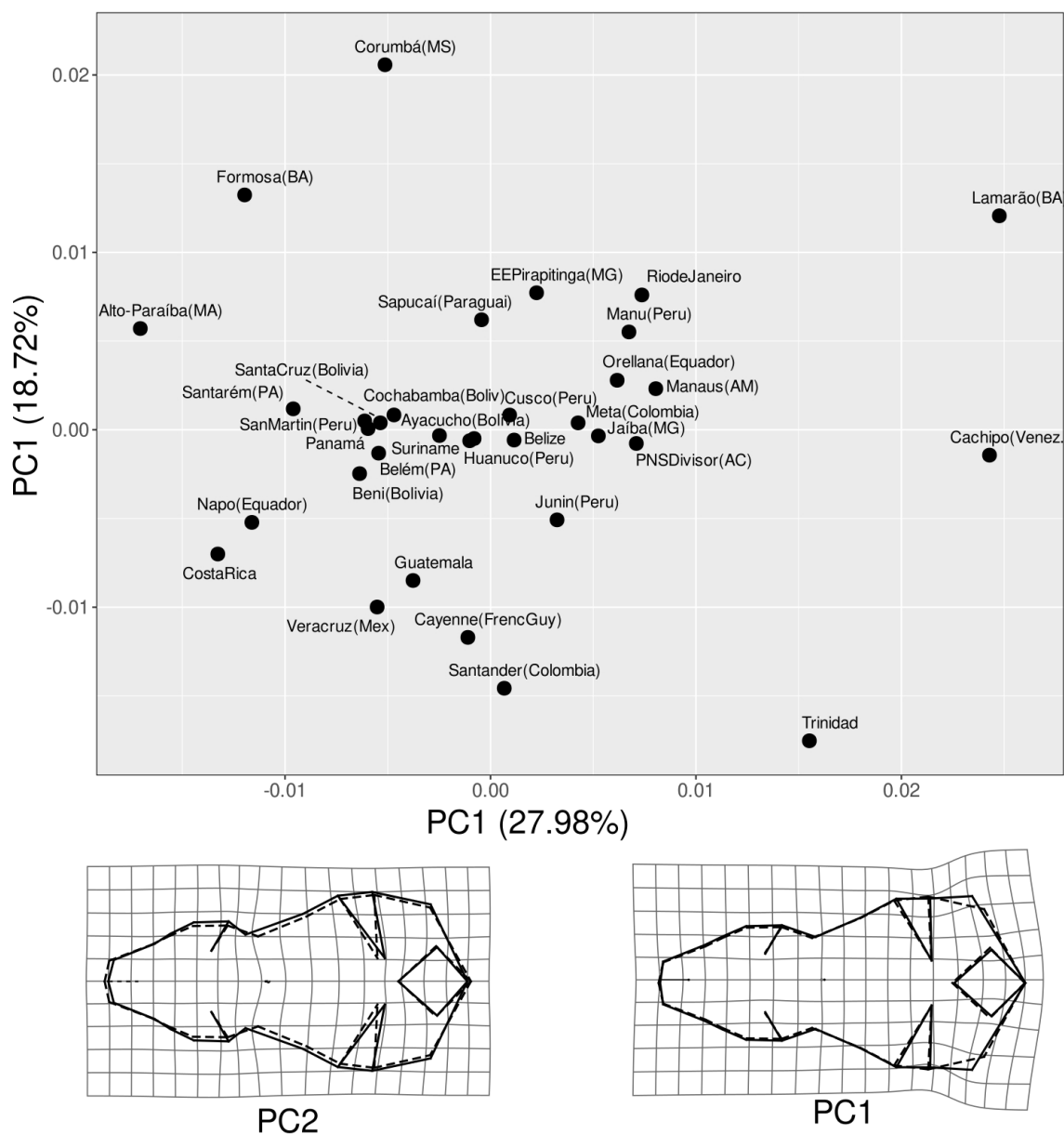Figure 6: Principal components for cranial shape variation among geographic sites in this study. The grid diagrams below the ordination plot depict shape changes associated with the PCs. The dashed line corresponds to the wireframe of the overall mean shape (the reference, with a score of 0 in all axes), and the solid line corresponds to the shape change associated with positive scores in each axis.

Comparison with phyllostomid integration and theoretical matrices

The mandibular integration matrices of *C. perspicillata* were compared with higher level phyllostomid integration and theoretical matrices through the combination of non-metric multidimensional scaling and independence graphs (Figure 7). In the NMDS ordination, the evolutionary matrices group together along the second (vertical) axis, separate from static and developmental matrices.

Integration matrices for *C. perspicillata* at the static and developmental levels are not associated with theoretical models, but both matrices connect with the static within-species pattern for nectarivores. At the same time, both the static and evolutionary patterns for *C. perspicillata* are correlated with the frugivore evolutionary pattern (Figure 7).
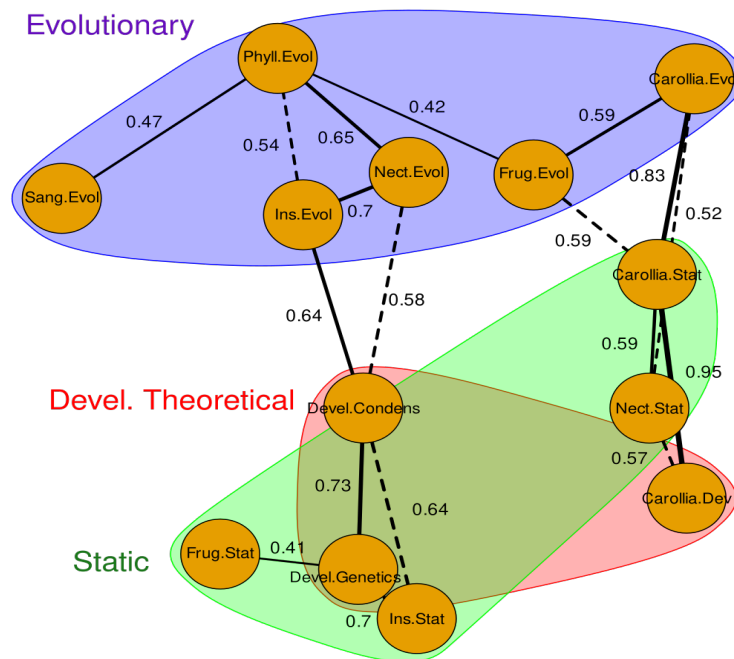
Figure 7: Independence graph showing associations among integration patterns estimated for *C. perspicillata* (this study) and those estimated by Monteiro and Nogueira (2010) for other levels of variation in Phyllostomidae, as well as theoretical matrices based on genetics and development. Numbers correspond to correlations with statistical support and edge thickness is proportional to the correlations. The arrangement of components is based on a non-metric multidimensional scaling ordination of matrix dissimilarities (NMDS1 and NMDS2 are the horizontal and vertical dimensions, respectively). Solid edges indicate the minimum spanning tree, whereas dashed edges indicate other associations with statistical support. Polygons join groups of matrices at the same level (Development theoretical, Static, Evolutionary). Vertices are labeled according to integration level (Devel = developmental, Stat = static, Evol = evolutionary) and lineage/guild (Frug = stenodermatine frugivores, Nect = nectarivores, Sang = sanguivores, Ins = insectivores+carnivores, Phyll = all phyllostomids). Theoretical patterns identified by Condens = cell condensation model and Genetics = shared developmental genes).

Discussion

The multi-level analysis of skull integration in *Carollia perspicillata* presented here indicated that developmental processes act structuring integration patterns at the intra-individual as well as at the static, within-population level. Conversely, at the evolutionary level, a complex and stronger pattern emerges. The strengthening of integration among morphogenetic components not associated by development is possibly due to functional demands and selection gradients arising from ecological differences among populations, as observed on a macro, interspecific scale for phyllostomid bats (Monteiro and Nogueira, 2010; Monteiro and Nogueira, 2011; Rossoni *et al.*, 2019).

Asymmetry and developmental integration

We observed a general pattern of association at the developmental level characterized by more integration between adjacent morphogenetic components than between components not sharing borders. It is clear along the mandible, and reiterated by the fact that the cranium is developmentally independent from the mandible. In the mandibular case, the expectation from developmental information, that predicted a separation in two distinct modules (alveolar regions and the mandibular processes) was not met (Atchley and Hall, 1991; Monteiro and Nogueira, 2010). This result might be explained by coordinated signaling to and between adjacent structures during morphogenesis (Szabo-Rogers *et al.*, 2009; Young *et al.*, 2015; Duclos *et al.*, 2019). The axis of developmental integration observed along the mandibular components from the middle to the posterodorsal processes was previously observed by Zelditch *et al.*(2008b) for rodents—deer mice (*Peromyscus maniculatus*) and fox squirrel (*Sciurus niger*). The high developmental correlation between the posterior alveolar and the masseter observed for *C. perspicillata* is not predicted in models of development or genetics, but was observed in within-species integration patterns for the mandible of nectarivores (Monteiro and Nogueira, 2010).

Static integration

Comparisons between within-individual and within-population correlations for cranial and mandible components have shown evidence that in some groups developmental and static levels present the same pattern (an indication that patterns between individuals reflect the developmental architecture), but in other groups they are not equivalent, indicating that different factors (like selection) affect on each level (Klingenberg, 2010; Klingenberg, 2013; Melo *et al.*, 2016). In our analysis, within-population pattern resembles that observed at the developmental level, but with a weaker integration, indicating that the developmental process prevails at this level.

Evolutionary integration

Classic publications in the field of integration and modularity, including Cheverud (1984) and (Wagner and Altenberg, 1996), argued that genetic and developmental integration patterns should evolve to match functional modules. Since multilevel analysis of integration and modularity are relatively rare (Klingenberg, 2013; Klingenberg, 2014; Sherratt and Kraatz, 2023), this hypothesis has not been extensively tested. There are examples both corroborating (Kent and Mardia, 2001; Young and Badyaev, 2006; Benítez *et al.*, 2022) contradicting (Breno *et al.*, 2011; Klingenberg, 2014) this hypothesis, or presenting mixed results (Sherratt and Kraatz, 2023). At the evolutionary level, cranium and mandible presented the highest integration among the analyzed levels in *C. perspicillata*. Unlike the developmental and static patterns, we observed relatively strong associations between non-adjacent components. Both the increased level of integration and the reorganization of the structure of associations among morphogenetic units are consistent with the influence of functional demands and selection gradients in this level of integration (Monteiro *et al.*, 2005; Monteiro and Nogueira, 2010; Arlegi *et al.*, 2019; Randau *et al.*, 2019; Raidan *et al.*, 2021; Rossoni *et al.*, 2024). Our study design does not allow for the identification of eventual selection agents, but we would hypothesize that dietary variation across the species distribution (Sánchez and Giannini, 2018) played a role in the reorganization of integration pattern—as happened at the macroevolutionary level (Monteiro and Nogueira, 2010; Monteiro and Nogueira, 2011; Dumont *et al.*, 2012; Rossoni *et al.*, 2019; Rossoni *et al.*, 2024).

A set of associations, that is evident at the evolutionary level and might constitutes a functionally integrated set, are the correlations between the maxilla and morphogenetic components in the medial posterior part of the mandible (masseter, condylar and angular). These components are the areas of insertion of pterygoid muscles (Santana, 2018)—the main muscle responsible for the lateral excursion of the mandible in bats. A motion that is important for *C. perspicillata*, because this bat chews in side-to-side cycles while feeding on *Piper* infructescences (Santana and Dumont, 2009; Santana, 2018). The anterior alveolar component is evolutionarily associated with all components but the maxilla and the posterior alveolar, both tooth bearing components that are anatomically close. The integration of the anterior alveolar with components located posteriorly, which are muscle insertion sites is consistent with the hypothesis of functional integration in shape differences among populations (Zelditch *et al.*, 2008b; Monteiro and Nogueira, 2010).

Attempts to comprehend the quantitative variation among populations in *C. perspicillata* have been limited by sampling design. For example, Jarrín-V and Menendez-Guerrero (2011), López-Aguirre *et al.* (2015), and Ruelas and Pacheco (2022) examined specimens from Ecuador, Colombia and Peru and Ecuador respectively. Pine (1972) and McLellan (1984) suggest that size is correlated with latitude in this species, with northern populations being larger than more southern ones. But none of the authors included specimens from populations located further south than the Amazon basin in their analysis. The ordination of mandibular shape did separate Peruvian and Colombian sites, but at the same time, did not provide evidence of range-wide geographic patterns. The lack of geographic structure in the principal components for cranial and mandibular shape is consistent with the lack of isolation among populations of *C. perspicillata*, observed both in the geographically restricted morphological analyses (Jarrín-V and Menendez-Guerrero, 2011; López-Aguirre *et al.*, 2015; Ruelas and Pacheco, 2022) and in a phylogeographic analysis based on the mitochondrial gene Cytochrome *b* (Velazco, 2013). Lack of geographic structure does not mean that differences among populations are random. They might as well be associated with adaptations to local conditions that do not follow large scale geographic gradients or might even be convergent among sites (Richardson *et al.*, 2014; Moreira and Smith, 2023).

Comparison with phyllostomid integration and theoretical matrices

The high partial correlation between the posterior alveolar and the masseter observed at all levels of variation in *C. perspicilata*, along with associations between the anterior alveolar and the mandibular processes, helps to explain why these integration patterns are more similar to the within-species pattern observed for nectarivorous phyllostomids (Monteiro and Nogueira, 2010) than to matrices based on developmental patterns and genetics. Also, and perhaps more interestingly, the shape changes associated with the main mandibular axis of variation (PC1) among populations of *C. perspicillata* are similar to changes that happened in the evolution of nectarivory and frugivory in phyllostomid bats—the reduction of the coronoid processes (nectarivory) and the vertical expansion of the anterior alveolar, forming the robust "chin" (frugivory) (Monteiro and Nogueira, 2010; Monteiro and Nogueira, 2011). Because *C. perspicillata* is in an intermediary clade between these two more ecologically specialized lineages (Glossophagines and Stenodermatines) (Rojas *et al.*, 2016), this similarity might reflect an ancestral integration pattern.

The association between evolutionary (among populations) integration in *C. perspicillata* and the frugivorous evolutionary pattern (family level) indicates that the reorganization of mandibular integration observed at the interspecific level during the dietary transitions from the insectivore ancestor (Monteiro and Nogueira, 2011) might also be observed at the intraspecific, among-population level. This reorganization was also reported for cranial integration patterns in this lineage of bats (Dumont *et al.*, 2012; Rossoni *et al.*, 2019; Rossoni *et al.*, 2024).

Final remarks

Our analysis of skull integration in *Carollia perspicillata* bridges developmental, micro- and macroevolutionary patterns in phyllostomid bats. It reaffirms the role of evolutionary processes such as selection, in the morphological diversification of the group, in addition to pointing out the role of development in structuring intra-individual and intra-population variation. These connections are essential since evolutionary diversification of morphology and ecology are based

primarily on the intraspecific variation structure of the form-performance-fitness relationship. This study reinforces the importance of population level analysis to the comprehension of overall diversification patterns.

References

Álvarez, A., Perez, S.I., Verzi, D.H. (2013). Ecological and phylogenetic dimensions of cranial shape diversification in South American caviomorph rodents (Rodentia: Hystricomorpha). *Biological Journal of the Linnean Society* 110:898–913.

Anthwal, N., Tucker, A.S. (2022). Evolution and development of the mammalian jaw joint: Making a novel structure. *Evolution & Development* 25:3–14.

Arlegi, M., Veschambre-Couture, C., Gómez-Olivencia, A. (2019). Evolutionary selection and morphological integration in the vertebral column of modern humans. *American Journal of Physical Anthropology* 171:17–36.

Atchley, W.R., Hall, B.K. (1991). A model for development and evolution of complex morphological structures. *Biological Reviews* 66:101–157.

Benítez, H.A., Püschel, T.A., Suazo, M.J. (2022). Drosophila Wing Integration and Modularity: A Multi-Level Approach to Understand the History of Morphological Structures. *Biology* 11:567.

Breno, M., Leirs, H., Dongen, S.V. (2011). No relationship between canalization and developmental stability of the skull in a natural population of *Mastomys natalensis* (Rodentia: Muridae). *Biological Journal of the Linnean Society* 104:207–216.

Cheverud, J.M. (1984). Quantitative genetics and developmental constraints on evolution by selection. *Journal of Theoretical Biology* 110:155–171.

Cheverud, J.M. (1996). Quantitative genetic analysis of cranial morphology in the cotton-top (*Saguinus oedipus*) and saddle-back (*S. fuscicollis*) tamarins. *Journal of Evolutionary Biology* 9:5–42.

Csárdi, G. et al. (2024). igraph: Network Analysis and Visualization in R. . . https://CRAN.R-project.org/package=igraph.

Dryden, I.L., Mardia, K.V. (2016). *Statistical shape analysis with applications in R*. New York: John Wiley and Sons. 454 p.

Duclos, K.K., Hendrikse, J.L., Jamniczky, H.A. (2019). Investigating the evolution and development of biological complexity under the framework of epigenetics. *Evolution & Development* 21:276–293.

Dumont, E.R., Davalos, L.M., Goldberg, A., Santana, S.E., Rex, K., Voigt, C.C. (2012). Morphological innovation, diversification and invasion of a new adaptive zone. *Proceedings of the Royal Society B: Biological Sciences* 279:1797–1805.

Esteve-Altava, B. (2017). In search of morphological modules: a systematic review. *Biological Reviews* 92:1332–1347.

Fleming, T.H., Dávalos, L.M., A. R. Mello, M. (2020). *Phyllostomid bats: a unique mammalian radiation*. Chicago, Illinois: University of Chicago Press. 470 p.

Goslee, S.C., Urban, D.L. (2007). The ecodist package for dissimilarity-based analysis of ecological data. *Journal of Statistical Software* 22:1–19.

Graham, J.H., Raz, S., Hel-Or, H., Nevo, E. (2010). Fluctuating asymmetry: methods, theory, and applications. *Symmetry* 2:466–540.

Grossnickle, D.M. et al. (2024). The hierarchical radiation of phyllostomid bats as revealed by adaptive molar morphology. *Current Biology* 34:1284–1294.e3.

Gual-Suárez, F., Medellín, R.A. (2021). We eat meat: a review of carnivory in bats. *Mammal Review* 51:540–558.

Hall, B.K. (2015). *Bones and cartilage: developmental and evolutionary skeletal biology*. New York: Elsevier. 892 p.

Hallgrímsson, B., Lieberman, D.E., Young, N.M., Parsons, T., Wat, S. (2006). Evolution of covariance in the cammalian skull. in Tinkering: The Microevolution of Development. *Novartis Foundation Symposium*. 289:164–190.

Houle, D., Pélabon, C., Wagner, G., Hansen, T. (2011). Measurement and meaning in biology. *The Quarterly Review of Biology* 86:3–34.

Jarrín-V, P., Menendez-Guerrero, P.A. (2011). Environmental Components and Boundaries of Morphological Variation in the Short-Tailed Fruit Bat (Carolliaspp.) in Ecuador. *Acta Chiropterologica* 13:319–340.

Kent, J.T., Mardia, K.V. (2001). Shape, Procrustes tangent projections and bilateral symmetry. *Biometrika* 88:469–485.

Klingenberg, C. (2003). Developmental instability as a research tool: using patterns of fluctuating asymmetry to infer the developmental origins of morphological integration. *In*: Polak, M. (eds.) *Developmental instability: causes and consequences*. Oxford: Oxford UniversityPress. p. 427–442.

Klingenberg, C.P. (2010). Evolution and development of shape: integrating quantitative approaches. *Nature Reviews Genetics* 11:623–635.

Klingenberg, C.P. (2011). MorphoJ: an integrated software package for geometric morphometrics. *Molecular Ecology Resources* 11:353–357.

Klingenberg, C.P. (2013). Cranial integration and modularity: insights into evolution and development from morphometric data. *Hystrix, the Italian Journal of Mammalogy* 24:43-58.

Klingenberg, C.P. (2014). Studying morphological integration and modularity at multiple levels: concepts and analysis. *Philosophical Transactions of the Royal Society B: Biological Sciences* 369:20130249.

Klingenberg, C.P. (2015). Analyzing fluctuating asymmetry with geometric morphometrics: concepts, methods, and applications. *Symmetry* 7:843–934.

Klingenberg, C.P., Barluenga, M., Meyer, A. (2002). Shape analysis of symmetric structures: quantifying variation among individuals and asymmetry. *Evolution* 56:1909–1920.

Klingenberg, C.P., McIntyre, G.S. (1998). Geometric morphometrics of developmental instability: analyzing patterns of fluctuating asymmetry with Procrustes methods. *Evolution* 52:1363–1375.

Koyabu, D. (2023). Evolution, conservatism and overlooked homologies of the mammalian skull. *Philosophical Transactions of the Royal Society B: Biological Sciences* 378:.

Law, C.J., Blackwell, E.A., Curtis, A.A., Dickinson, E., Hartstone-Rose, A., Santana, S.E. (2022). Decoupled evolution of the cranium and mandible in carnivoran mammals. *Evolution* 76:2959–2974.

Legendre, P., Legendre, L. (2012). *Numerical Ecology*. New York: Elsevier. 990 p.

López-Aguirre, C., Pérez-Torres, J., Wilson, L.A.B. (2015). Cranial and mandibular shape variation in the genus *Carollia* (Mammalia: Chiroptera) from Colombia: biogeographic patterns and morphological modularity. *PeerJ* 3:e1197.

Loy, A., Ciucci, P., Guidarelli, G., Roccotelli, E., Colangelo, P. (2021). Developmental instability and phenotypic evolution in a small and isolated bear population. *Biology Letters* 17:.

Magwene, P.M. (2001). New tools for studying integration and modularity. *Evolution* 55:1734–1745.

Mammal Diversity Database (2024). Mammal Diversity Database.

Mardia, K.V., Bookstein, F.L., Moreton, I.J. (2000). Statistical assessment of bilateral symmetry of shapes. *Biometrika* 87:285–300.

Martín-Serra, A., Nanova, O., Varón-González, C., Ortega, G., Figueirido, B. (2019). Phenotypic integration and modularity drives skull shape divergence in the Arctic fox (*Vulpes lagopus*) from the Commander Islands. *Biology Letters* 15:20190406.

McLellan, L.J. (1984). A morphometric analysis of *Carollia* (Chiroptera, Phyllostomidae). *American Museum Novitates* 2791:1–35.

Melo, D., Porto, A., Cheverud, J.M., Marroig, G. (2016). Modularity: genes, development, and evolution. *Annual Review of Ecology, Evolution, and Systematics* 47:463–486.

Meloro, C., Tamagnini, D. (2021). Macroevolutionary ecomorphology of the Carnivora skull: adaptations and constraints in the extant species. *Zoological Journal of the Linnean Society* 196:1054–1068.

Milošević-Zlatanović, S., Vukov, T., Chovancová, G., Anderwald, P., Corlatti, L., Tomašević Kolarov, N. (2022). Cranial integration and modularity in chamois: The effects of subspecies and sex. *Journal of Mammalian Evolution* 30:269–280.

Monteiro, L.R., Bonato, V., Reis, S.F. (2005). Evolutionary integration and morphological diversification in complex morphological structures: mandible shape divergence in spiny rats (Rodentia, Echimyidae). *Evolution & Development* 7:429–439.

Monteiro, L.R., Nogueira, M.R. (2010). Adaptive radiations, ecological specialization, and the evolutionary integration of complex morphological structures. *Evolution* 64:724–744.

Monteiro, L.R., Nogueira, M.R. (2011). Evolutionary patterns and processes in the radiation of phyllostomid bats. *BMC Evolutionary Biology* 11:1–23.

Monteiro, L.R., Reis, S.F. (1999). *Princípios de morfometria geométrica*. Ribeirão Preto, SP: Holos Editora. p.

Moreira, L.R., Smith, B.T. (2023). Convergent genomic signatures of local adaptation across a continental-scale environmental gradient. *Science Advances* 9:eadd0560.

Nogueira, M.R., Monteiro, L.R., Peracchi, A.L., de Araújo, A.F.B. (2005). Ecomorphological analysis of the masticatory apparatus in the seed-eating bats, genus *Chiroderma* (Chiroptera: Phyllostomidae). *Journal of Zoology* 266:355–364.

Oksanen, J. et al. (2024). vegan: Community Ecology Package. . . https://CRAN.R-project.org/package=vegan.

Palmer, A.R., Strobeck, C. (2003). Fluctuating asymmetry analyses revisited. *In*: Polak, M. (eds.) *Developmental instability: causes and consequences*. : Oxford University Press New York. p. 279–319.

Pine, R.H. (1972). *The Bats of the Genus Carollia*. Technical Monograph, College Station: Texas A & M University Press. 125 p.

Raidan, C., de Andrade Costa, B.M., Marroig, G., Aprígio Assis, A.P., Paresque, R. (2021). Morphological integration and cranial modularity in six genera of echimyid rodents (Rodentia: Echimyidae). *Journal of Mammalogy* 103:648–662.

Randau, M., Sanfelice, D., Goswami, A. (2019). Shifts in cranial integration associated with ecological specialization in pinnipeds (Mammalia, Carnivora). *Royal Society Open Science* 6:190201.

Richardson, J.L., Urban, M.C., Bolnick, D.I., Skelly, D.K. (2014). Microgeographic adaptation and the spatial scale of evolution. *Trends in Ecology & Evolution* 29:165–176.

Richtsmeier, J.T., Flaherty, K. (2013). Hand in glove: brain and skull in development and dysmorphogenesis. *Acta Neuropathologica* 125:469–489.

Rohlf, F. (2015). The tps series of software. *Hystrix* 26:9–12.

Rojas, D., Warsi, O.M., Dávalos, L.M. (2016). Bats (Chiroptera: Noctilionoidea) challenge a recent origin of extant Neotropical diversity. *Systematic Biology* 65:432–448.

Rolland, J. et al. (2023). Conceptual and empirical bridges between micro- and macroevolution. *Nature Ecology & Evolution* 7:1181–1193.

Rossoni, D.M., Costa, B.M.A., Giannini, N.P., Marroig, G. (2019). A multiple peak adaptive landscape based on feeding strategies and roosting ecology shaped the evolution of cranial covariance structure and morphological differentiation in phyllostomid bats. *Evolution* 73:961–981.

Rossoni, D.M., Patterson, B.D., Marroig, G., Cheverud, J.M., Houle, D. (2024). The role of (co)variation in shaping the response to selection in New World leaf-nosed bats. *The American Naturalist* 203:E107–E127.

Ruelas, D., Pacheco, V. (2022). Variación intraespecífica de *Carollia brevicaudum* y *Carollia perspicillata* (Phyllostomidae: Chiroptera) de Perú y Ecuador. *Neotropical Biodiversity* 8:253–266.

Sánchez, M.S., Giannini, N.P. (2018). Trophic structure of frugivorous bats in the Neotropics: emergent patterns in evolutionary history. *Mammal Review* 48:90–107.

Santana, S.E. (2018). Comparative anatomy of bat jaw musculature via diffusible iodine-based contrast-enhanced computed tomography. *The Anatomical Record* 301:267–278.

Santana, S.E., Dumont, E.R. (2009). Connecting behaviour and performance: the evolution of biting behaviour and bite performance in bats. *Journal of Evolutionary Biology* 22:2131–2145.

Sherratt, E., Kraatz, B. (2023). Multilevel analysis of integration and disparity in the mammalian skull. *Evolution* 77:1006–1018.

Szabo-Rogers, H.L., Geetha-Loganathan, P., Whiting, C.J., Nimmagadda, S., Fu, K., Richman, J.M. (2009). Novel skeletogenic patterning roles for the olfactory pit. *Development* 136:219–229.

R Core Team (2024). *R: A Language and Environment for Statistical Computing. R Foundation for Statistical Computing*. Vienna, Austria. https://www.R-project.org/.

Van Dongen, S. (2006). Fluctuating asymmetry and developmental instability in evolutionary biology: past, present and future. *Journal of Evolutionary Biology* 19:1727–1743.

Velazco, P.M. (2013). On the phylogenetic position of *Carollia manu* Pacheco et al., 2004 (Chiroptera: Phyllostomidae: Carolliinae). *Zootaxa* 3718:.

Voss, R.S., Fleck, D.W., Strauss, R.E., Velazco, P.M., Simmons, N.B. (2016). Roosting Ecology of Amazonian Bats: Evidence for Guild Structure in Hyperdiverse Mammalian Communities. *American Museum Novitates* 3870:1–43.

Wagner, G.P., Altenberg, L. (1996). Perspective: complex adaptations and the evolution of evolvability. *Evolution* 50:967–976.

Wasserstein, R.L., Schirm, A.L., Lazar, N.A. (2019). Moving to a world beyond " p < 0.05". *The American Statistician* 73:1–19.

Young, N.M., Winslow, B., Takkellapati, S., Kavanagh, K. (2015). Shared rules of development predict patterns of evolution in vertebrate segmentation. *Nature Communications* 6:.

Young, R.L., Badyaev, A.V. (2006). Evolutionary persistence of phenotypic integration: influence of developmental and functional relationships on complex trait evolution. *Evolution* 60:1291–1299.

Zelditch, M.L., Goswami, A. (2021). What does modularity mean?. *Evolution and Development* 23:377–403.

Zelditch, M.L., Wood, A.R., Bonett, R.M., Swiderski, D.L. (2008a). Modularity of the rodent mandible: Integrating bones, muscles, and teeth. *Evolution & Development* 10:756–768.

Zelditch, M.L., Wood, A.R., Swiderski, D.L. (2008b). Building developmental integration into functional systems: function-induced integration of mandibular shape. *Evolutionary Biology* 36:71–87.

Zepeda Mendoza, M.L. et al. (2018). Hologenomic adaptations underlying the evolution of sanguivory in the common vampire bat. *Nature Ecology & Evolution* 2:659–668.

Supplementary Materials for chapter 4:

Supplementary Table S1. Partial correlations for asymmetry distance matrices (developmental level of integration and modularity) between cranial and mandible morphogenetic components. Superior diagonal indicates the partial correlation and the inferior indicates the associated *p* value based on random

	Basicranium	Maxilla	Coronoide	Condylar	Angular	Masseter	P. alveolar	A. alveolar
Basicranium	–	0.249	-0.035	0.094	0.010	-0.044	0.057	-0.022
Maxilla	0.001	–	-0.033	-0.008	-0.044	-0.027	-0.003	0.034
Coronoide	0.840	0.841	–	0.506	-0.069	0.328	-0.271	0.036
Condylar	0.002	0.613	0.001	–	0.052	0.353	-0.281	0.100
Angular	0.403	0.906	0.985	0.069	–	0.088	-0.050	0.056
Masseter	0.916	0.808	0.001	0.001	0.007	–	0.829	-0.212
P. alveolar	0.043	0.548	1.000	1.000	0.953	0.001	–	0.282
A. alveolar	0.758	0.723	0.154	0.004	0.049	1.000	0.001	–

Supplementary Table S2. Partial correlations for distance matrices based on within-population symmetrized data (static level of integration and modularity) between cranial and mandible morphogenetic components. Superior diagonal indicates the partial correlation and the inferior indicates the associated *p* value based on random permutations (Mantel test).

	Basicranium	Maxilla	Coronoide	Condylar	Angular	Masseter	P. alveolar	A. alveolar
Basicranium	–	0.053	0.003	0.047	0.001	-0.036	0.036	0.022
Maxilla	0.048	–	0.007	0.003	0.014	0.013	0.026	-0.015
Coronoide	0.438	0.405	–	0.263	-0.020	0.221	-0.179	0.061
Condylar	0.042	0.444	0.001	–	0.031	0.352	-0.250	0.105
Angular	0.464	0.301	0.776	0.128	–	0.064	-0.021	-0.012
Masseter	0.917	0.328	0.001	0.001	0.012	–	0.695	-0.249
P. alveolar	0.103	0.185	1.000	1.000	0.770	0.001	–	0.348
A. alveolar	0.219	0.706	0.014	0.002	0.651	1.000	0.001	–

Supplementary Table S3. Partial correlations for distance matrices based on among-population symmetrized data (evolutionary level of integration and modularity) between cranial and mandible morphogenetic components. Superior diagonal indicates the partial correlation and the inferior indicates the associated *p* value based on random permutations (Mantel test).

	Basicranium	Maxilla	Coronoide	Condylar	Angular	Masseter	P. alveolar	A. alveolar
Basicranium	–	0.235	0.247	0.025	0.008	0.212	-0.157	-0.160
Maxilla	0.025	–	-0.195	0.195	0.190	0.050	0.286	0.050
Coronoide	0.026	0.967	–	0.116	-0.078	0.323	-0.220	0.313
Condylar	0.391	0.058	0.139	–	-0.173	0.345	-0.291	0.248
Angular	0.447	0.053	0.751	0.965	–	0.113	-0.181	0.253
Masseter	0.017	0.315	0.004	0.001	0.101	–	0.826	-0.210
P. alveolar	0.955	0.013	0.988	1.000	0.973	0.001	–	0.133
A. alveolar	0.025	0.253	0.003	0.005	0.003	0.992	0.057	–

Conclusão geral

Essa tese propôs o exame da estabilidade do desenvolvimento e os padrões de integração morfológica e modularidade, usando o morcego neotropical *Carollia perspicillata* como espécie modelo. Para tanto, foram examinados diferentes complexos morfológicos (crânio, membro anterior e posterior) de espécimes provenientes de diferentes localidades ao longo da distribuição da espécie depositados em coleções científicas.

Foi detectada a presença de efeito sistêmico da instabilidade do desenvolvimento, medida pela assimetria flutuante. Interessantemente esse efeito não é homogeneamente distribuído nos diferentes complexos e tampouco é distribuído de forma aleatória. O nível de ID apresentado pelos caracteres é negativamente associado à relevância funcional por eles apresentados. O nível de DI apresentado foi menor em caracteres funcionalmente associados ao voo, seguido por aqueles associados à mastigação, enquanto os associados ao pouso e suspensão apresentaram o maior nível.

Essa diferença entre os níveis de ID levanta uma interessante questão a ser examinada em estudos futuros. Qual o papel da escolha do caractere no tipo de resultado encontrado em estudos que avaliam a relação ID e adequabilidade ambiental, valor adaptativo ou medidas de desempenho regulatório, por exemplo? Se os caracteres funcionalmente mais importantes são mais tamponados durante o desenvolvimento, em relação a distúrbios, pode ser que eles apresentem um sinal maior de ID expresso na assimetria e por isso sejam mais informativos em estudos de monitoramento. Uma outra questão a ser examinada em estudos futuros é a relevância da variação em caracteres do crânio vs membros para gradientes de seleção intrapopulacionais. Se as asas são menos assimétricas que o crânio por serem funcionalmente mais relevantes, é possível que os gradientes de seleção associados aos membros anteriores sejam maiores que os associados ao crânio.

Foi observada maior AF em populações de *C. perspicillata* em localidades da Diagonal de Formações Secas da América do Sul, o que indica que estresse ambiental, mesmo que de origem natural, pode aumentar a instabilidade do desenvolvimento dessa espécie. Esse resultado reforça a importância da realização cuidadosa de avaliações do impacto do estresse ambiental causado

por fatores antropogênicos (levando em consideração ecologia das espécies), para além da atenção à escolha das variáveis a serem analisadas.

Além de marcador para a ID, as assimetrias flutuantes permitiram a avaliação dos padrões de integração do desenvolvimento (isolado de fatores genéticos e ambientais) tanto nos membros quanto no crânio de *C. perspicillata*. Os comprimentos lineares dos ossos pertencentes aos membros anterior e posterior foram usados para a análise da integração nos níveis estático e evolutivo dos membros anterior e posterior. Para a análise dos padrões de integração no crânio e na mandíbula foi usada a forma dos componentes morfogenéticos que os compõem. É importante ressaltar que as medições de integração realizadas dependem do contexto teórico. Os comprimentos de elementos ósseos são interpretados como resultado da dinâmica das populações celulares que compõem as condensações formadoras, assim como eventos de remodelagem a partir de estímulos funcionais. A forma dos componentes morfogenéticos, por outro lado, resulta de diferenças em direções dos eixos de crescimento em diferentes partes do componente. A discussão sobre o significado biológico das medições têm ocupado menos espaço que os métodos estatísticos mais apropriados para o estudo da integração.

O padrão de integração de desenvolvimento no crânio foi marcado pela associação de caracteres adjacentes entre si, possivelmente como consequência da sinalização coordenada durante a morfogênese. O nível estático apresentou um padrão similar, indicando que o desenvolvimento estrutura as diferenças interindividuais em *C. perspicillata*.

No nível evolutivo (entre populações), os padrões de integração em ambos os complexos estudados foram mais complexos e também mais fortes que o observado nos níveis de desenvolvimento e estático. A reorganização dos padrões de associação nesse nível indica que gradientes de seleção atuando nos padrões de associação entre as estruturas morfológicas estudadas.

Esse trabalho foi o primeiro a demonstrar por uma perspectiva morfológica a existência de módulos de desenvolvimento integrando elementos do autopódio em morcegos. Este resultado é consistente com evidências da biologia do desenvolvimento que indicam que falanges e metacarpos apresentam relativa independência quanto à regulação do seu desenvolvimento. No nível estático, entre indivíduos, não foi encontrado padrão de associação entre estruturas

serialmente homólogas nos membros, a maioria das associações observadas conecta elementos pertencentes ao mesmo membro. Um padrão consistente com o observado em outros grupos em que membros anteriores e posteriores apresentam relativa independência entre si.

Populações de localidades cuja vegetação é mais fechada apresentam membros posteriores relativamente mais longos—por potencialmente gerar um incremento de manobrabilidade (capacidade de mudar a forma da asa e o coeficiente de sustentação) e por consequência reduzir o custo energético do voo. Os padrões de integração de desenvolvimento e estático em *C. perspicillata* mostram similaridades com o nível estático (dentro da espécie) de nectarívoros da família Phyllostomidae. Os níveis estático e evolutivo intraespecíficos foram ambos associados à matriz evolutiva (entre espécies) de frugívoros mais especializados (subfamília Stenodermatinae). Esses resultados reforçam o papel do desenvolvimento na estruturação do padrão de integração no nível estático. No nível evolutivo (entre populações), gradientes de seleção, provavelmente relacionados à dieta, podem fortalecer a integração entre componentes que não são integrados do ponto de vista de desenvolvimento.

Os resultados dessa tese reafirmam a importância das questões conceituais, metodológicas, e da biologia dos organismos modelo no planejamento e execução de investigações científicas. Além disso, reforçam a importância da compreensão de como os processos de desenvolvimento e microevolutivos atuam sobre estrutura de variação nos níveis intraindividual, interindividual e evolutivos.